

UNCLASSIFIED

AD NUMBER
AD859724
NEW LIMITATION CHANGE
TO Approved for public release, distribution unlimited
FROM Distribution authorized to U.S. Gov't. agencies and their contractors; Critical Technology; JUN 1969. Other requests shall be referred to Dean of Engineering, Air Force Institute of technology, ATTN: AFIT-SE, Wright-Patterson AFB, OH 45433.
AUTHORITY
AFIT memo dtd 22 Jul 1971

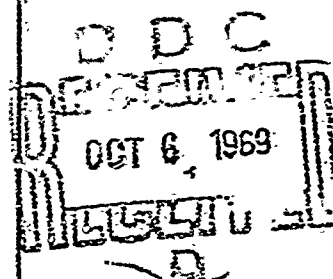
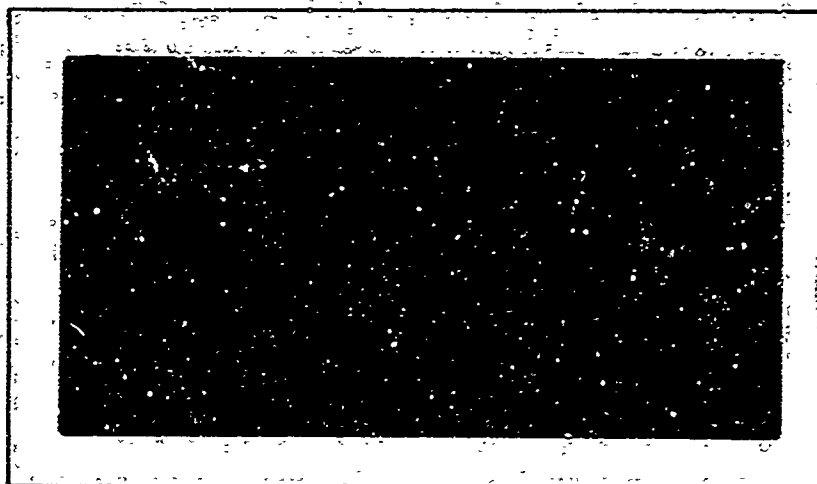
THIS PAGE IS UNCLASSIFIED

AD859724

AIR FORCE INSTITUTE OF TECHNOLOGY



AIR UNIVERSITY
UNITED STATES AIR FORCE



SCHOOL OF ENGINEERING

WRIGHT-PATTERSON AIR FORCE BASE, OHIO

GSF/MC/69-4

COMPRESSIBILITY OF SIMULATED LUNAR

SOILS IN AIR AND IN ULTRAHIGH

VACUUM

THESIS

GSF/MC/69-4

Dwayne G. Lee
Captain CE

This document is subject to special export controls and each transmittal to foreign governments or foreign nationals may be made only with prior approval of the Dean of Engineering, Air Force Institute of Technology (AFIT-SE), Wright-Patterson AFB Ohio, 45433

GSF/MC/69-4

**COMPRESSIBILITY OF SIMULATED LUNAR SOILS IN AIR
AND IN ULTRAHIGH VACUUM**

THESIS

**Presented to the Faculty of the School of Engineering
of the Air Force Institute of Technology**

**in Partial Fulfillment of the
Requirements for the Degree of
Master of Science**

by

**Dwayne G. Lee, BS
Captain CE**

Graduate Space Facilities Engineering

June 1969

**This document is subject to special export controls and
each transmittal to foreign governments or foreign nationals
may be made only with prior approval of the Dean
of Engineering, Air Force Institute of Technology (AFIT-
SE). Wright-Patterson AFB, Ohio**

45433

Acknowledgements

I wish to express my sincere thanks to all those individuals who assisted me in the experimentation that was required before this report could be written. A particular note of thanks goes to: Mr. Wolfe of the AFIT Shops for fabrication of some necessary equipment; Mr. S. G. Lee of the AFIT Laboratories for his ever-present help during the experimentation; Sgt. Norm Swenson of the Aerospace Research Laboratories for his assistance in the use of their facilities; and finally to Maj. Stewart W. Johnson, Associate Professor, Department of Mechanics, AFIT, for his wealth of experience and assistance throughout the entire span of this report.

Dwayne G. Lee

Contents

	Page
Acknowledgements	ii
List of Figures.....	v
List of Tables.....	vii
Abstract	
I. Introduction.....	1
Background.....	1
Statement of the Problem	3
Scope	3
Organization.....	4
II. Experimentation.....	5
Preliminary Considerations.....	5
Sample Selection and Preparation.....	9
Description of Vacuum Apparatus	11
Description of Test.....	15
Instron Tests.....	16
III. Discussion and Results	21
Introduction.....	21
Discussion.....	27
Boundary Effects.....	33
Results.....	35
IV. Conclusions and Recommendations	46
Conclusions.....	46
Recommendations.....	47
Bibliography.....	49
Appendix A: Comminution of Basalt.....	52
Appendix B: Mineralogy of the Rocks Tested.....	57

GSF/MC/69-4

Appendix C: Analysis of Force Measuring Device.....	59
Appendix D: Raw Data and Sample Calculations	74
Appendix E: Assumptions	136
Appendix F: Analysis of the Boundary Effects	142

List of Figures

Figure	Page
1 Varian VI-360 System	13
2 Soil Containers.....	13
3 Typical Loading-Rate Curve	17
4 Sample Loaded in the Instron.....	19
5 Sample Loaded in the Chamber Apparatus	19
6 Data Runs # 3, 26, 44	22
7 Data Runs # 7, 37, 9, 40	23
8 Data Runs # 12, 23, 19, 39	24
9 Data Runs # 16, 35, 17, 38	25
10 Data Runs # 15, 29, 3, 42.....	26
11 M_v vs. e_i , 10^{-10} Torr and Atmosphere, $\Delta P=40$	36
12 M_v vs. e_i , 10^{-10} Torr and Atmosphere, $\Delta P=60$	37
13 M_v vs. e_i , 10^{-8} Torr and Atmosphere	40
14 Soil Sample before Loading	45
15 Soil Sample after Loading.....	45
16 Shaker Box.....	54
17 Grain Size Analysis	55
18 Photomicrographs of the Soil Grains	56
19 Schematic of the Chamber Apparatus	60
20 Detail of the Linear Motion Feedthrough	60
21 Chamber Apparatus Installed in Chamber	61

22	Chamber Apparatus Seen from Top.....	61
23	Moments about the Pivot Point.....	68
24	Raised Platform	71
25	Reduced Volume Used in Calculations	76
26	Data Run # 22	82
27	Data Run # 21.....	83
28	Data Run # 2	84
29	Data Run # 10	85
30	Data Run # 6	86
31	Data Run # 13.....	87
32	Range on e_i from 1.10 to 1.40	88
33	Range on e_i from 1.40 to 1.70	89
34	Range on e_i from 1.70 to 2.00	90
35	Atmospheric Tests	91
36	10^{-8} Torr Tests	92
37	10^{-10} Torr Tests	93
38	Flow Pattern of the Soil	146

List Of Tables

Table		Page
I	Calibration Test.....	65
II	Summary of Data Runs.....	78
III		94
through		to
XIX	Raw Data from Tests on Chamber Apparatus	114
XX		115
through		to
XL	Raw Data from Tests on Instron	135
XLI	Comparison of Green's Standards and the Surveyor Results.....	137

Abstract

A simulated lunar soil of comminuted tholeiitic basalt powder with particles less than 60 microns in size was tested in one dimensional compression to determine the effect of the initial void ratio and the ambient pressure on the compressibility of the soil. The initial void ratio ranged from 1.12 to 2.00 and the ambient pressure was restricted to three levels; atmospheric pressure, 10^{-8} Torr, and 10^{-10} Torr. The compression tests were performed in a vacuum chamber to allow control of the ambient pressure. The results of the tests indicate that the compressibility of the powders increased as the initial void ratio increased. Also the powders tended to become less compressible as the ambient pressure decreased. No change was noted between air and 10^{-8} Torr; but the coefficient of volume compressibility between air and 10^{-10} Torr decreased 16% for an initial void ratio of 2.00 and 75% for an initial void ratio of 1.20.

Abstract

A simulated lunar soil of comminuted tholeiitic basalt powder with particles less than 60 microns in size was tested in one dimensional compression to determine the effect of the initial void ratio and the ambient pressure on the compressibility of the soil. The initial void ratio ranged from 1.12 to 2.00 and the ambient pressure was restricted to three levels; atmospheric pressure, 10^{-8} Torr, and 10^{-10} Torr. The compression tests were performed in a vacuum chamber to allow control of the ambient pressure. The results of the tests indicate that the compressibility of the powders increased as the initial void ratio increased. Also the powders tended to become less compressible as the ambient pressure decreased. No change was noted between air and 10^{-8} Torr; but the coefficient of volume compressibility between air and 10^{-10} Torr decreased 16% for an initial void ratio of 2.00 and 75% for an initial void ratio of 1.20.

I. Introduction

Background

The field of soil mechanics is far from an exact science. Only recently have attempts been made to be more precise in predicting the mechanical response of a soil under load. The bulk of available data originated from one of two sources; laboratory tests and in situ observations. Both of these sources have been significant in the development of soil mechanics. They furnish the best sources of information because of the large number of variables involved in describing soil behavior under load. Because of the nature of information gained from these sources, the relationships that exist in soil mechanics are primarily empirical ones. If either of these inputs of information are absent, then the conclusions based upon observations of only one source become speculative. If for some reason either source is not available, then the only alternative is to exhaust the remaining source and extract from it as much information as possible. In the case of lunar soils, the in situ information is meager consisting only of the Surveyor and Luna 13 mission results. Because of this shortcoming it is difficult to formulate an intelligent statement about the response of the lunar surface material to an imposed load. Consequently, the bulk of the information about the mechanical properties of the lunar surface must come from laboratory tests. This

paper is a report of an attempt to add some small amount to that knowledge that will be required to understand the mechanical response of the lunar surface material.

There are a number of soil properties that will change significantly under the lunar environment. Those properties that reflect the strength of the soil and its response to an applied load should be the first ones investigated because these will have direct influence on future lunar missions. Bearing capacity, shear strength, compressibility, and penetration resistance are a few of the properties that should be high on a priority list. It would be difficult to assess which of these is the most important but the property that was investigated in this study was the compressibility of a soil under simulated lunar atmospheric conditions. The compressibility of a soil as determined by the one dimensional compression test has been an old acquaintance of the soils engineer. The test is generally performed in a cylindrical apparatus approximately 4 in. in diameter and 1 in. high. The sides of the container prevent lateral movement of the soil and impose the condition of no lateral strain (Ref 24:56). The change in volume for a given increase in load is measured and the resulting information when plotted is known as a compressibility curve. Even though the test is titled a one dimensional compression test, this name has arisen from common usage and is not a precise description of the state of stress in the soil. Once the results are obtained, they are used in a

semi-empirical relation to calculate the settlements in a soil under an imposed surface load. Without the results of the compressibility test the only way that settlements can be determined is to physically load the soil in situ and observe the settlement. Such a technique is not practical on the lunar surface. The degree of settlement of the surface under an imposed load should be an important parameter to the early lunar missions, and to fully understand this parameter the difference in compressibility of a fine-grained soil in vacuum as compared to air must be known.

Statement of the Problem

The purpose of this investigation was to determine the effect of the initial void ratio and the ambient pressure level on the compressibility of simulated lunar soil subjected to one dimensional compression.

Scope

The compressibility of the soil was determined from void ratio versus pressure, e - P , curves for the samples tested. The void ratio, e , is defined as the ratio of the volume of voids to the volume of solids in the sample. The e - P curve is a plot of the change in void ratio as the applied surface load changes. Obtaining this curve while independently varying the initial void ratio, e_i , and the ambient pressure was the objective of the experimentation.

The entire process consisted of comminution of rocks to pro-

duce powders, sieving the powders for grain size control, performing the one dimensional compression test while measuring the applied force and the corresponding decrease in volume, and plotting the e - P curve for each test. The details of this sequence are described in the body of the report.

The experimentation was limited in scope in several respects. The only variables in the tests were the initial void ratio and the ambient pressure level. The ambient pressures used were atmospheric pressure, 10^{-8} Torr, 10^{-10} Torr. The initial void ratio ranged from 1.12 to 2.00. The grain size was restricted to particles passing a #250 sieve or approximately less than 60 microns in size. Only one type of rock, tholeiitic basalt, was comminuted.

Organization

The material is presented in the following sequence: a description of the test apparatus, instrumentation, and procedures; a statement of the experimental results; a discussion of the results; and recommendations for additional work to be done in the area. If the reader desires to obtain as much information as possible about the work that was done with a minimum of reading the suggested sections and sequence of readings would be as follows: abstract; introduction; Chapter III, the Results section only; conclusions; and Appendix E.

II. Experimentation

Preliminary Considerations

Several factors should be considered before a detailed discussion of the actual experimentation is presented. These factors were taken into account during the design of the experiment to insure that the results would be valid and some conclusions could be drawn.

The tests were performed in a vacuum chamber capable of operation in the 10^{-10} Torr range to create the required variation in ambient conditions. So that a comparison of the results between the atmospheric tests and the vacuum tests would be valid, both vacuum and atmospheric tests from which conclusions were drawn were performed on the chamber apparatus.

The purpose of the experiment was to determine the effects of a change in ambient pressure on the coefficient of volume compressibility of a rock powder. The soil mechanics parameter that represents the e-P curve is the coefficient of volume compressibility, M_v . M_v is defined by the equation

$$M_v = a_v / (1 + e)$$

a_v is the slope of the chord of the e-P curve between an initial load and a final load on the soil

e_i is the initial void ratio

(Ref 22:170)

M_v is therefore not a constant but depends on the slope of the e - P curve and the initial void ratio. It is also related to the more familiar Young's Modulus by the equation

$$E = (M_v)^{-1} \left[1 - 2v^2 / (1 - v) \right]$$

v is Poisson's ratio for the soil

(Ref 16:68)

This equation is valid only for the one dimensional compression case of no lateral strain which was the assumed condition in the soil mass. Defining the initial load as P_0 and the load increment as ΔP , M_v becomes

$$M_v = (1 + e_i)^{-1} \left[\frac{e \text{ (at } P_0) - e \text{ (at } P_0 + \Delta P)}{P} \right]$$

The test that was performed was a one dimensional compression test. Certain deviations from the normal test procedure were included because of special problems associated with this particular experiment. The sample size was selected as approximately 0.7 in. high and 1.0 in. in diameter in a cylindrical configuration. This is substantially different from the normal size of the apparatus used for one dimensional testing of soils with nominal dimensions of 1.00 in. high and 4.0 in. in diameter (Ref 24:260). The sample was purposely kept small so that the outgassing problems associated with the vacuum system

would be within the capacity of the system to handle. The primary phenomena associated with a change in the response of the soil to changes in ambient pressure is the change in the degree of surface cleanliness of the soil grains (Ref 25:3748). The larger the soil sample, the lesser the degree of surface cleanliness and thus the less the difference of the observed results. Consequently some compromise had to be attained between the standard size of sample and a smaller sample size that would produce results that truly illustrate the effects of a change in the environment. The size that was selected was chosen based on those considerations. Another problem associated with the size of the soil container was the sensitivity of the results to slight changes in the size of the container. Several tests were performed with containers with small changes in internal dimensions and it was found that the results were sensitive to changes in geometry. Consequently, the results presented are a function of the geometry of the test and would change as the scaling of the test apparatus was changed. This scaling problem restricts the interpretation of the results in such a way that only relative differences between the data can be discussed and the absolute value of the results is subject to some question. However, since all of the tests were performed with the same internal dimensions, they are all subject to the same scaling problems and comparisons within the test data are quite valid.

The tamping device that was used to apply the load to the surface of the soil was designed in such a manner that there was 0.10 in. clearance between the wall of the container and the edge of the tamper. This was also a deviation from the standard test but was felt to be necessary because of the problems associated with metal-metal contacts in ultrahigh vacuum. To eliminate the difficulties inherent in determining the frictional interaction at the interface of the tamper and the wall in the vacuum and its effect on the computed compressibility of the powders, this clearance space was designed into the apparatus. All of the tests that were run were performed with the same tamper-wall clearance. Again, this design change affects the absolute values of the results but since only comparisons between tests are made, the conclusions are valid.

The final deviation from the standard one dimensional test was the design of the container itself. The containers are shown in Fig. 2. The container used in the vacuum chamber was made from stainless steel because of its excellent outgassing properties. The teflon container could not be used in the vacuum chamber because of its poor outgassing properties, however it was used in atmospheric tests. These containers were of a cylindrical configuration with vertical slits cut in the sides. The slits were placed in the sides of the steel container to increase the capability of the soil to outgas. If these slits had not been present, a soil grain in the bottom of the container

would have seen the vacuum through the height of the column of soil. Because of the slits in the side that same soil grain had to look only along a radius to see the vacuum. The degree of surface cleanliness that was obtained would probably not have been achieved if these slits had not been present.

These above discussed considerations were made before the actual experimentation was started and they do have a significant effect on the results. The important result of these factors is that the absolute value of the results is highly speculative but the relative value of the results is quite valid. Consequently, all of the conclusions made consider only relative changes and general trends in the observed data.

Sample Selection and Preparation

The rocks chosen for comminution were samples of tholeiitic basalt furnished by the U.S. Bureau of Mines. An analysis of these rocks is included in Appendix B. These rocks were selected because they are one of Green's standards for lunar research (Ref 8) and because they closely approximate the results of the chemical analysis of the lunar surface from the Surveyor missions. A comparison of chemical compositions is given in Appendix E. The rocks had been previously crushed mechanically and were less than one inch in size. They were placed in a furnace and heated to 600^o C for approximately 45 hours. This was done to drive off as much water vapor as pos-

ible from the surface of the rocks since this is the area from which most of the powders were derived. Also the furnace was flushed with argon during this heating to minimize oxidation of the surface of the rocks which would change their mineralogical content. After the rocks were dried, they were stored in a dessicated atmosphere to prevent further adsorption of water vapor. Before comminution, the rocks were placed in a shaker box and the interior of the box was flushed with argon so that the comminuting process would be conducted in an inert atmosphere. This comminution process is discussed in detail in Appendix A. After comminution in the inert atmosphere, the powders were sieved to collect all particles that passed a #250 sieve. A grain size analysis is shown in Fig. 17 in Appendix A. This sieving process was conducted in an enclosed box that had been flushed with argon during the sieving operation. This procedure was also followed to minimize surface contamination. In the initial stages of testing, the powders were tested in the same day in which they were comminuted because the degree of cleanliness of a surface is directly related to the age of that surface (Ref 12:27). Later a compression test was conducted on powders that had been prepared one month prior to the test. No difference in the results were observed and consequently all later tests were conducted with powders that were not more than one month old. After the powders of the proper size were collected, they were stored in a dessicated atmosphere to prevent the adsorption of water

vapor.

On the day in which the test was to be performed, the powders were placed in a testing container whose volume had been accurately measured. The method of placement was varied to eliminate the possibility of systematic error. For initial void ratios below 1.60 the samples were packed to the desired void ratio for testing by either applying a uniform pressure across the entire face of the sample or by using a rod and rodding the sample into its final configuration. Vibration could not be used because of the slits in the sides of the containers. For initial void ratios of 1.70 and above the initial configuration was attained by pouring the powders into the containers from a short height and not applying any pressure to the surface. After the container had been filled it was weighed and the initial void ratio was determined. The density of the solid particles was assumed to be the same as the density of the rock prior to comminution. This density was measured and found to be $2.85 \pm 0.012 \text{ gm/cm}^3$. The same technique of sample preparation was used for tests performed both in the vacuum chamber and on the Instron.

Description of Vacuum Apparatus

The vacuum system used to create the pressure environment for testing was a Varian VI-360 ultrahigh vacuum system. This system has the capability of operating in the low 10^{-11} Torr range when emp-

vapour.

On the day in which the test was to be performed, the powders were placed in a testing container whose volume had been accurately measured. The method of placement was varied to eliminate the possibility of systematic error. For initial void ratios below 1.60 the samples were packed to the desired void ratio for testing by either applying a uniform pressure across the entire face of the sample or by using a rod and rodding the sample into its final configuration. Vibration could not be used because of the slits in the sides of the containers. For initial void ratios of 1.70 and above the initial configuration was attained by pouring the powders into the containers from a short height and not applying any pressure to the surface. After the container had been filled it was weighed and the initial void ratio was determined. The density of the solid particles was assumed to be the same as the density of the rock prior to comminution. This density was measured and found to be $2.85 \pm 0.012 \text{ gm/cm}^3$. The same technique of sample preparation was used for tests performed both in the vacuum chamber and on the Instron.

Description of Vacuum Apparatus

The vacuum system used to create the pressure environment for testing was a Varian VI-360 ultrahigh vacuum system. This system has the capability of operating in the low 10^{-11} Torr range when emp-

ty and can easily operate in the 10^{-10} Torr range under a gas load. Rough pumping is accomplished by five sorption pumps. The other pumps in the system are a titanium sublimation pump and a 500 liter per second ion pump all of which are bakeable to 250°C . The entire system with control panel is shown in Fig. 1. The chamber is 18 in. in diameter, 30 in. tall internally, and can be separated in the center to allow access to the interior. The top of the bell jar is connected to a motor driven hoist to permit raising and lowering. This connection may be sealed with either a Viton gasket, which permits operation to 10^{-8} Torr without bakeout, or a copper gasket clamped with Wheeler flanges, which permits operation to 10^{-10} Torr with a bakeout. The two feedthroughs that were used for the test were the linear motion feedthrough, which permitted one inch of precision horizontal travel, and the electrical feedthrough. There are essentially four gages used in the system to monitor the pressure at various stages during pump-down. A bourdon gage operates during the first stage of rough pumping and a thermocouple gage operates during the latter stages of rough pumping. For the range of 1×10^{-4} to 5×10^{-9} Torr a pressure gage on the ion pump records the pressure. From 5×10^{-9} to 2×10^{-11} Torr a mode ion gage is used. The significant advantage of this system is that it does not use any diffusion or oil type pumps thus eliminating the possibility of contamination by backstreaming of oil into the vacuum.

A certain number of internal modifications were required to a-

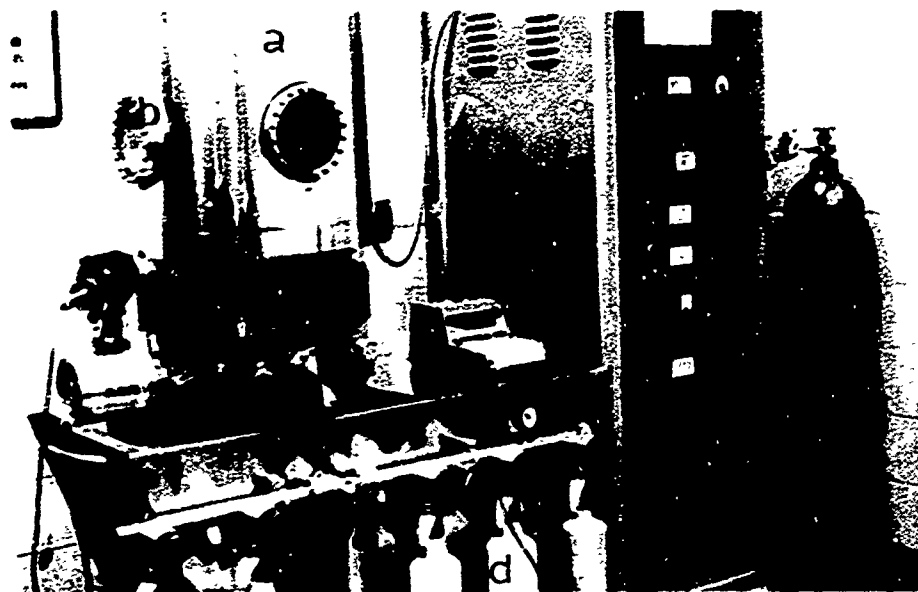


Fig. 1 Varian VI-360 System. (a) Bell Jar
(b) Viewing Ports (c) Wheeler Flanges
(d) Sorption Pumps (e) Control Panel

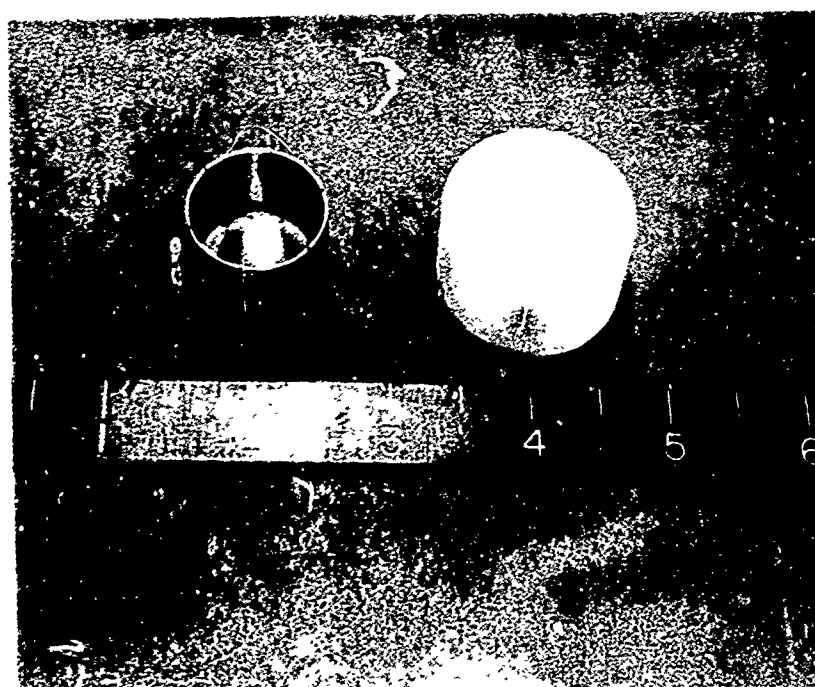


Fig. 2 Soil Containers (Scale in inches)

dapt the system to perform the desired tests. The staging platform was approximately 12 in. below the viewing ports, consequently a stainless steel table was made to elevate the working area to the level of the viewing ports so the experiments could be seen from the exterior of the chamber. A system of arms and levers was constructed to transfer the horizontal motion of the linear motion feedthrough into a nearly vertical motion at the surface of the soil sample to be tested. The known stiffness of the lever system was used in the determination of the force applied to the sample. Because of the importance of this aspect of the instrumentation this device is discussed in detail in Appendix C.

The containers that were used to hold the sample are shown in Fig. 2. A stainless steel container was used for the bulk of the experiments, and a teflon container was used to test for the friction effects involved. The teflon container was used only for tests in atmosphere and was not used in the vacuum chamber.

A heating coil was constructed that could be placed near the soil sample to introduce the capability of intense local heating near the sample. The element consisted of two large coils, 2 in. in diameter, around the sample. The wire used was standard heavy gauge heating element wire and was coiled in 1/4 in. coils. The wire was connected to an external power supply and was operated for two hours at 6.0 amps during the bakeout of the system. This increased the local tem-

perature near the sample to approximately 300° C.

The final portion of the apparatus was a cathetometer which was placed outside the chamber and measured the vertical deformation or axial strain in the soil as the load was applied. This device is also discussed in more detail in Appendix C.

Description of Test

The tests were performed at three pressure levels; atmospheric, 10^{-8} Torr, and 10^{-10} Torr. All of the tests were performed on the chamber apparatus to insure compatibility of results. The atmospheric tests were conducted by placing the sample in the chamber, closing the chamber with the Viton gasket installed, and creating a small vacuum of approximately 10 in. This was done to insure a proper seal of the Viton gasket. The chamber was then backfilled with nitrogen gas to a pressure of about 28 in. Thus the atmospheric tests were conducted in about a 1 in. vacuum and a nitrogen atmosphere. The 10^{-8} Torr tests also used the Viton gasket however the complete pumping cycle of the system was required to attain this vacuum level. Only one test sample at 10^{-8} Torr had been exposed to a bakeout. The 10^{-10} Torr tests were exposed to a system bakeout of 200° C for 18 hours and exposure to the sample heating coil at approximately 300° C for 2 hours. In some instances the sample heating coil malfunctioned and this is noted where applicable. All of the 10^{-10} Torr tests used the copper gasket and the Wheeler flanges to seal the bell jar. The system

is capable of a bakeout to 250°C but the linear motion feedthrough that was used as an attachment is limited to a 200°C exposure temperature.

The compressibility test was performed when the desired vacuum environment had been created in the chamber. This test consisted of applying an input to the linear motion feedthrough which transmitted a corresponding force to the surface of the sample. This applied force was measured along with the corresponding deflection of the sample. An additional force increment was applied and the increased deflection measured, and so forth until the total load on the sample was approximately 60 psi. This force and deflection measuring system is discussed at great length in Appendix C. The force could be measured with an accuracy of $\pm 10\%$ and the deflection could be read to $\pm 0.01\text{ mm}$. From this information the void ratio at any force increment could be determined and the corresponding e-P curve could be plotted. The time rate at which the load was applied is shown for a typical test as Fig. 3. The void ratio could be determined to ± 0.02 and the total volume of the sample at any time was known to $\pm 0.01\text{ cm}^3$.

Instren Tests

Additional tests in atmosphere were performed on an Instron machine for two reasons. First, since this instrument was much more accurate than the chamber apparatus, a comparison of the results of tests from the Instron and the chamber apparatus permitted

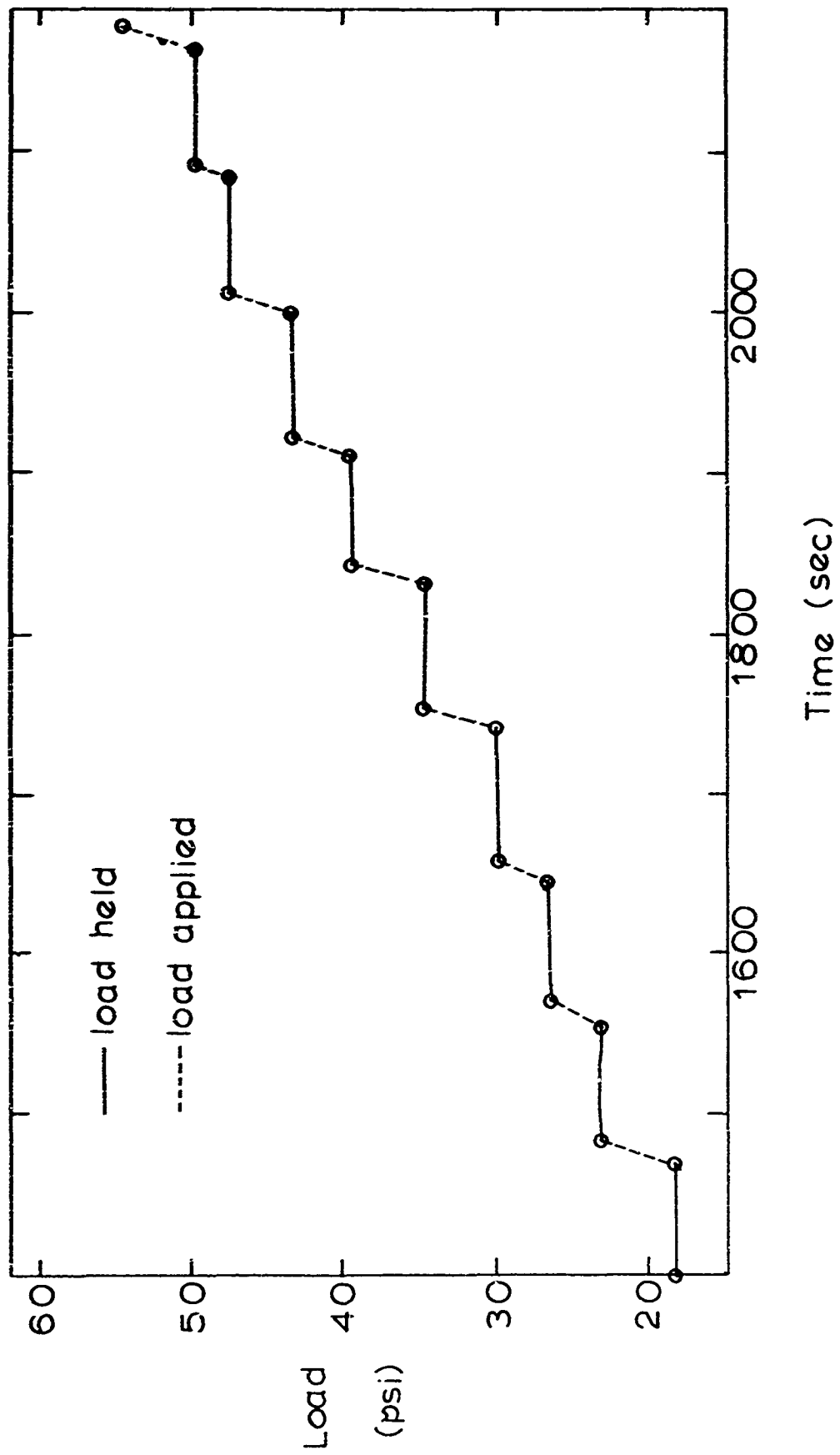


Fig.3 Typical Loading-Rate Curve

an analysis of the accuracy of the chamber apparatus. Second, the additional atmospheric tests provided more information on the behavior of the powders under atmospheric conditions particularly the frictional effects of the boundaries of the containers.

The Instron is a commercially-available test apparatus designed to permit the capability of testing a wide variety of materials in tension or compression. A load cell incorporated into the stationary base of the machine was capable of recording loads up to 50 lbs. full scale. A moveable crosshead containing the tamping device and the soil container was placed on top of the compression load cell. The same container and tamper size was used for these tests as was used for the chamber tests. The only difference was the geometry of loading since the crosshead of the Instron would move directly into the soil sample and not along the arc of a circle as in the chamber apparatus. Fig. 4 shows the sample loaded in the Instron and Fig. 5 shows the sample loaded in the chamber. The movement of the crosshead was controlled by a synchronous motor and was calibrated to be 0.005 in./min. This loading rate corresponded to the approximate loading rate of the chamber tests. The output of the load cell was fed into a chart recorder which was driven by another synchronous motor operating off of the same power source as the crosshead motor. The load cell was accurate to $\pm 0.5\%$ on all force readings. The accuracy of measuring the displacement in the soil could be varied by

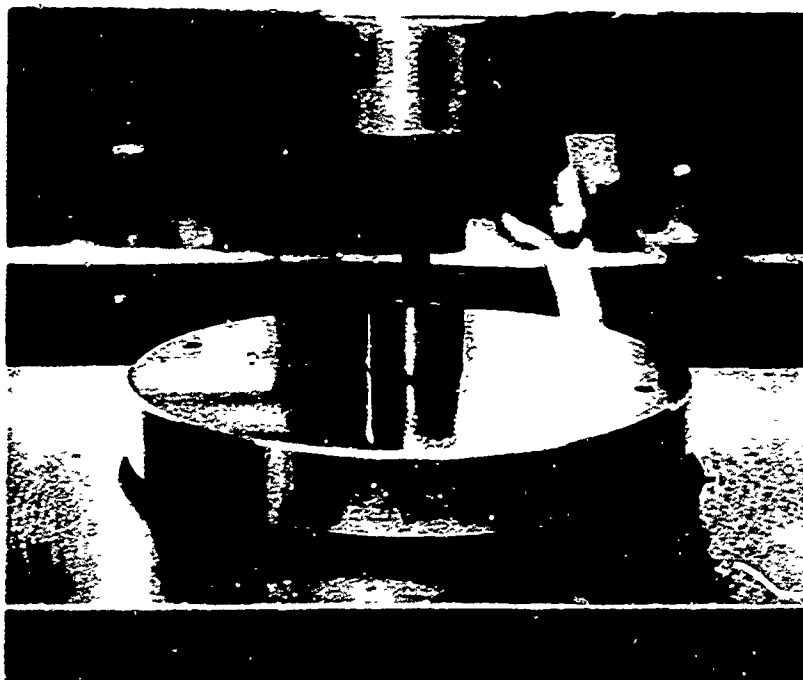


Fig. 4 Sample Loaded in the Instron

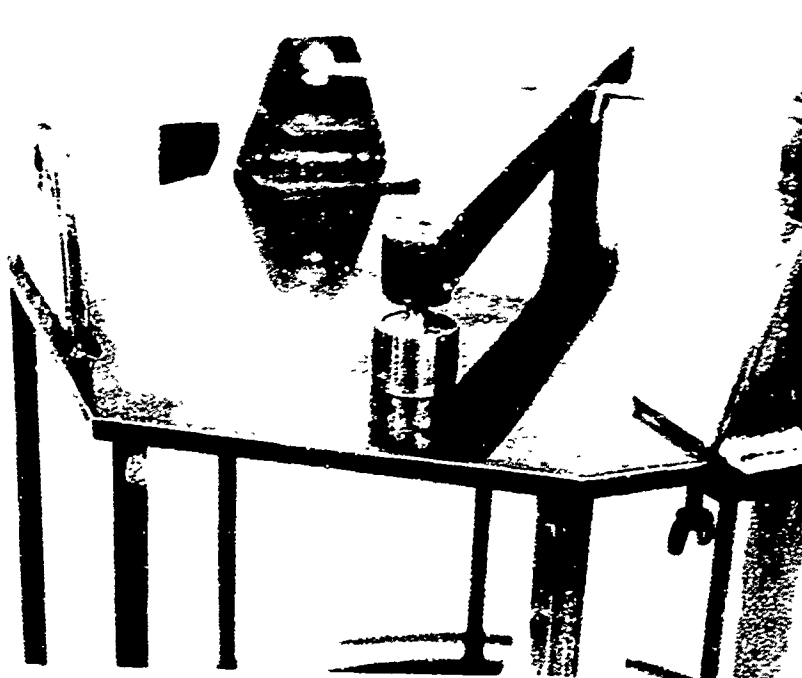


Fig. 5 Sample Loaded in the Chamber Apparatus

proper selection of the chart speed. The accuracy chosen was slightly greater than the accuracy of displacement measurement available on the chamber apparatus and was ± 0.00005 in. By making this choice, the tests on the Instron were duplicates of the chamber tests except for three respects which were the straight downward motion of the tamper relative to the sample, improved accuracy of the force and displacement measurements, and performance of the tests in air as opposed to a nitrogen environment.

The Instron was also used to determine the effects of the frictional resistance developed at the boundaries of the container by performing the tests in a teflon container. A detailed discussion of these tests and their analysis is included in Appendix F.

III. Discussion and Results

Introduction

A total of 15 tests were run in the vacuum chamber, six of which were at atmospheric pressure, three at 10^{-8} Torr, and six at 10^{-10} Torr. The data collected from these tests is included in Appendix D. Table II in that appendix is a summary listing of all tests performed. The corresponding void ratio versus pressure curves for some of the tests are presented as Figs. 6 through 10. The e-P curves for the remaining tests performed in the vacuum chamber are in Appendix D as Figs. 26 through 31. Figs. 26 and 27 were tests performed in the vacuum chamber but there were no other test performed in vacuum at similar initial void ratios. Figs. 28, 29 and 30 are the e-P plots of the three tests performed in the 10^{-8} Torr range. Fig. 31 is a plot at a 10^{-10} Torr test on a sample with an $e_i = 1.517$ and is essentially the same result as obtained in Data Run #12 with $e_i = 1.497$. The e-P plot for Data Run #12 is shown in Fig. 8. Also included in Appendix D, as Figs. 32 through 37 are additional non-dimensional plots of the same information with the volume normalized to the initial volume and the applied load to a 60 psi value and plotted on a semilog scale. These plots are included in the Appendix for information and do not show any results that cannot be gained from Figs. 6 through 10.

The tests performed on the Instron in the stainless steel con-

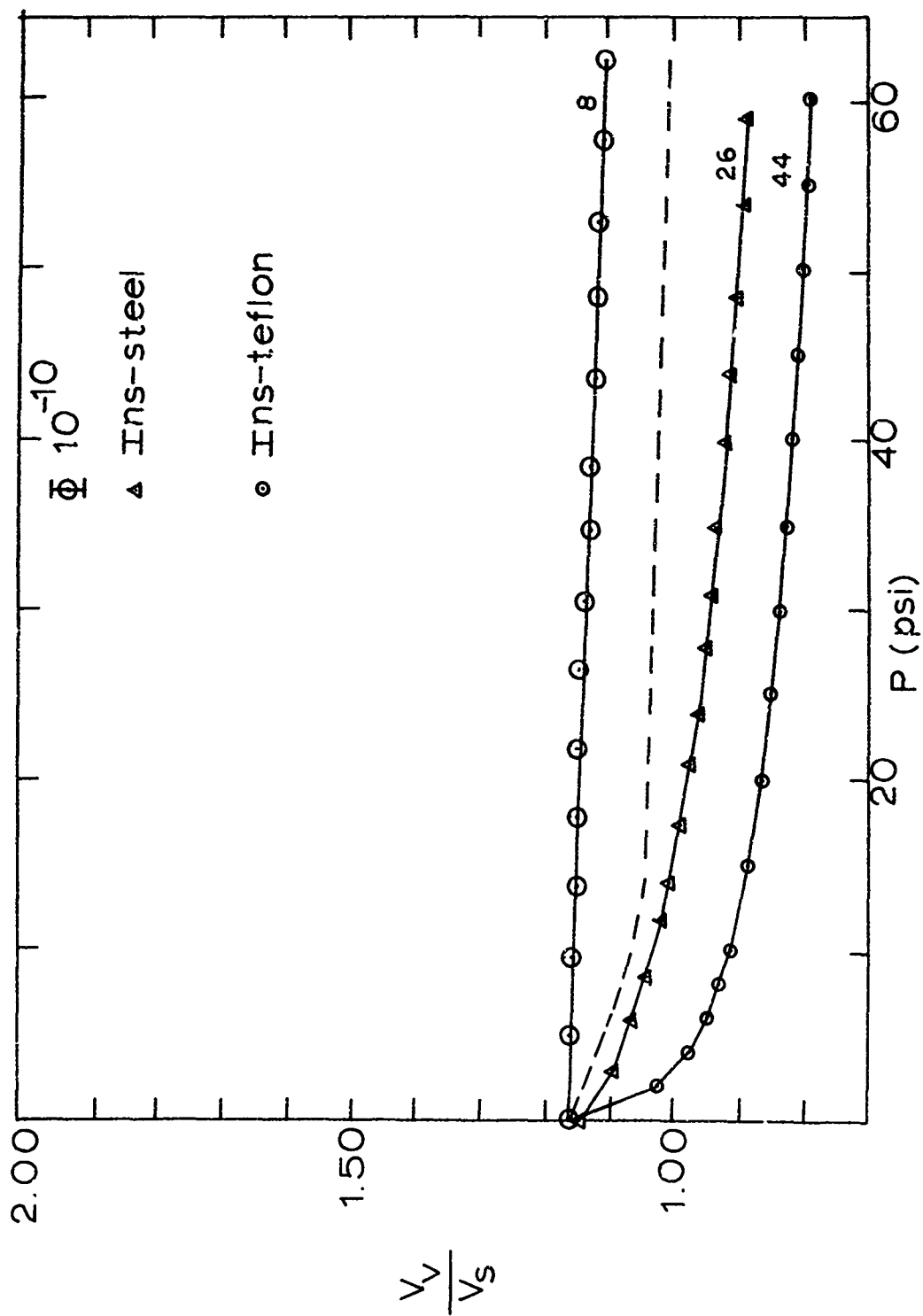


Fig.6 Data Runs Nos. 8, 26, 44

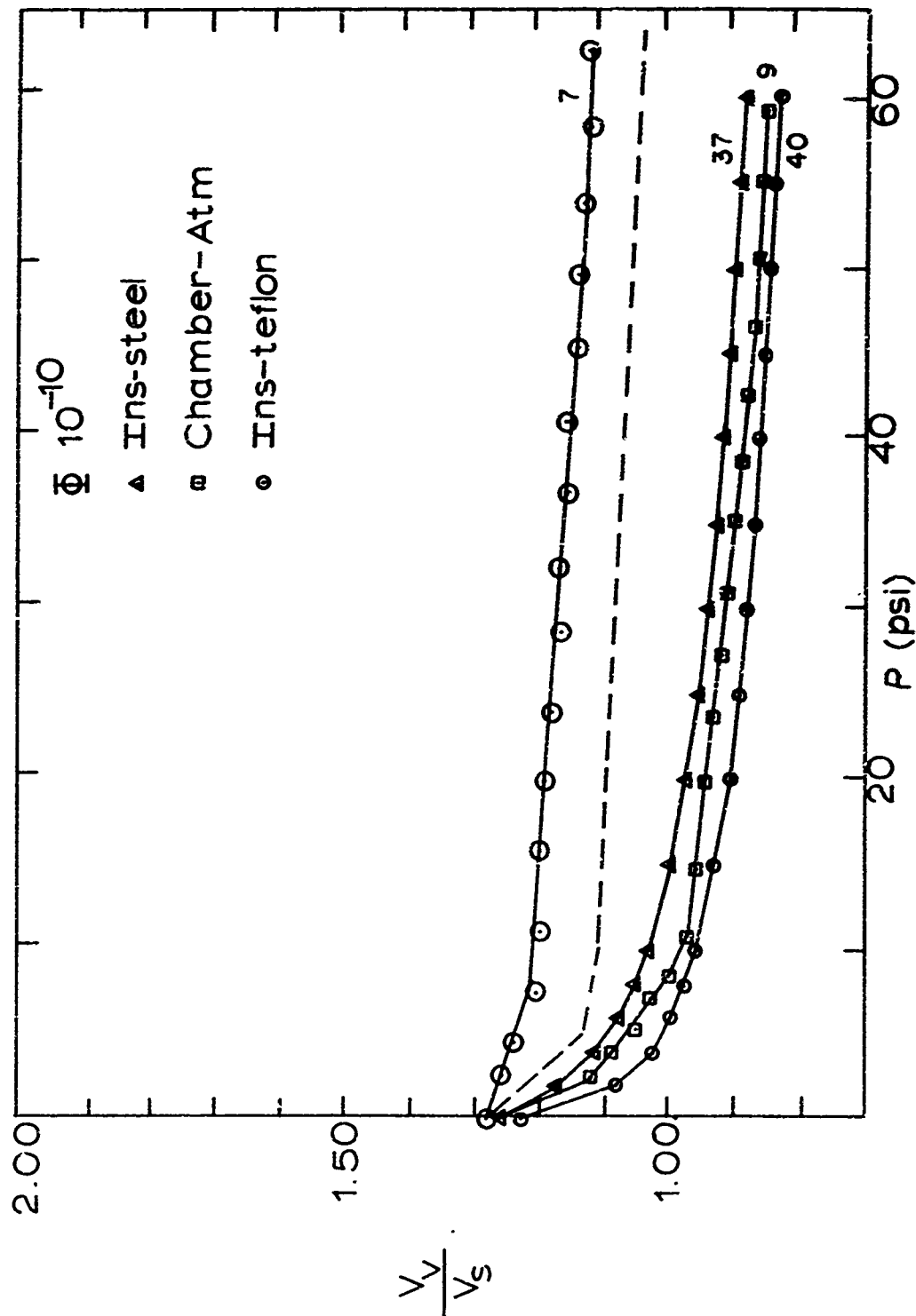


Fig. 7 Data Runs Nos 7, 37, 9, 40

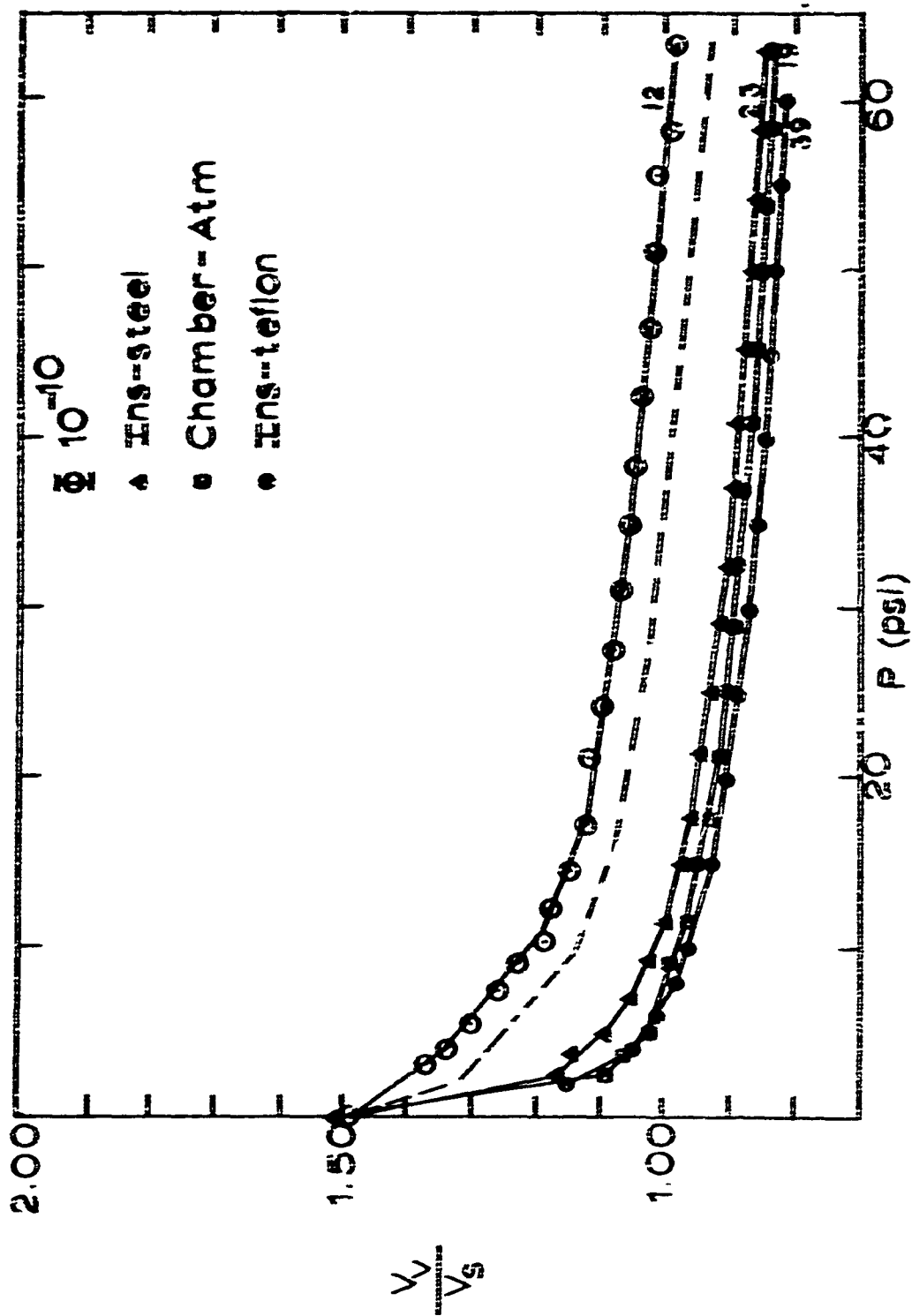


Fig.8 Data Runs Nos. 12, 23, 19, 39

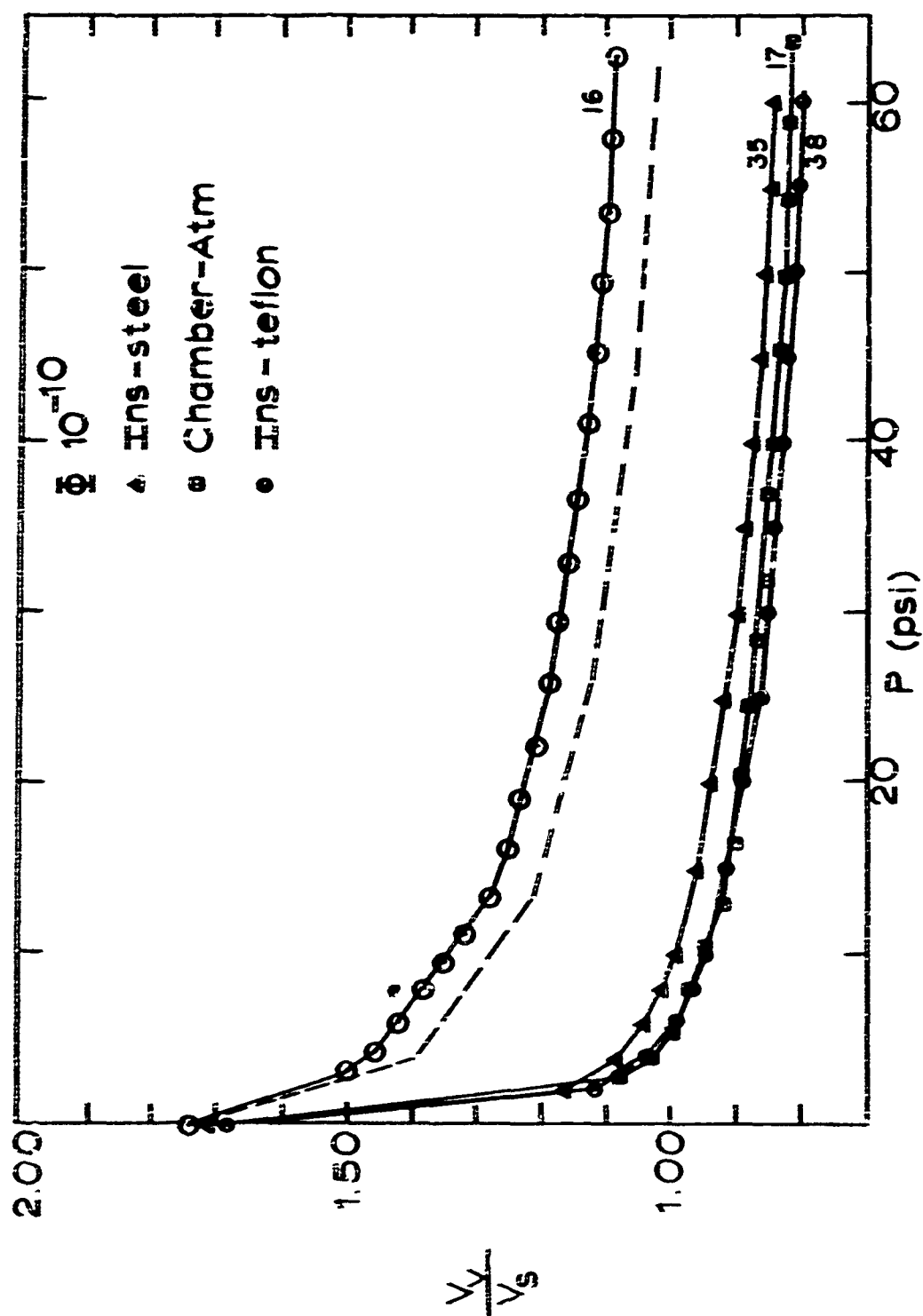


Fig. 9 Data Runs Nos 16, 35, 17, 38

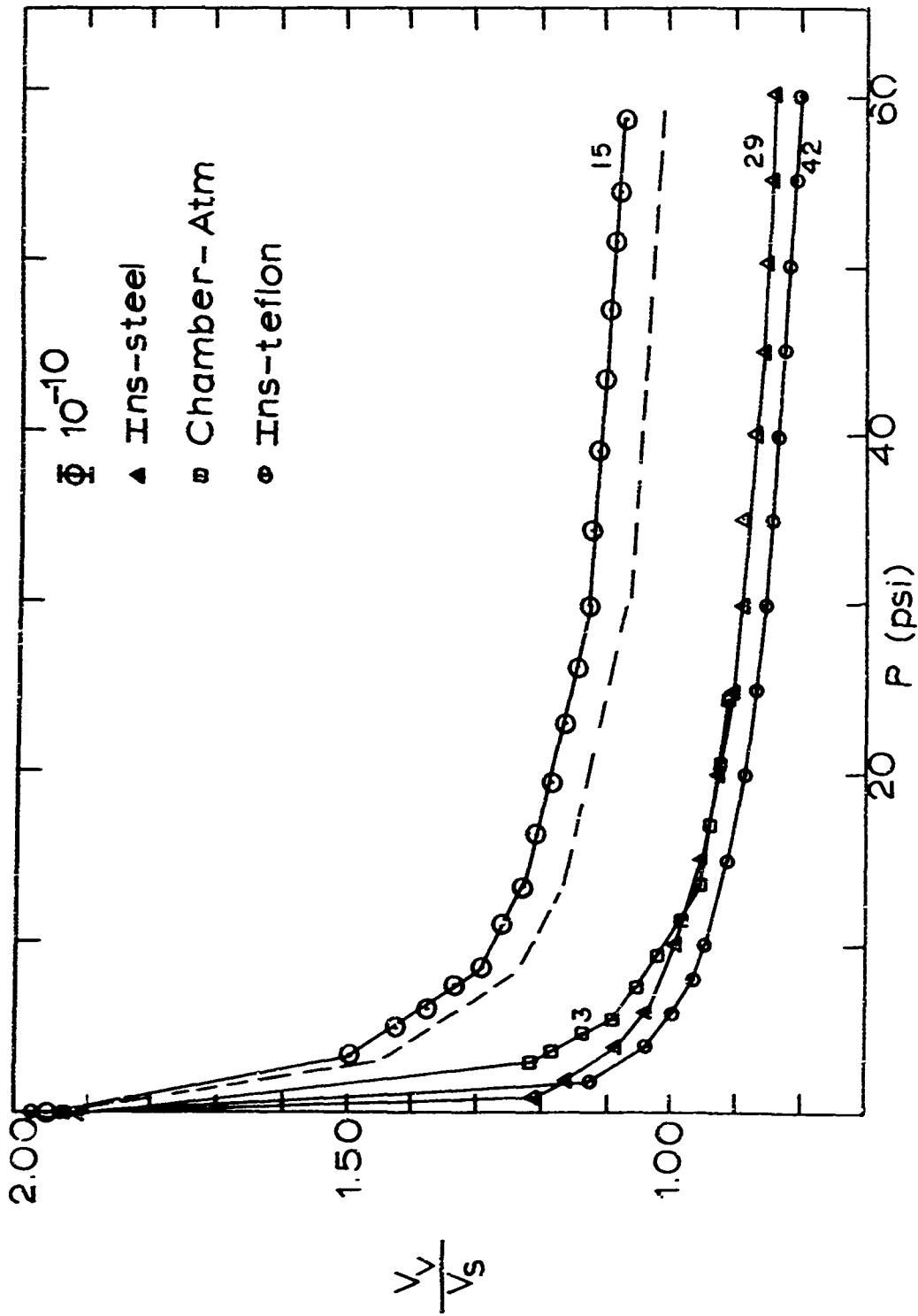


Fig.10 Data Runs Nos.15,29,3,42

tainer in all cases produced results that were within the error limits of the tests performed in the vacuum chamber at atmospheric pressures. This can be seen by examination of Figs. 7 through 10 which show that for tests in the steel container the lower error limit of the Instron test overlaps the upper error limit for the chamber test. Perhaps the weakest aspect of the experiment in the chamber is the lack of precision of the force measurement. The compatibility of the chamber and the Instron results in atmosphere can be interpreted one of two ways. Either the e-P curves are insensitive to a force variation of 10% or the actual measurement capability of the chamber system is better than + 10%. In either case, the results of the Instron test indicate that the e-P curves from the chamber tests are accurate descriptions of the response of the soil to one dimensional compression for the given loading geometry.

A cursory examination of the above mentioned figures indicates that the vacuum environment did have some effect. Before the size of this effect or its possible cause is discussed, an analysis of the forces at work in the sample should be made.

Discussion

As an external load is applied to the surface of a soil, certain internal reactions are created in the soil to oppose the application of that load. The degree to which each of these reactions participate is directly related to the compressibility of that soil. These internal re-

sponses may be broken down into a number of factors.

1. Elastic response of the soil grains. As the load is applied to the surface, the individual soil grains will undergo some elastic deformation. This deformation will be recovered when the load is removed and its apparent magnitude may be calculated from standard equations relating the mechanical properties of the grains to their deformation, such as is found in Yong and Warkentin, equation 8.6 (Ref 28). The actual contribution of this term is small in the tests conducted because the largest percentage of the volume change noted was irreversible and not due to an elastic deformation. As the initial void ratio decreased the size of the contribution of this term would increase; however, for the same initial void ratio, the elastic response of the grains should not be affected by a change in the environmental pressure. Consequently whatever the elastic response was at atmospheric pressure, it was the same at 10^{-10} Torr for a sample with the same initial void ratio. This term then cannot account for the observed differences between the atmospheric data and the 10^{-10} Torr data.

2. Electrostatic forces. Because of the small size of the grains tested it is possible that a buildup of electrostatic charges on the grains during preparation and handling could create forces that would have a significant effect on the resistance of the soil to a compressive load. Experimental work conducted by Kitchenier and Prosser (Ref

13:407) has shown that water vapor will dissipate this electrostatic charge. The relative humidity of the laboratory was 25-35% which would be sufficient to dissipate such an electrostatic charge. Consequently, if this force were present at all, its magnitude was of no relative significance for the atmospheric tests. For similar tests conducted in vacuum, the same authors indicate that the glow discharge from starting the ion pump will dissipate all electrostatic charge in the chamber (Ref 13). If the particles are not disturbed by handling or tumbling after the glow discharge of the pump, no further electrostatic charges can be built up. From these observations, it is concluded that electrostatic attraction or repulsion of individual soil grains was not a significant factor in either the atmospheric or vacuum tests.

3. Cohesive forces. These are attractive surface forces that act within the soil and contribute significantly to the resistance of the soil to an applied external load. The size of the cohesive force in a soil mass is dependent principally on the nature of the adsorbed film that exists on each individual grain (Ref 24:16). For this discussion they will be considered to be forces that arise from either Van der Waals attraction or chemical bonding at grain contacts. At atmospheric pressure the degree of chemical bonding that occurs is negligible because of the thickness of the adsorbed surface film. The Van der Waals forces however can constitute a sizeable attractive force on

the macroscopic scale (Ref 18:13) and probably are significant in a soil mass. As the sample is exposed to a vacuum, the adsorbed surface film is stripped away to some lesser extent depending on the degree of surface cleanliness of the soil grains. As a result of this change in surface film, the Van der Waals forces will increase and the possibility exists that atomic bonding may occur at isolated spots throughout the soil mass where two grains contact at asperities and the surface film has been completely removed. Ryan (Ref 19:234) found that silicates with air-formed surfaces at low loads in vacuum showed an increase in cohesion probably caused by Van der Waals forces. These same surfaces at higher loads showed a much greater increase in cohesion and this was attributed to the formation of much stronger chemical or atomic bonds. Consequently Ryan has found both factors to be at work in the soil mass. Vey and Nelson (Ref 25) have also found that cohesion increases in a vacuum and feel that the effect is primarily an increase in Van der Waals forces. Salisbury and Glaser found that the increase could be from either chemical bonds or Van der Waals forces (Ref 20:81, 94). Almost all of the investigators have found that cohesion does increase in a vacuum but as already shown they are not in agreement as to what is the cause of the increase. In any case, cohesion most likely was a factor in producing the differences between the atmospheric and vacuum test data for this experiment.

4. Friction forces. The frictional forces that are developed in the soil mass during the test are essentially of two kinds. First is the interparticle friction between individual soil grains and second is the frictional interaction of the soil mass with the boundaries of the container. The grain-grain friction is an inherent property of any granular mass and is simply the frictional resistance of the grains as they are subjected to forces in an attempt to move one grain relative to another. This frictional property will certainly change as the vacuum level is changed because of the change in the nature of the adsorbed surface film. The change in the internal frictional properties has been observed by several investigators to increase (Refs 25, 23, 9, 26). This phenomena was also involved in the tests conducted in this study and thus is a contributor to the observed differences seen between the atmospheric and vacuum test data. The other frictional phenomenon that is at work is the effect of changes in frictional forces at the container boundary on changes in calculated stiffness of the soil sample. The soil container and the tamper were designed so that physical contact between the two was not permitted. For the tests conducted the tamper was about 0.10 in. from the wall of the soil container. As the load was applied, frictional shear forces created between the soil and the wall reduced the effective pressure seen by the soil sample. Also the soil grains along the bottom of the container would have a tendency to move as the result of shear forces developed

in that region. These forces would develop because the soil grains would attempt to move out from under the applied load. If movement occurred, it would increase the void ratio of the soil in the region of the grain movement and thus the soil would not respond along the bottom of the container as it would in an ideal one dimensional compression test. These effects were created by the geometry of the test apparatus and were not a property of the soil. As the vacuum level increased, the frictional resistance at the boundaries increased and consequently the ability of the wall to carry a larger share of the load increased, and the resistance to shear on the bottom increased. These effects then would contribute to the observed differences between the atmospheric and vacuum test data.

In summary, of the forces at work in the soil mass opposing the application of an external compressive load, only three can account for the observed differences between the atmospheric and vacuum data. These are the cohesion of the soil, the interparticle friction, and the effects of the boundaries of the container. Of these three only the boundary effect is undesirable since it arises from the experimental apparatus and is not a natural response of the soil. If the effect of the boundary could be eliminated from the observations, then the observed difference could be related only to an increase in cohesion and interparticle friction. With the type of experiment that was conducted, it was not possible to separate or isolate the individual

effects of cohesion and interparticle friction. An attempt was made however to place limits on the boundary effect.

Boundary Effects

Although the boundary effects could not be eliminated either experimentally or theoretically, an attempt was made to determine an upper limit for the magnitude of their influence. Several tests were conducted on the Instron in atmosphere with several types of containers. Tests were run with a stainless steel container, a teflon container, and a teflon container with an aluminum foil bottom. These tests permitted changes in the frictional properties of the wall and the bottom and combinations of each to determine the degree and magnitude of the frictional resistance of the walls and the bottom of the container. Teflon was used because it has the lowest coefficient of friction of any known solid (Ref 3:113). Consequently the teflon container represented the lowest possible frictional response at the boundaries. The results of these test with the steel and the teflon containers are shown as the appropriate two curves on Figs. 6 through 10. The resulting e-P plot for the teflon container is always below the corresponding plot for the steel container. This is the anticipated result because of the reduced frictional response at the boundaries of the teflon container. The resulting plot for the aluminum foil bottom is not shown in these figures but it fell intermediate to the curves for the steel and teflon containers leading to the con-

clusion that in the teflon container without foil some movement of soil was occurring along the walls and on the bottom. It could not be determined if the same movement was occurring in the steel container but it was felt that it was. This possible movement of soil grains is a major deviation from the standard one dimensional test and has an effect on the results. Nevertheless since all conclusions are based on comparisons of test data, only when the boundary conditions differed from test to test would they affect the conclusions drawn. Frictional forces developed at the boundaries were different for tests in vacuum than for tests in air. Therefore, determination of the magnitude of the change in the frictional response of the boundary of the steel container between the air tests and the vacuum tests would permit conclusions to be drawn that were not functions of the container boundaries. The precise determination of that magnitude was not possible but an upper bound of its effect was found. The method used to determine this upper bound was rather indirect and is discussed at length in Appendix F. The result of this determination was to lower the vacuum compressibility curve to account for the increased frictional response of the boundaries under vacuum. This lower limit on the vacuum compressibility curve is shown in Figs. 6 through 10 as a dashed line. For samples of the same initial void ratio the difference between this curve and the e - P curve for a sample tested in air can be attributed to changes in internal friction and soil cohesion.

Results

Figs. 11 and 12 indicate the dependency of the volume compressibility on the initial void ratio. These figures have taken two values of final loads of 40 and 60 psi, respectively, and an initial load of 0 psi, and have plotted the variation of M_v with e_i . Each data point on these plots represents an e-P curve using the steel container. As the initial void ratio increases from 1.1 to 2.0 the coefficient of volume compressibility, M_v , increases in almost a linear fashion. Even though the increase in M_v is nearly linear, it does appear to level off at an e_i near 1.90. Tests at values of e_i larger than 2.00 were not made so that this tendency to level off could not precisely be determined. The dependence of M_v on e_i does not appear to be a function of the ambient pressure level since the same general shape and slope of curves was obtained for tests performed at both levels of ambient pressure. These results are in agreement with Hendron (Ref 10:58) and Schultz and Moussa (Ref 21:336). This direct dependency of M_v on e_i is the type of dependency that would be expected. The higher the initial void ratio is the looser the packing configuration of the soil mass will be. This loose state represents an unstable configuration and the application of an external load tends to force the soil grains to a more stable and denser configuration (Ref 14:151). In conclusion, the variation of M_v with e_i is almost directly linear with M_v but appears to be leveling off as e_i approaches 2.0.

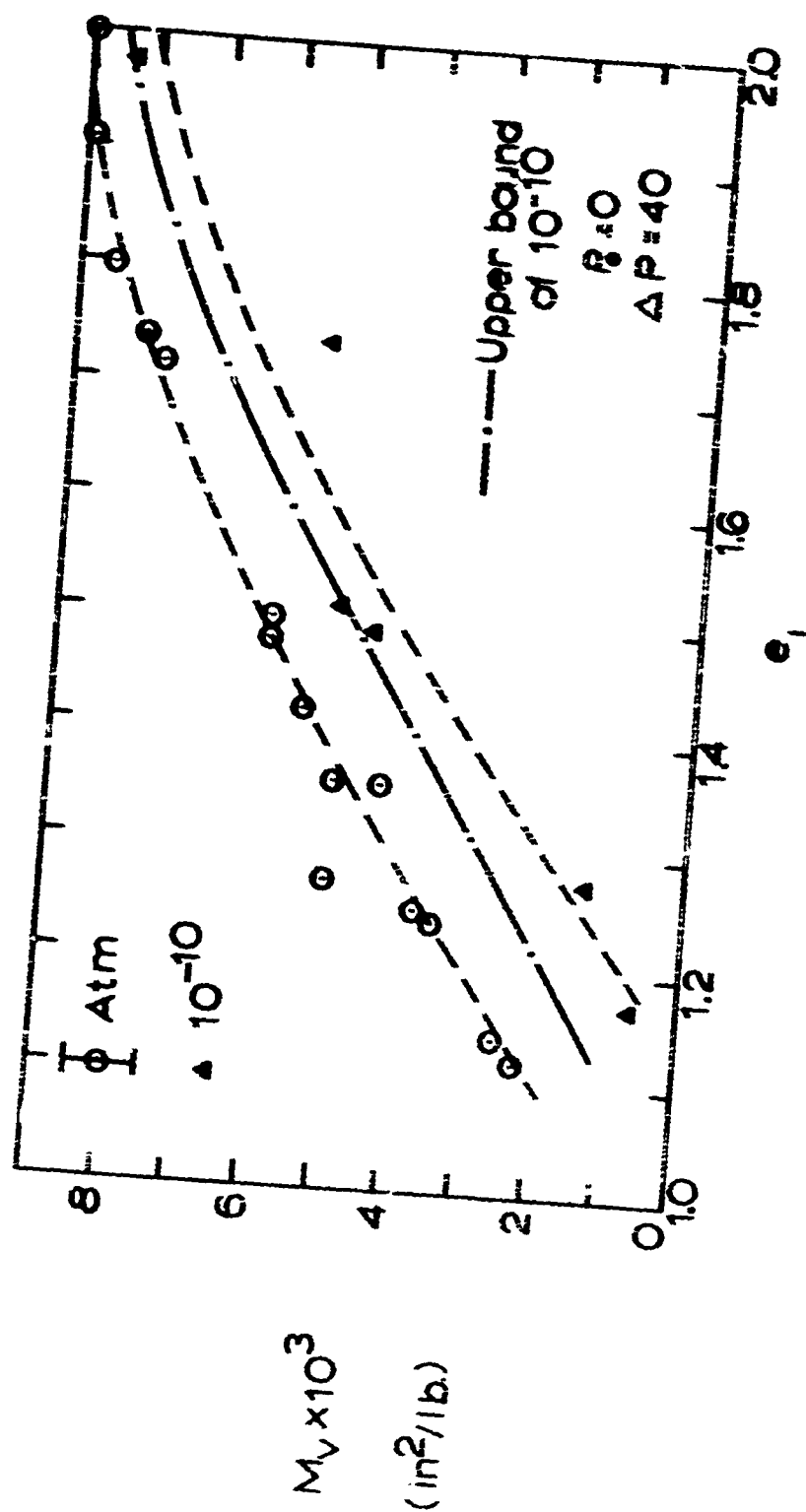


Fig 11 M_v vs e_1

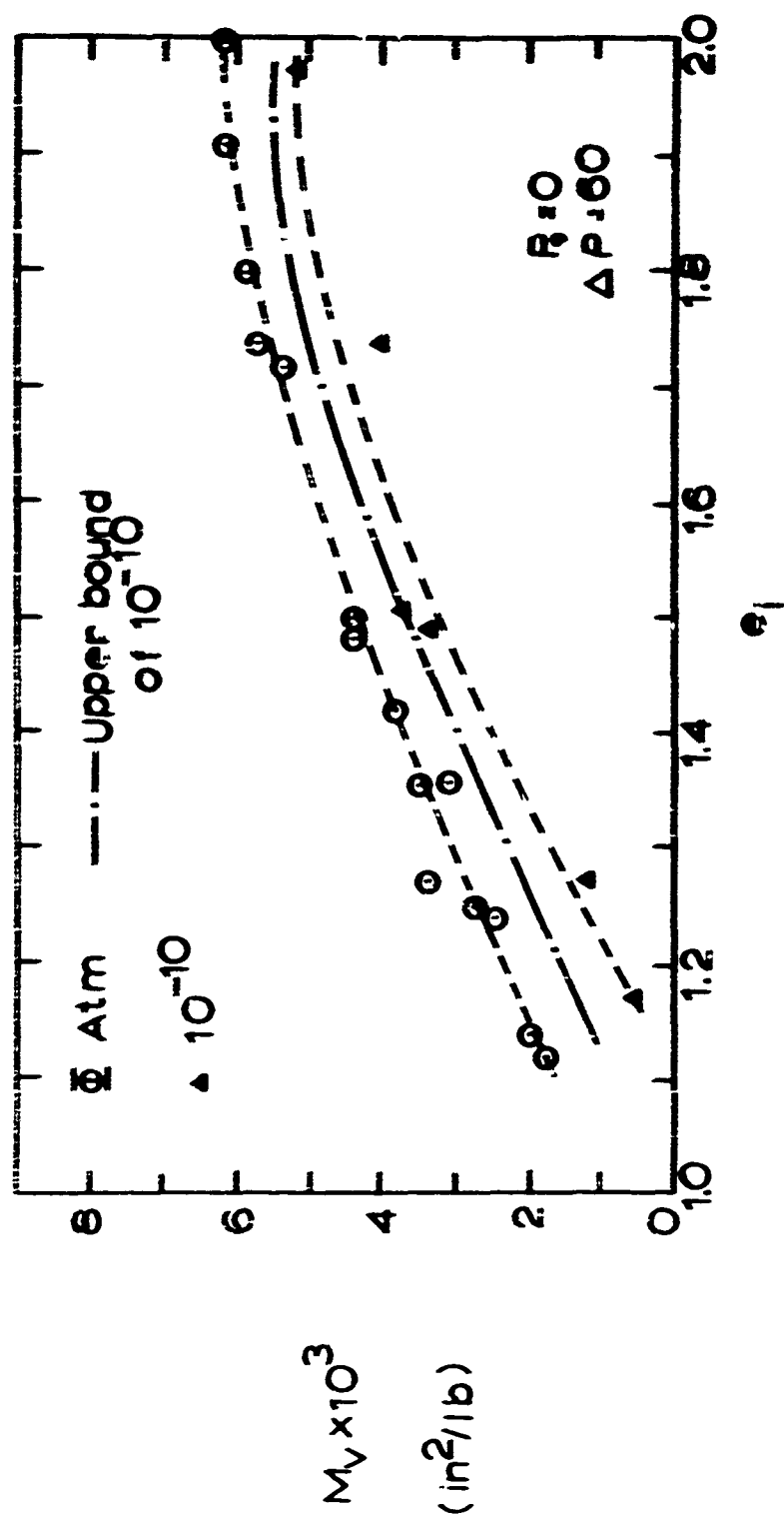


Fig.12 M_v vs e_l

The dependency of M_v on the ambient pressure is illustrated by Figs. 6 through 10 and Figs. 11 and 12. The data of Fig. 9 is representative of all of the data taken from the experiments. These four tests plotted in Fig. 9 were all for soil samples of an initial void ratio near 1.70. Attention is drawn to the two tests performed in the vacuum chamber at 10^{-10} Torr and atmospheric pressure. The only parameter that was varied between these two tests was the ambient pressure level; but when the compressibility tests were performed, the resulting e - P curves were widely separated. This separation is shown in Fig. 9. The curves start at the same point, the void ratios drop off at decreasing rates until the applied load reaches the 15 to 20 psi range, and then the void ratios tend to decrease with little change in rate up to a load of 60 psi. For the 10^{-10} Torr plot the total decrease in the void ratio was significantly less than for the atmospheric plot. The dependence of M_v on ambient pressure is also shown in Figs. 11 and 12 by the fact that data points for atmospheric and vacuum tests fall on two different lines. The comparable e - P curves of Fig. 9 indicate that the compressibility decreases as the ambient pressure decreases. This is true because the soil becomes stiffer in the vacuum and is better able to resist an applied load and thus it is compressed less. This decrease in compressibility can be seen in Figs. 11 and 12 by the lower position of the vacuum data on the graph. The decrease in M_v with an ambient

pressure change from atmospheric to 10^{-10} Torr does not appear to vary significantly with e_i . In Fig. 12 M_v between atmospheric and 10^{-10} Torr tests decreased approximately 0.0015 in $^2/\text{lb}$ for an $e_i = 1.20$ and approximately 0.0010 in $^2/\text{lb}$ for an $e_i = 2.00$. This represents a percent decrease in M_v of 75% for $e_i = 1.20$ and 16% for $e_i = 2.00$. The explanation for this dependency of M_v on the ambient pressure level involves a complex interaction of several forces. The effect, however, seems to depend more on the surface cleanliness of the grains than on the absolute vacuum level although these two are interrelated. This was evident from the results of Data Run #7. During the pumpdown phase of this test a leak developed which prohibited the attainment of a 10^{-10} Torr vacuum although the system was baked out for 26 hours and the sample was baked individually for two hours. Under these baking conditions the sample was as clean or cleaner than the other samples tested at 10^{-10} Torr but the vacuum level was in the 10^{-8} Torr range. The results of this test indicate that the soil behaved the same as the soil in the other 10^{-10} Torr tests and not at all like other soil samples tested at 10^{-8} Torr. The other 10^{-8} Torr tests were performed without any bakeout on the system. Therefore the surface cleanliness that resulted was only that due to the stripping away of the surface adsorbed film by the creation of the vacuum at room temperature. The effect of this vacuum level on M_v , as compared to atm. pheric tests, was not signi-

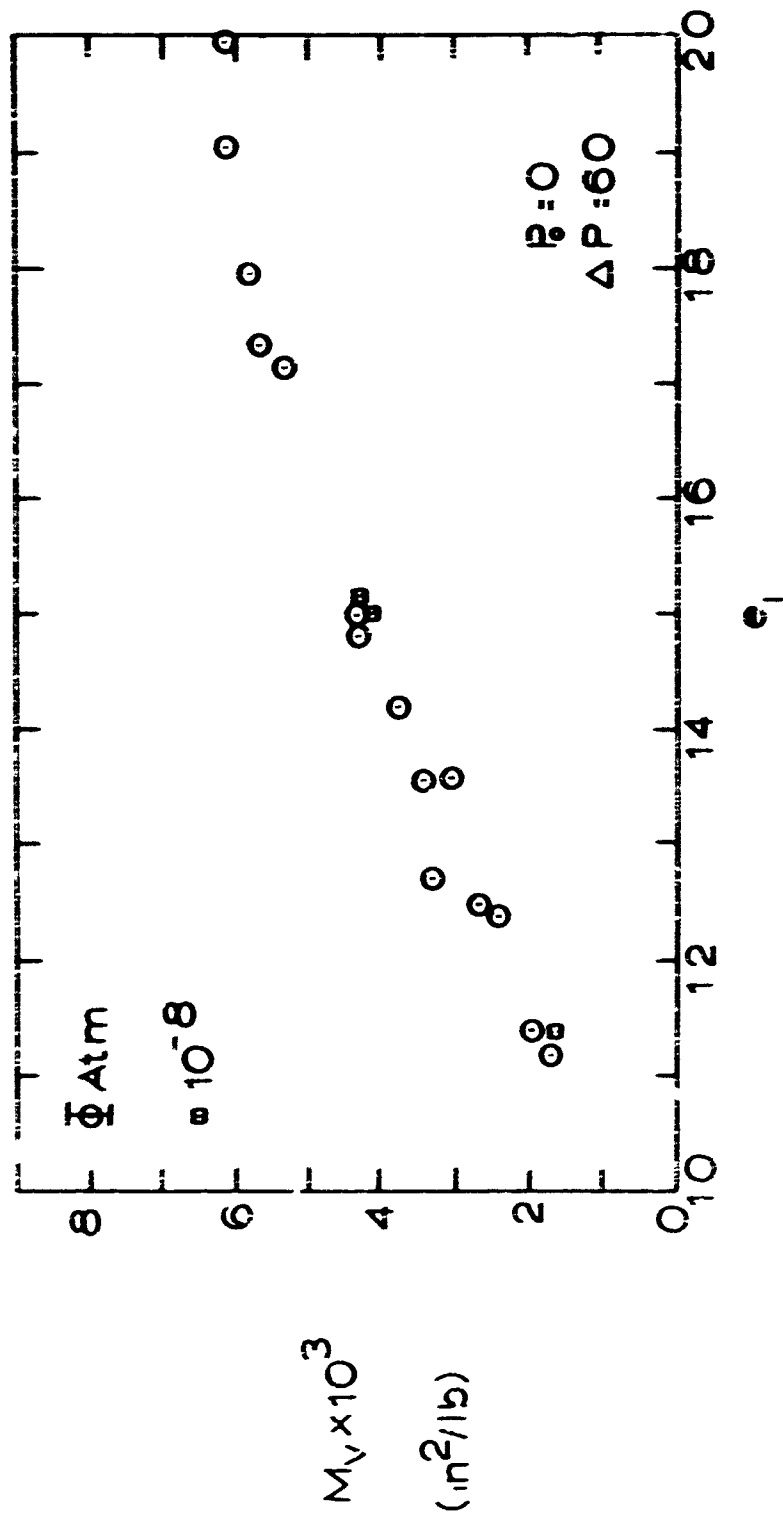


Fig.13 M_V vs. e_1

ificant. Examination of Fig. 12 which shows the variation of M_v on e_i for ambient pressures of atmosphere and 10^{-8} Torr, indicates that the 10^{-8} Torr data falls somewhat below the atmospheric data but the differences involved are within the experimental error. Thus the effect of a 10^{-8} Torr vacuum without bakeout on the compressibility of the soil was found to be non-existent; or if it did exist, it was below the sensitivity of the instrumentation. These results are consistent with the work of Waters who worked in a 10^{-8} Torr environment with just a 150°C bakeout. He noted no effect on the shear strength of amorphous soid (Ref 27:101). Because of these early results in the 10^{-8} Torr tests, no further tests were performed under these conditions. In conclusion it seems that the most important parameter affecting the compressibility was the degree of surface cleanliness of the individual particles. The two internal forces that are most dependent on the degree of surface cleanliness are the inter-particle friction and the soil cohesion. It was apparently an increase in these two forces that caused the observed decrease in M_v . It could not be determined if the increased cohesion was the result of an increase in Van der Waals forces or if some localized atomic bonding had occurred. Also separation of the effects of internal friction and cohesion could not be made.

The frictional effects of the boundaries appeared to increase in magnitude as the initial void ratio decreased. On Figs. 6 through 10

the separation of the two curves for the tests on the Instron in the steel and the teflon containers gives a qualitative measure of the frictional response at the boundaries. Comparing these curves for an $e_i = 1.15$, Fig. 6, and $e_i = 1.70$, Fig. 9, the separation for the smaller value of e_i is substantially the larger of the two. This would imply that the change of the frictional characteristics of the boundary for the samples with the lower initial void ratios had a more significant effect on the state of stress in the soil. The apparent explanation for this is that the more dense samples were able to transfer more of the vertical pressure to the side walls closer to the top. As the load was applied, some pressure was distributed from the surface of the soil to the walls at some depth below the surface. In the denser samples, this load reached higher up on the wall and as a result the wall carried more of the applied load and reduced the effective pressure on the soil. An alternative explanation for the observed increase in frictional effects at boundaries with decreased void ratio can be offered. There may have been a greater tendency in the denser samples for the soil to move adjacent to the container boundaries. As the initial void ratio increased, it was apparently easier for the soil grains to move relative to each other than to shear along the boundaries. Consequently there was greater movement along the boundaries of the container for the more dense samples. Either or both of these alternative mechanisms could be operative.

ative in the soil mass and could have produced the observed results. Further examination of the Instron tests in steel and in teflon containers in Figs. 6 through 10 indicates the frictional effect seems to be larger, percentagewise, up to loads of 20 psi. At loads of greater than 20 psi the effect of the friction seemed to level off at some constant per cent of the applied load. This corresponds with the results of Leonards and Girault who found that an appreciable amount of side friction develops in the initial compression stage and thereafter continues to increase at a decreasing rate (Ref 15:216). Their tests were performed with sand in a one-dimensional consolidometer. Frictional effects are present in almost any form of the one dimensional compression test. They must be understood before test results can be interpreted and then applied to predict response of soil to loading in the field.

The possible modes of failure of a soil in a vacuum environment are essentially two. The soil can either fail in shear or in compression. The shear failure will result in the plastic flow of soil from under the load to regions of less applied pressure while the compressive failure will be common to loose material where the soil will deform under the load without any plastic flow but with the development of a straight-walled failure area in the soil (Ref 9:3). The soil that was tested in this investigation tended to fail in both shear and compression; however, the failure was predominantly a

compressive one. Examination of Fig. 14, the soil sample before testing, and Fig. 15, the soil sample after testing, indicates the compressive mode of failure. These figures are for an atmospheric test.

Some plastic behavior was noticed in that the soil on the surface was bulged up at the end of a test. This occurred only for the tests of the material of the lower initial void ratios. This bulging was extremely small and was visually estimated to be less than 0.01 in. measured relative to the top of the container wall. For the material of an initial void ratio greater than 1.50, this bulging was not noticed but the failure appeared to be purely compressive although there may have been some shear failure in the soil mass. The fact that the straight wall failure mode was observed in all tests under all conditions established that the compressive mode was the dominant failure mechanism.



Fig. 14 Soil Sample before Loading



Fig. 15 Soil Sample after Loading

IV. Conclusions and Recommendations

Conclusions

The following conclusions were drawn from the experimental work performed:

1. The compressibility of the rock powders increased as the initial void ratio increased. This increase was essentially linear until it appeared to reach an upper limit at approximately an initial void ratio of 1.90.

2. The compressibility of the powders was not a function of ambient pressure between atmospheric pressure and 10^{-8} Torr unless some means of increasing the degree of surface cleanliness was imposed.

3. An increase in compressibility of powders is observed in experiments between ambient pressures of 10^{-10} Torr and atmospheric. This change was apparently induced by creating a higher degree of a surface cleanliness on each soil grain, which in turn had two important results;

- a. An increase in the grain-grain frictional resistance.
- b. An increase in the soil cohesion from either an increase in the Van der Waals forces, or isolated chemical bonding, or both.

The total decrease in the coefficient of volume compressibility was

essentially constant so that the per cent decrease in M_v from an environment of air to 10^{-10} Torr was 75% for $e_i = 1.20$ to 16% for $e_i = 2.00$. The 10^{-10} Torr environment increased the stiffness of the soil so that it could withstand larger applied loads for the same volume change as in air.

4. The failure mode of the soil was in both shear and compression with the compressive failure dominant. For an initial void ratio greater than 1.50, no shear failure was observed.

Recommendations

There are a number of recommendations for continued study in the area of this analysis.

1. As the vacuum results were accumulated, it became apparent that there was insufficient information as to how these powders behaved in an atmospheric environment. A much more intelligent approach to the problem could have been taken if more were known on the atmospheric behavior of these powders. Consequently the most immediate recommendation would be to conduct extensive testing of the powders under atmospheric conditions to determine their mode of behavior. Specifically tests could be run insuring the condition of no lateral strain, the geometry of the container and the tamper could be varied, the soil should be tested to higher values of applied loads, the effects of the frictional properties of the container need to be isolated, and finally, loading, unloading, and reloading cycles

could be run to determine the capacity of the material to store energy.

2. A better design of a force measuring device would be desirable for the vacuum chamber apparatus. This was perhaps the least precise feature of the vacuum testing although it was substantiated by the results of the tests on the Instron.

3. No effort was made to determine the effect of varying degrees of exposure time to the vacuum on the compressibility of the sample. This would help determine the degree of surface cleanliness that was obtained initially as the vacuum was created and how much additional gain would exist as the exposure to the vacuum lengthened.

The establishment of any type of permanent structure on the lunar surface will require an intimate knowledge of the settlement characteristics of the material on and near the surface. If such a knowledge is to be obtained, a better understanding of the behavior of granular material compressed in a vacuum environment will be needed.

Bibliography

1. Bishop, A.W. and Henkel, D.J. The Measurement of Soil Properties in the Triaxial Test (2nd Ed.). London: Edward Arnold, 1957.
2. Bowers, R.C., et al. "Frictional Properties of Plastics." Modern Plastics. 31 No. 6: pp 131-144 (Feb 1954).
3. Brenner, Walter, et al. High Temperature Plastics. New York: Reinhold Publishing Corporation, 1962.
4. Christensen, E.M., et al. "Lunar Surface Mechanical Properties" Surveyor V Mission Report Part II, Science Results. NASA Tech Rep No. 32-1244. Pasadena, Calif.: Jet Propulsion Laboratory, California Institute of Technology, Nov 1961.
5. Fegelson, David E. "Simulated Lunar Rocks" Proceedings of the Working Group on Extraterrestrial Resources: NASA SP-177. Washington, D.C.: National Aeronautics and Space Administration, 1968.
6. Franzgrote, Ernest J., et al. "Chemical Analysis of the Moon at the Surveyor VII Landing Site: Preliminary Results. " Surveyor VII Mission Report Part II, Science Results. NASA Tech Rept No. 32-1264. Pasadena, Calif.: Jet Propulsion Laboratory, California Institute of Technology, March 1968.
7. Gilboy, G. "The Compressibility of Sand-Mica Mixtures." Proceedings, ASCE, 54: pp 555-568 (1928).
8. Green, J. "Selection of Rock Standards for Lunar Research." Annals of the New York Academy of Sciences. 123: 1123-1147 (July 15, 1965).
9. Halajian, J.D. Soil Behavior in a Low and Ultrahigh Vacuum. Grumman Research Dept. Report RE-197J. Bethpage, New York: Grumman Aircraft Engineering Corporation, Dec 1964.
10. Hendron, A.J. The Behavior of Sand in One Dimensional Compression. PhD Thesis: University of Illinois, Urbana, 1963
11. Higdon, Archie, et al. Mechanics of Materials. New York: John Wiley & Sons, Inc., 1960.

12. Houwink, G. and Salomon, G. Adhesion and Adhesives (2nd Ed).
New York: Elsevier Publishing Co., 1965
13. Kitchner, J.A. and Prosser, A.P. "Direct Measurement of the
Long-Range Van Der Waals Forces." Proceedings of the Roy-
al Society of London. A242: 403-409 (Nov 19, 1957).
14. Ko, Hoa-Yin and Scott, R.F. "Deformation of Sand in Hydro-
static Compression." Jour. of Soil Mechanics and Foundations
Division, Proceed. ASCE, Vol 93, No. SM3: (May 1967)
15. Leonards, G.A. and Girault, P. "A Study of the One-Dimension-
al Consolidation Test." Proceedings, 5th International Confer-
ence on Soil Mechanics, 1: pp 123-127 (1961).
16. Majumder, D.K. and LaFrance, G.G. "Stress-Strain Relation-
ships in Triaxial and Consolidation Tests." Civil Engineering:
pg 68 (Jul 66).
17. Mohr, G. and Karafiath, L.L. Determination of the Coefficient
of Friction Between Metals and Nonmetals in Ultrahigh Vacuum.
Grumman Research Dept. Report RE-311. Bethpage, New York:
Grumman Aircraft Engineering Corporation, Dec 1967.
18. Ottewill, R.H. "Attractive Forces Between Surfaces" in As-
pects of Adhesion 2. Cleveland, Ohio: CRC Press, 1966.
19. Ryan, J.A. and Baker, M.B. "Adhesional Behavior of Air and
Ultrahigh Vacuum Formed Silicate Surfaces in Relation to the
Moon." in Adhesion or Cold Welding of Materials in Space
Environments. Philadelphia, Pa.: American Society for Tes-
ting and Materials, 1967.
20. Salisbury, J.W. and Glaser, P.G. Studies of the Characteristics
of Probable Lunar Surface Materials. AFCRL-64-970, Special
Reports, No. 20. Bedford, Mass.: Air Force Cambridge Re-
search Laboratories, Jan 1964.
21. Schultz, E. and Moussa, A. "Factors Affecting the Compres-
sibility of Sand." Proceedings, 5th International Conference on
Soil Mechanics, 1: pp 335-340 (1961).
22. Scott, Ronald F. Principles of Soil Mechanics. Reading, Mass.:
Addison-Wesley Publishing Company, 1963.
23. Sjaastad, Gerald D. The Effect of Vacuum on the Shearing Re-

sistance of Ideal Granular Systems. PhD Thesis: Princeton University, 1963

24. Terzaghi, Karl and Peck, Ralph B. Soil Mechanics in Engineering Practice. New York: John Wiley & Sons, Inc., 1948.
25. Vey, E. and Nelson, J.D. "Relative Cleanliness as a Measure of Lunar Soil Strength." Journal of Geophysical Research. 73, #12: pp 3747-3764 (15 Jun 1968).
26. Vey, E. and Nelson, J.D. Studies of Lunar Soil Mechanics. NASA Contract No. NASr-65(02), IITRI Project No. M272 (Phase III), May 1966.
27. Waters, Ronald H. The Effect of Porosity on Shearing Resistance and Thermal Conductivity for Amorphous Soils in Vacuum. PhD Thesis: Texas A & M, Jan 1967.
28. Yong, R. and Warkentin, B. Introduction to Soil Behavior. New York: The Macmillan Co., 1966.

Appendix A

Comminution of Basalt

The process of preparing the powder used during the test consisted of comminuting basaltic rocks in a shaker box with an outside diameter of 4 in. and made of 4140 steel which had been toughened and hardened. The box is shown in Fig. 16.

Approximately 200 grams of one inch or less rocks were placed between the two moveable rings inside the walls of the box. Then a neoprene gasket was placed over the top, the lid was bolted down, and the inside of the box was flushed with argon by two gas ports in the top of the lid. The shaker box was then bolted to a one dimensional, sinusoidal input shake table and vibrated at 12.5 ± 0.5 cps with a displacement of 0.30 ± 0.02 inches. This input produced an average acceleration of about 2.5 g's. Approximately one hour of shaking time produced about 40 grams of powder passing a #250 sieve.

The powders were derived from the outer surfaces of the rocks. Since the rocks were baked at 600°C for 45 hours prior to grinding and then stored in a sealed container with a dessicated atmosphere, the outer surfaces of the rocks were essentially moisture free. Consequently, the moisture in the resulting powders was kept to a minimum.

A hydrometer analysis of the powders was performed and the results are shown as Fig. 17. Some photomicrographs of the grains

GSF/MC/69-4

were taken by the Air Force Materials Lab, Wright-Patterson AFB,
and two of these are shown as Fig. 18.



Fig. 16 Shaker Box

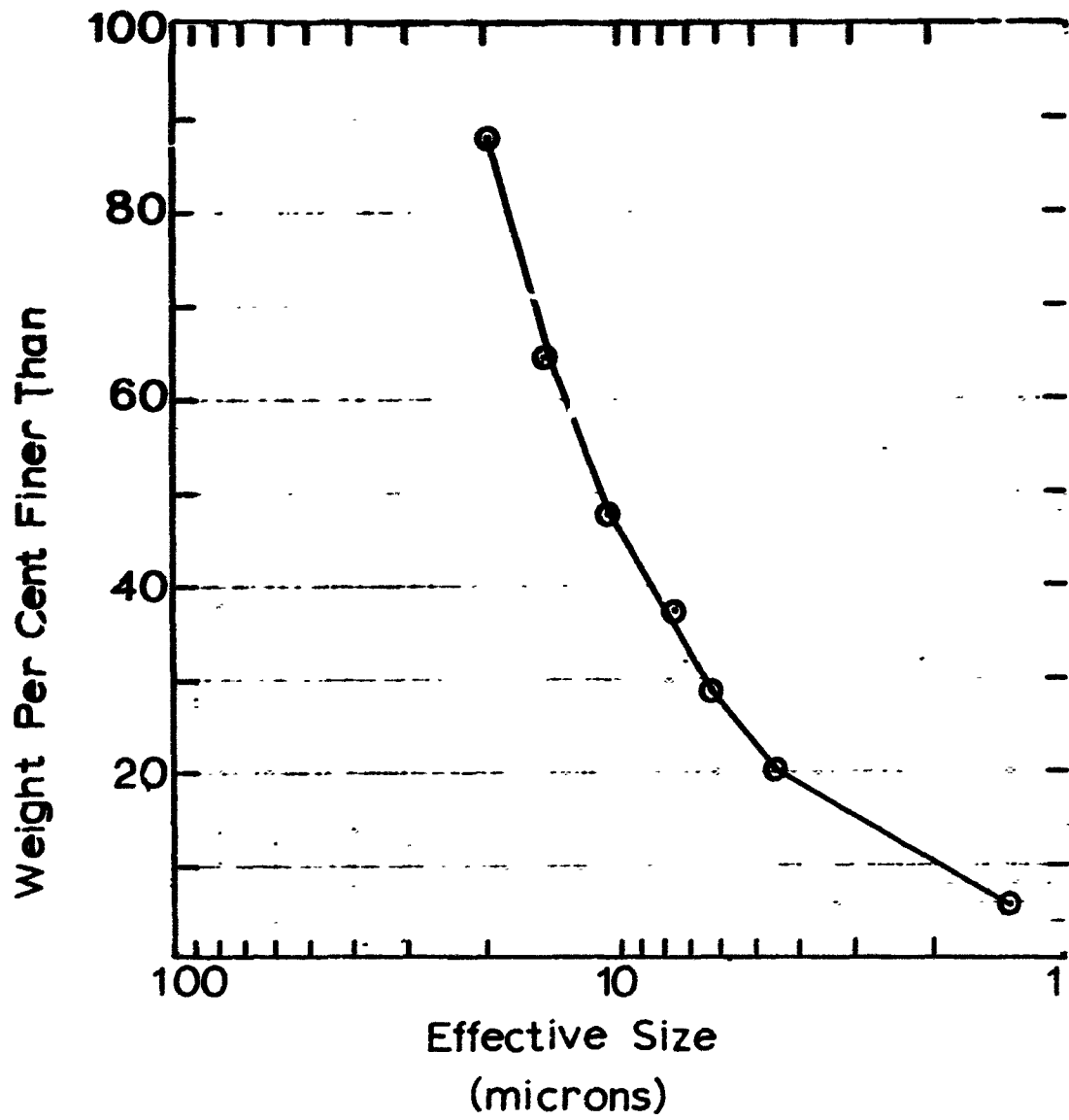


Fig.17 Grain Size Analysis



(a)



(b)

Fig. 18 Photomicrographs of the Soil Grains

Appendix B

Mineralogy of the Rocks Tested

The rocks that were comminuted to produce the powders that were tested were furnished by Dr. Thomas Atcheson of the U.S. Bureau of Mines, Twin Cities Mining Research Center. These rocks were selected because they are one of Green's standards for lunar research (Ref 8) and also because their composition closely approximates the results of the alpha scattering experiments of Surveyor V, VI, and VII. A comparison of the results of Surveyor V, VI, VII, and Green's standards are given in Appendix E. The information given below was compiled by the Bureau of Mines and was taken from Fongelson (Ref 5:80-81).

Content

Plagioclase (39 %) $\text{NaAlSi}_3\text{O}_8$ - $\text{CaAl}_2\text{Si}_2\text{O}_8$

Two types: Largest grain size approximately 0.15

mm x 0.03 mm

Smallest grain size approximately

0.10mm x 0.025mm

Olivine (10.5%) Fe_2SiO_4 ; Mg_2SiO_4

Average grain size approximately 0.04mm in diameter

Augite (10.5%) $(\text{Ca}, \text{Mg}, \text{Fe}^{+2}, \text{Ti}, \text{Al})_2(\text{Si}, \text{Al})_2\text{O}_6$

GSF/MC/60-4

Average grain size approximately 6.6mm in diameter

Plagioclase microlites (12%)

Glass (12%)

Magnetite and ilmenite (8%)

Chlorite (4%)

Quartz (1%)

Others (less than 2%)

Appendix C

Analysis of Force Measuring Device

Description

The force measuring device consists of a system of stainless steel arms, levers, and rods which was treated as a stiff spring. The overall spring constant of the system was determined and the system was calibrated by comparison with the force as determined by a pressure transducer. Initially an attempt was made to find a transducer or load cell that was commercially available that would serve the intended purpose. The specifications for this device were sensitivity on the 0-50 lb. range, capable of operation in an ultrahigh vacuum, unaffected by exposure temperatures to 200° C, and retention of its sensitivity and accuracy after repeated exposure to these environmental conditions. No such product was found. Pressure transducers were eliminated because their output signal is a change in capacitance and that type of signal would be lost when transmitted through the chamber wall on passing through two uninsulated wires. Load cells that could meet the specifications could not be found.

The spring system is shown in Fig. 19. The linear motion feed-through of the vacuum chamber, as shown in Fig. 20, was capable of a total horizontal travel of 1 in. The drive mechanism consists of a knob permitting 0.1 in. of travel per revolution. A digital counter

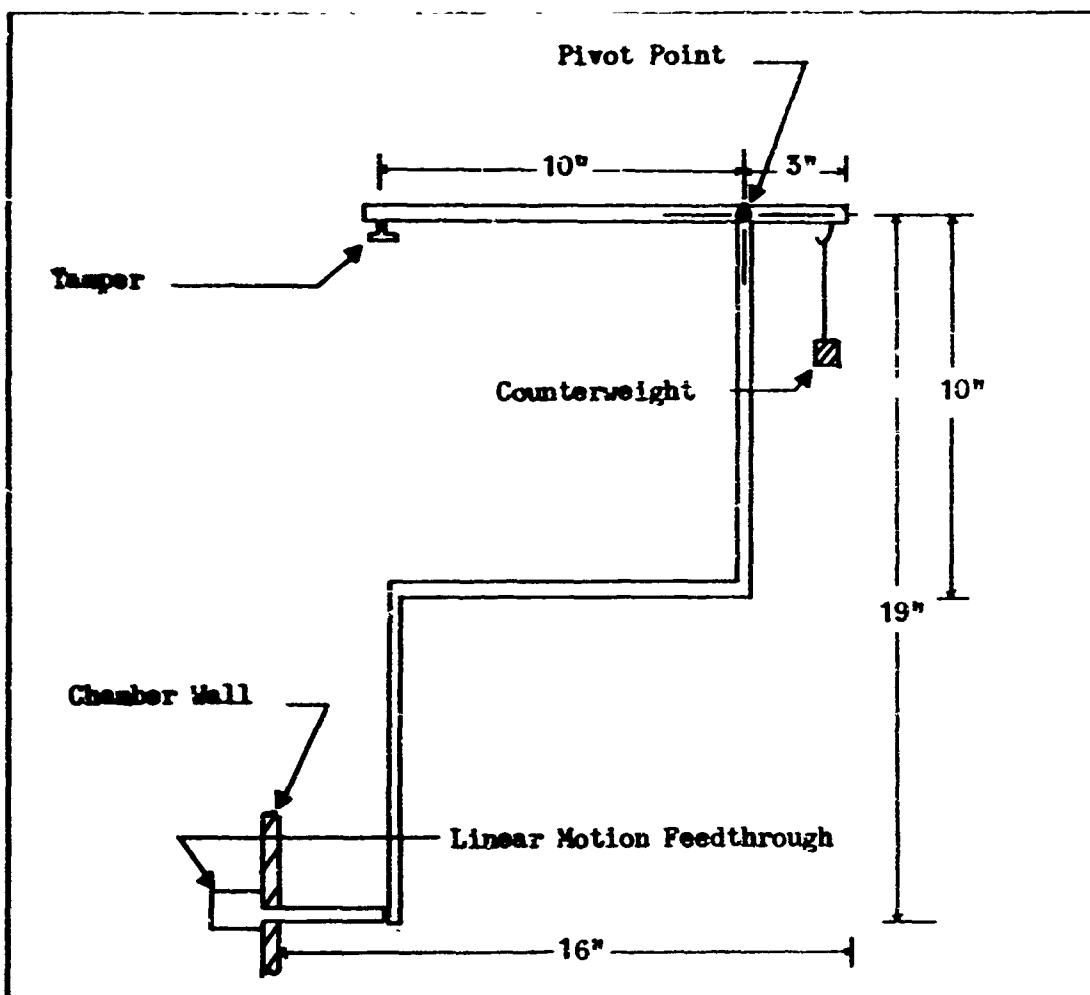


Fig. 19 Schematic of Linear Motion Feedthrough

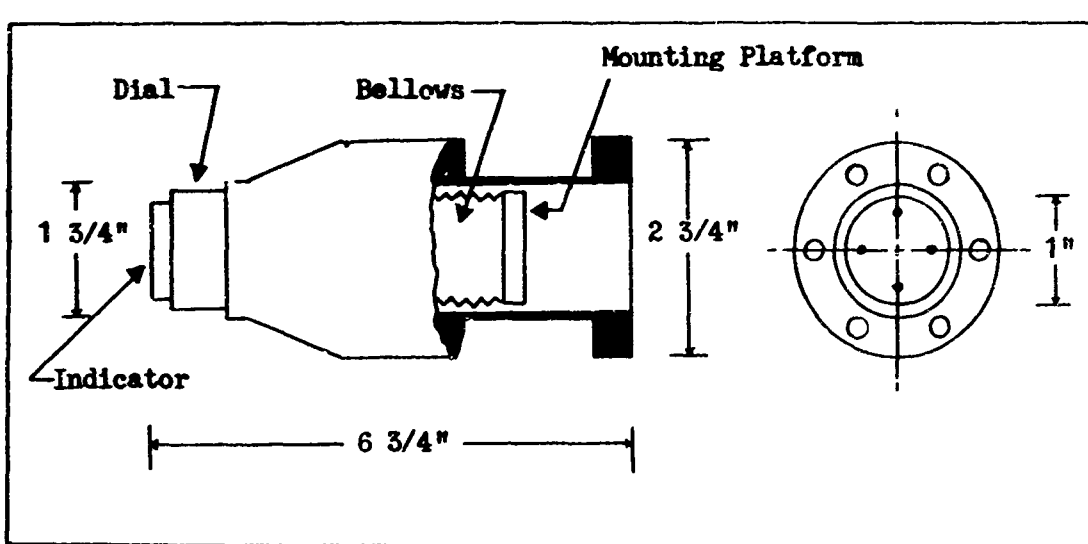


Fig. 20 Detail of Linear Motion Feedthrough

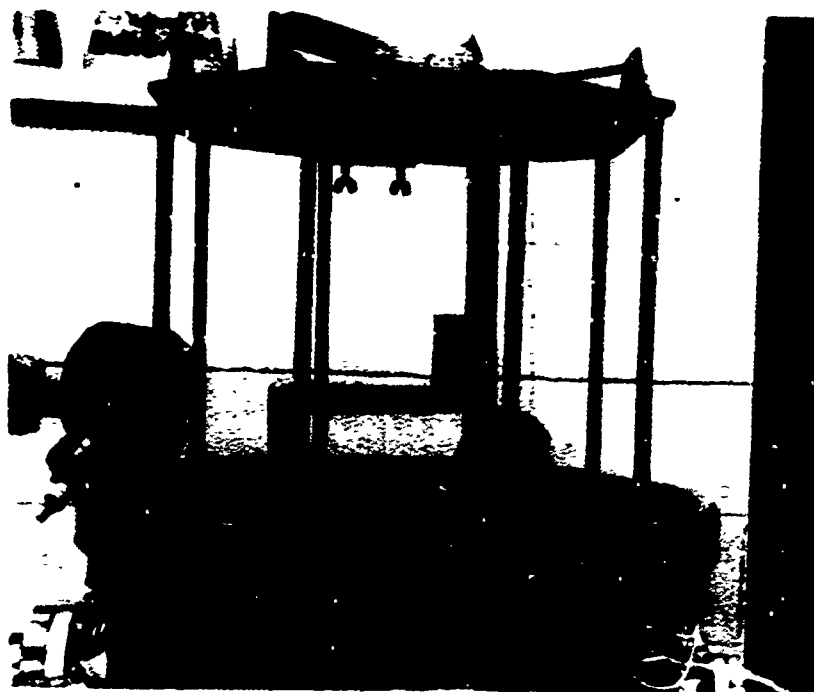


Fig. 21 Chamber Apparatus Installed in Chamber

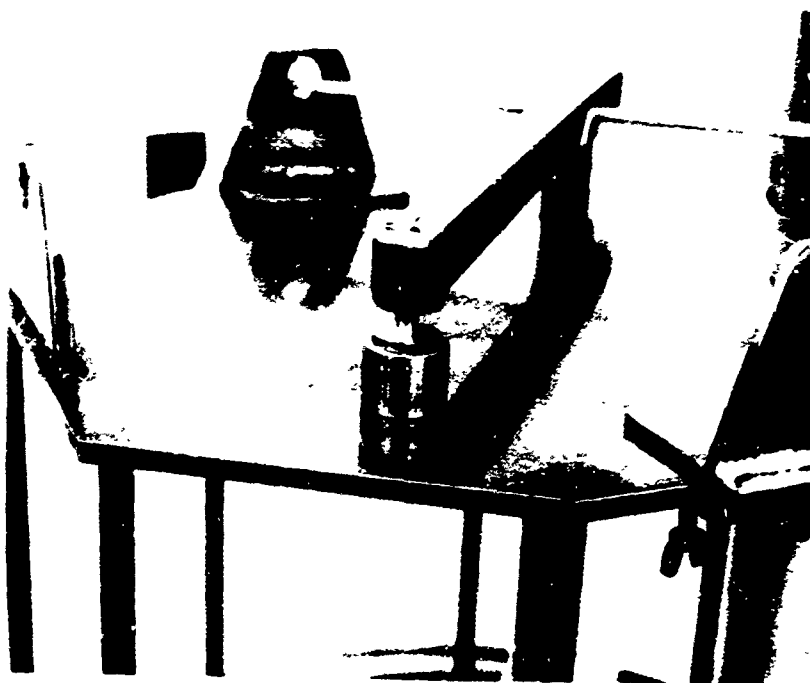


Fig. 22 Chamber Apparatus Seen from Top

geared to the drive mechanism read out the travel to 0.001 in. within 1% accuracy. Axial loads of up to 100 lbs. and vertical loads of 3 lbs. were possible. The operating conditions for the experiments conducted were axial loads of less than 50 lbs. and shear loads of essentially zero. The connection between the feedthrough and the lever system was a bearing connection to minimize these shear loads. The feedthrough was the limiting factor in the maximum allowable bakeout temperature since it could not be exposed to temperatures greater than 200° C.

The system of lever arms was constructed of 18-8 stainless steel, 3/4 in. tubing. They were welded together and all joints were rigid connections. The counterweight was suspended to offset the weight of the device so that when no load was applied the tamper would be suspended in mid-air. A 1/4 in. shaft passed through the pivot point and was the point about which the system rotated.

The tamper was the device that applied the pressure to the surface of the soil sample and was fastened loosely under the force arm. It had free travel within a 3/8 in. diameter circle in a plane parallel to the force arm but remained in contact with the underside of the force arm at all times. The face of the tamper was 51/64 in. in diameter and was made from 2024 aluminum.

Calibration

The calibration consisted of essentially three steps. First the

amount of travel of the tamper for a given input to the feedthrough was determined. Second the amount of force applied to a practically rigid object for a given input to the feedthrough was determined. Third and finally, the results of the first two steps were used to determine the force applied to a soil sample while that same force was measured with a pressure transducer to determine the accuracy of the system.

The free space travel of the tamper was determined by repeated trials. Each time the vertical displacement was measured with the cathetometer which was used in the actual experimentation. The results of this work were that for 88 trials of an input on the feedthrough of 0.025 in. the average vertical displacement in the tamper was 0.34 mm. A 90% confidence interval yielded an average of 0.34 ± 0.005 mm. This data was determined with the apparatus in the same configuration that was used for the tests.

The amount of force delivered by the tamper was calculated by placing a 1 in. solid steel cylinder under the tamper and putting a Kistler, Model 701 H quartz pressure transducer, under the steel cylinder. The output of the transducer was fed to a strip recorder which was calibrated and checked periodically with known weights. The output of the transducer was a small capacitive signal which was amplified before it was sent to the recorder. The time constant of the amplifier could be varied so that it was long enough to record the signal before it died out. As the input to the feedthrough was applied, the

deformation of the steel cylinder was negligible, and the force was transmitted to the output of the recorder. This process was repeated for 55 trials and the average resulting force was 2.50 lbs. for a feedthrough input of 0.025 in. No attempt was made to determine error bounds at this phase because the error could be determined exactly by testing a soil sample with the transducer underneath.

A sample of soil was then placed between the tamper and the transducer. The input to the feedthrough was increased by 0.025 in. for each increment. At each increment the displacement in the sample was measured by reading the change in the position of the crosshairs of the cathetometer, the force was calculated from the results of the previous calibration data, and the force was read out directly on the strip recorder from the transducer. Accepting the force as read by the transducer as the true value of force seen by the sample, the error associated with each value of calculated force was determined. This process was repeated four times and the results of the first test constitute Table I. In this table column (1) is the readout of the feedthrough, column (2) is the increment of increase of the feedthrough, and column (3) is the reading of the cathetometer. These three columns represent the raw data of the experimental work done. Column (4) is the increment of increase of the cathetometer, and the summation of this column represents the total deformation experienced by the soil. Column (5) is calculated from the calibration data of the

Table I

Calibration Test

(1)	(2)	(3)	(4)	(5)	(6)	(7)
460	0	28.64	0	0	0	0
470	10	28.66	0.02	0.01000	0	0
495	25	29.07	0.41	0.02500	0	0
520	25	29.34	0.27	0.01990	0.00510	0.510
545	25	29.62	0.28	0.02060	0.00440	0.440
570	25	29.92	0.30	0.02210	0.00290	0.290
595	25	30.23	0.31	0.02280	0.00220	0.220
620	25	30.44	0.21	0.01550	0.00950	0.950
645	25	30.64	0.20	0.01470	0.01030	1.030
670	25	30.82	0.18	0.01320	0.01180	1.180
695	25	30.91	0.09	0.00663	0.01837	1.837
720	25	31.03	0.12	0.00884	0.01616	1.616
745	25	31.12	0.09	0.00663	0.01837	1.837
770	25	31.18	0.06	0.00442	0.02058	2.058
795	25	31.26	0.08	0.00588	0.01912	1.912
820	25	31.32	0.06	0.00442	0.02058	2.058

7)	(8)	(9)	(10)	(11)
	0	0	0	0
	0	0	0	0
	0	0.072	0.072	100.00
10	0.510	0.178	0.250	105.00
10	0.950	0.250	0.500	90.00
20	1.240	0.428	0.928	33.80
20	1.460	0.428	1.356	7.70
50	2.410	0.858	2.214	8.86
30	3.440	1.070	3.284	4.75
30	4.620	1.250	4.534	1.90
37	6.457	1.710	6.244	3.41
16	8.073	1.890	8.134	-0.65
37	9.900	1.990	10.124	-2.20
38	11.958	2.140	12.264	-2.50
12	13.870	2.420	14.684	-5.56
38	15.928	2.390	17.074	-6.70

force measured on the transducer as the true force seen by the soil sample. Two immediate observations can be made. First the error involved is totally unpredictable for values of total force less than 1.50 lbs.; second, above 1.50 lbs. the error is less than 10%. These observations remained valid for the rest of the calibration tests. This initial calibration of the device was made and various aspects of the system were checked during the progress of the experimentation. All of these checks indicated that there was no change in these original calibration constants.

One might wonder why such a technique was employed to measure forces. A portion of this problem has been discussed in explaining that no commercial equipment was found that could meet the specifications to withstand the experimental environment. Additionally this system was mechanically simple and reliable. It easily fit into the vacuum chamber and presented no outgassing problem for the vacuum system.

Elasticity Analysis

The lever arm system to be a consistent measuring device had to operate within the elastic limit of 2% of its elements. The arms were made of 18-8 stainless steel and were 3/4 in. tubing with a 0.132 in. wall thickness. The maximum moment in the system occurred at the pivot point and was 450 in-lbs. This value assumes a load of 45 lbs. applied to the sample which exceeds any force actually

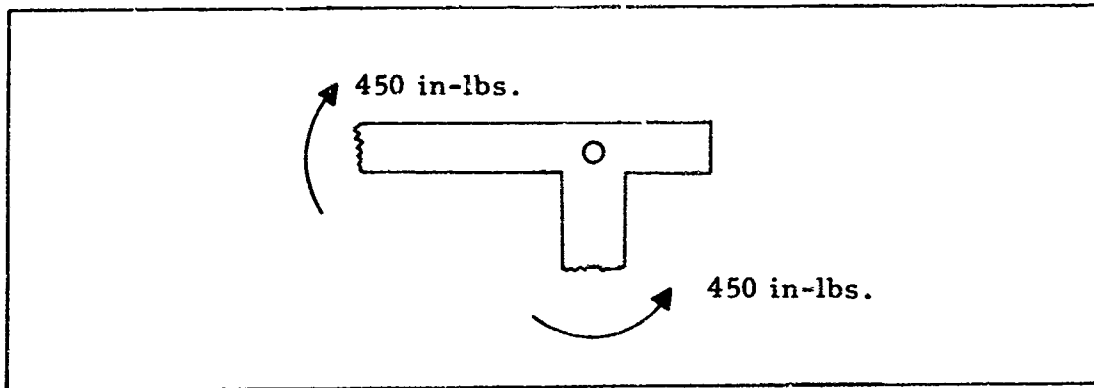


Fig. 23 Moments about the pivot point

used. Using the equations of classical elasticity the stress in the tubing at the pivot point was 18 ksi. With reference to Fig. 23, the stress concentration factor caused by the presence of the hole is 2.3 (Ref 11:389). The ratio of the diameter of the hole to the width of tubing is $1/3$. This increased the maximum value of stress in the tubing to 41.2 ksi. The yield point stress for 18-8 stainless steel, cold rolled, is 165 ksi (Ref 11:472). Therefore the system operates well within the range of elastic behavior.

Changes in the Spring Constant

There is the possibility that the overall spring constant of the system changed during experimentation as the vacuum level increased. This could have occurred for basically two reasons.

1. The friction between the moving parts of the spring system could have increased in the vacuum. There were essentially two moving parts; the shaft-arm connection on which the force arm rotates and the contact between the linear motion feedthrough and the vertical

section of the lever arm.

2. The lever arms were made from 3/4 in. stainless steel tubing which was constructed in atmosphere and welded shut. The gasses inside the tubing were at atmospheric pressure and remained at that pressure at all times. As the vacuum level increased the lever arm experienced a uniform pressure exerted equally in all directions from the inside out. This would serve to increase the stiffness of the lever arms and thus the spring system.

Both of these phenomena mentioned above would have a tendency to increase the stiffness of the spring system. The effect this would have on the resulting e-P curves is discussed below.

The equation for the force resulting from a deflection of a spring is $F = Kx$ where K is the spring constant.

Consider two cases,

Case A. Atmospheric test

$K = K_1$ and is measured in atmosphere as was done when the spring system was calibrated. Consequently all tests in atmosphere were within the accuracy of the force as determined by the calibration tests. The force measured and the force seen by the sample will be the same and will be

$$F = Kx = K_1 x.$$

Case B. Vacuum test

$K = K_2$ and K_2 is greater than K_1 because of the increased stiff-

ness due to the parameters mentioned above. Since no correction was made for the increased stiffness, the spring constant that is assumed to exist is K_1 . Therefore the force that is measured is $K_1 x$ while the force that the sample actually sees is $K_2 x$ and since K_2 is greater than K_1 the force that is recorded is less than the actual force. If the correction could be made in the e-P curves the data points of the vacuum data would have to be shifted to the right which would tend to increase the separation between the 10^{-10} Torr curve and the atmospheric curve. Consequently if the stiffness of the spring does increase a significant amount, it tends to reduce the magnitude of the observed results and not amplify them. The results then are a conservative estimate of the true curves when considering this aspect alone.

Effects of Table Movement

The stainless steel table on which the sample was tested, Fig. 24, rested upon three 2 in. flanges welded to the interior of the vacuum chamber. These flanges were 1/4 in. thick stainless steel and were loaded as a cantilevered beam 1 1/2 in. from the weld during the test. The maximum stress in each flange was 35 ksi which is less than the yield point stress for the steel. The table was secured to these flanges to prevent movement during the test; however, the possibility exists that the table could have slipped slightly during a test. If this had occurred, the vertical crosshair of the cathetometer which was centered on the focusing point would have moved abruptly off that

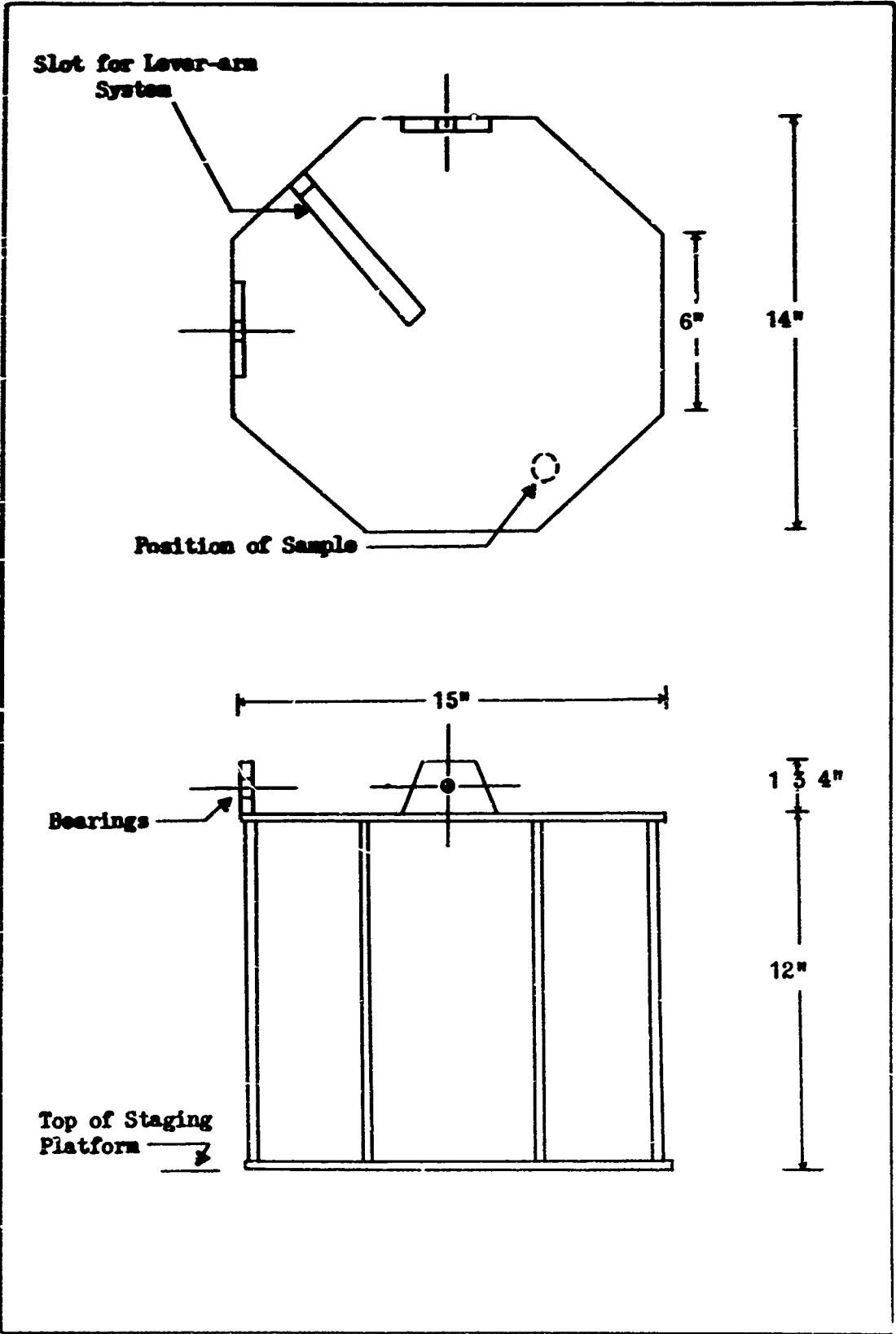


Fig. 24 Raised Platform

point. No such movement was observed. Also the net force seen by the sample would be reduced because of the force dissipated in moving the table. The true e-P curve would shift to the left from the measured curve thus the measured results would be a conservative estimate. However, it may be concluded that no table movement large enough to affect the results occurred since it would have been observed in the scope by the movement of the vertical crosshair away from the focusing point.

Component Specification

The tamper moved on the arc of a circle and not in a straight vertical line. The average angle of rotation was approximately 1° and the maximum rotation was 2.3° . With such small angles of rotation, the average travel of the tamper was assumed to be linear.

The cathetometer was mounted on a tripod outside the chamber and was capable of 16 cm. total vertical travel. The focusing range with the adapter attached extended from 60 cm. to infinity. The vernier permitted adjustments to 0.01mm. Using the cathetometer in this manner the axial strain or deformation in the sample was measured directly. In testing soils in a triaxial test apparatus under a no lateral strain condition, the volume change can be measured three ways but the most accurate is the direct observation of the axial strain (Ref 1:143). Consequently use of the cathetometer was the most accurate means available for measuring volumetric changes in these tests.

GSF/MC/69-4

The precision of the digital counter of the linear motion feed-through was 0.001 in. + 1% of total motion. The accuracy of this device far exceeded that of the cathetometer and the error introduced from this source was ignored.

Appendix D

Raw Data and Sample Calculations

Raw Data

All of the raw data for the conducted tests is included in this appendix. Tables III through XIX are the data taken for the tests performed in the vacuum chamber. Tables XX through XL are the data taken from the Instron tests. Table II is a summary of all of the tests performed and contains comments on deviations from the normal test procedure.

Sample Calculations

On tables III through XIX, the first column is the readout of the linear motion feedthrough on the vacuum chamber. An increase of one unit corresponds to an input of 0.001 in. of horizontal travel. The second column is the reading of the microscope or cathetometer which was positioned exterior to the chamber. The cathetometer scale reads in millimeters. These two columns represent the data taken during any test on the chamber apparatus. The third column is the void ratio and this value is computed from the data of the first two columns by the following sequence of steps.

Step 1. The increment of increase in the cathetometer is computed by subtracting the previous reading. For example, if the scope

read 13.50 on the previous reading and 13.75 on the present reading, the increment of increase would be 0.25 mm. This represents the deformation of the soil for that increment of input.

Step 2. The increment of increase for each input is added to the previous increment so that the total deformation of the soil sample for any input to the feedthrough is known. For the last reading on the feedthrough this would represent the total deformation of the soil sample.

Step 3. The effective height of the sample under the tamper is computed by subtracting the amount of deformation from step 2 from the original height of the container.

Step 4. The volume of the soil under the tamper that is being compressed is computed by taking the effective height and multiplying by the area of the tamper.

Step 5. The void ratio is computed in the following manner:

$$e = V_v / V_s = (V_{tot} - V_s) / V_s = (V_{tot} / V_s) - 1$$

This equation assumes that the water present in the soil occupies negligible volume, which was the case for the tests performed.

$$V_{tot} = (\text{area of tamper}) \times (\text{effective sample height})$$

$$V_s = \frac{(\text{weight of soil}) \times (\text{correction factor})}{(\text{density of the solid particles})}$$

The soil weight was determined prior to the test by weighting the soil and container on an analytical balance. The density of the solid par-

ticles was assumed to be the density of the rock prior to comminution. The correction factor was a geometric factor to account for the fact that the weight of soil that was under the tamper was less than the weight of the entire amount of soil in the container. This correction factor, CF, was

$$CF = \left[\frac{\text{radius of tamper}}{\text{radius of container}} \right]^2 \left[\frac{\text{weight of the entire soil mass}}{\text{weight of the soil in the reduced volume}} \right]$$

This correction factor that was used involved a basic assumption in the calculation of the void ratio. The volume of soil that was used to compute the void ratio was the volume directly under the tamper

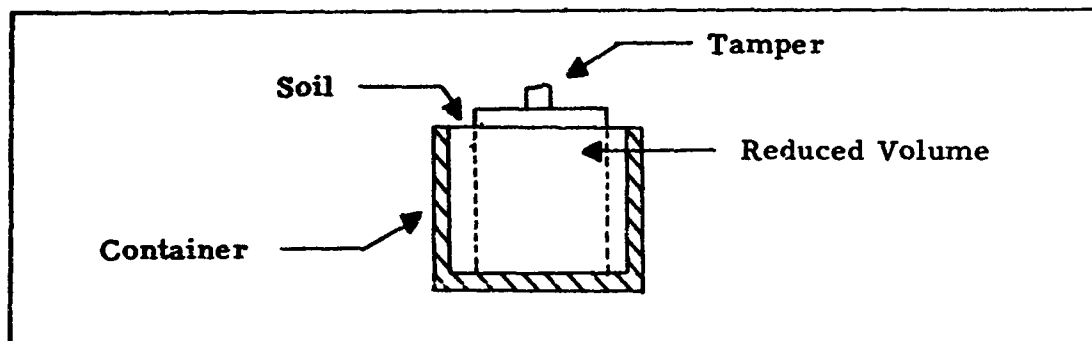


Fig. 25 Reduced Volume Used in Calculations

as shown in Fig. 25. By applying this correction factor the assumption is made that the mass of soil initially in that reduced volume remains constant during the compression of the sample. This would require that no loss of mass across the imaginary boundary would occur and that no shear forces are developed in the soil. This is known not to be the case and results in an incorrect value for the void ratio. There is some net loss of mass across that boundary that is not ac-

counted for in the calculation. Consequently the calculated value of the void ratio is too small and the true value is somewhat greater. All of the data and calculations were then sufficient to compute the void ratio which is the number in the third column. The load on the sample is in the fourth column and was computed from the calibration data obtained prior to the test. This computation is exactly the same as described in Appendix C and will not be discussed further here.

The data in Tables XX through XL are the raw data taken from the tests on the Instron machine. The method of calculation is exactly the same as in the chamber apparatus. The first column is the force applied to the sample and is a direct readout of the machine. The second column is the cumulative deflection of the sample under the tamper and represents the same information as was obtained at the end of step 2 in the chamber apparatus. Steps 3 through 5 are the same as for the chamber apparatus, and the last column is the force applied to the sample divided by the area of the tamper.

Table II
Summary of Data Runs

Data Run ¹	Test Apparatus	Container	Ambient Pressure	e_1	Remarks
1	Chamber	Steel	Atm	2.102	Unable to complete test because linear feed-through reached end of extension.
2	"	"	1.0×10^{-8}	1.143	
3	"	"	Atm	1.954	
4	"	"	2.0×10^{-8}	1.282	A malfunction of the hoist moved the sample from underneath the tamper preventing a test.
5	"	"	Atm	1.262	
6	"	"	3.2×10^{-8}	1.519	
7	"	"	2.0×10^{-8}	1.282	Attempted to attain UHV but could not. Sample was exposed to individual bakeout for 2 hours and a system bakeout for 26 hours.
8	"	"	6.2×10^{-10}	1.173	Individual heater malfunctioned.
9	"	"	Atm	1.277	
10	"	"	6.2×10^{-8}	1.497	
11	"	"	5.2×10^{-10}	1.412	Sample moved out from under tamper from an external disturbance. Unable to test.
12	"	"	2.1×10^{-9}	1.491	

GS- / 12/69-4

Data Run #	Test Apparatus	Container	Ambient Pressure	σ_i	Remarks
13	Chamber	Steel	6.6×10^{-10}	1.517	Individual heater malfunctioned
14	"	"	Atm	1.377	
15	"	"	5.1×10^{-10}	1.989	
16	"	"	3.7×10^{-10}	1.742	
17	"	"	Atm	1.738	
18	"	"	1.2×10^{-9}	1.302	Tamper caught at top and did not apply its load normal to the surface. As the load increased, the soil flowed to the elevated end of the tamper. The results were invalid.
19	"	"	Atm	1.477	
20	"	Glass	5.5×10^{-10}	1.200	Last TV test before breakdown of rough pumping system. Data is not included because there is nothing to compare it with.
21	"	Steel	Atm	1.359	
22	"	"	"	1.238	
23	Instron	"	"	1.496	
24	"	"	"	1.497	
25	"	"	"	1.744	
26	"	"	"	1.140	
27	"	"	"	2.030	
28	"	"	"	1.450	This test was a

Data Run#	Test Apparatus	Container	Ambient Pressure	e_i	Remarks
					loading, unloading and reloading test to determine the hysteresis in the soil. Time did not allow further examination thus the results are omitted.
29	Instron	Steel	Atm	1.912	
30	"	"	"	1.743	Prior to the test, the soil was accidentally vibrated and slumped down one side of the container. No test was performed.
31	"	"	"	1.494	
32	"	"	"	1.416	
33	"	"	"	1.120	
34	"	"	"	1.805	
35	"	"	"	1.716	
36	"	"	"	1.361	
37	"	"	"	1.256	
38	"	Teflon	"	1.681	
39	"	"	"	1.544	
40	"	"	"	1.242	
41	"	"	"	1.066	
42	"	"	"	1.910	
43	"	"	"	1.332	
44	"	"	"	1.143	

GSF/AC/69-4

Data Run#	Test Apparatus	Container	Ambient Pressure	σ_1	Remarks
45	Instron	Teflon	Atm	1.341	These last three tests were run with a teflon container and a piece of aluminium foil in the bottom.
46	"	"	"	1.245	
47	"	"	"	1.138	

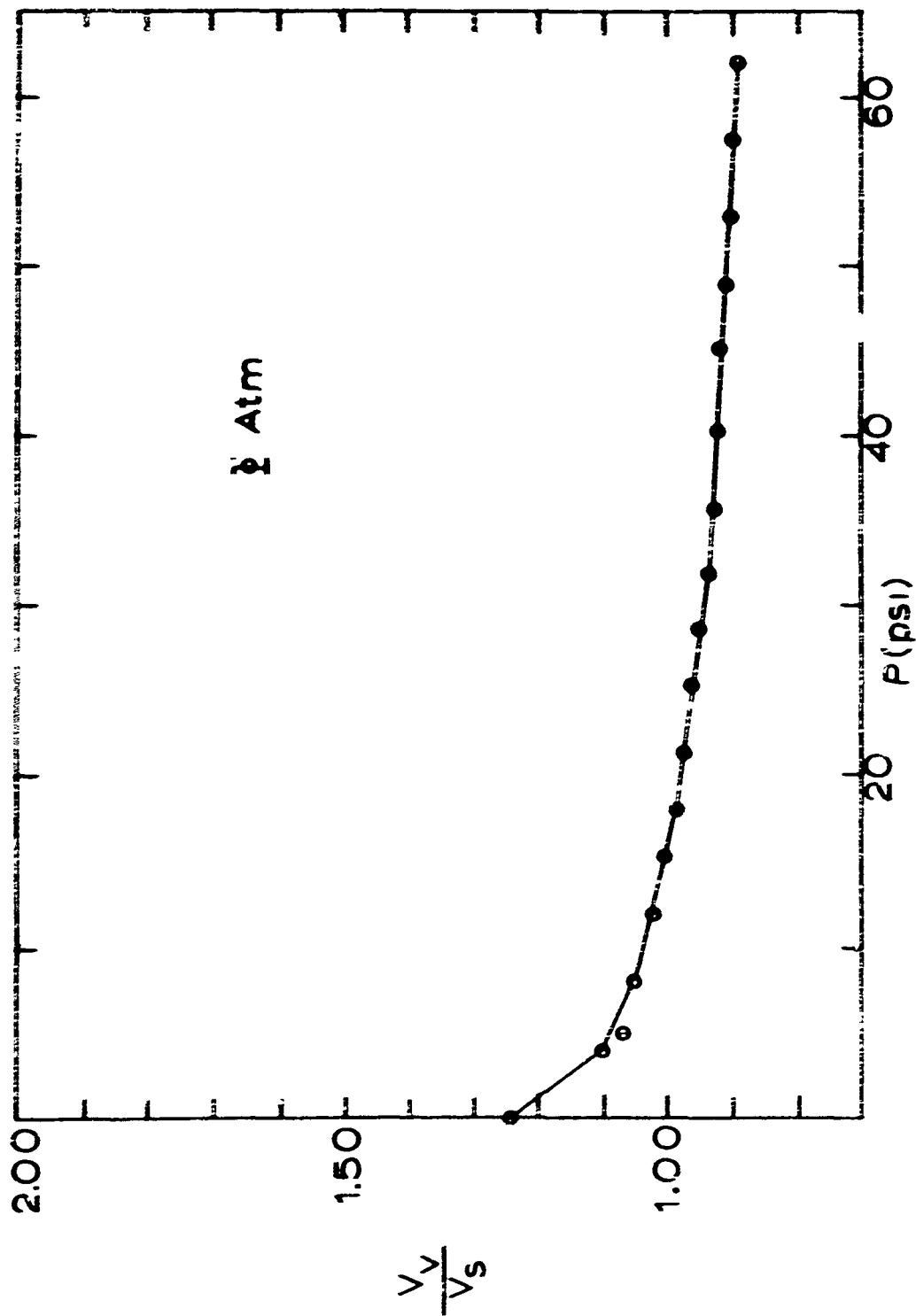


Fig.26 Data Run No.22

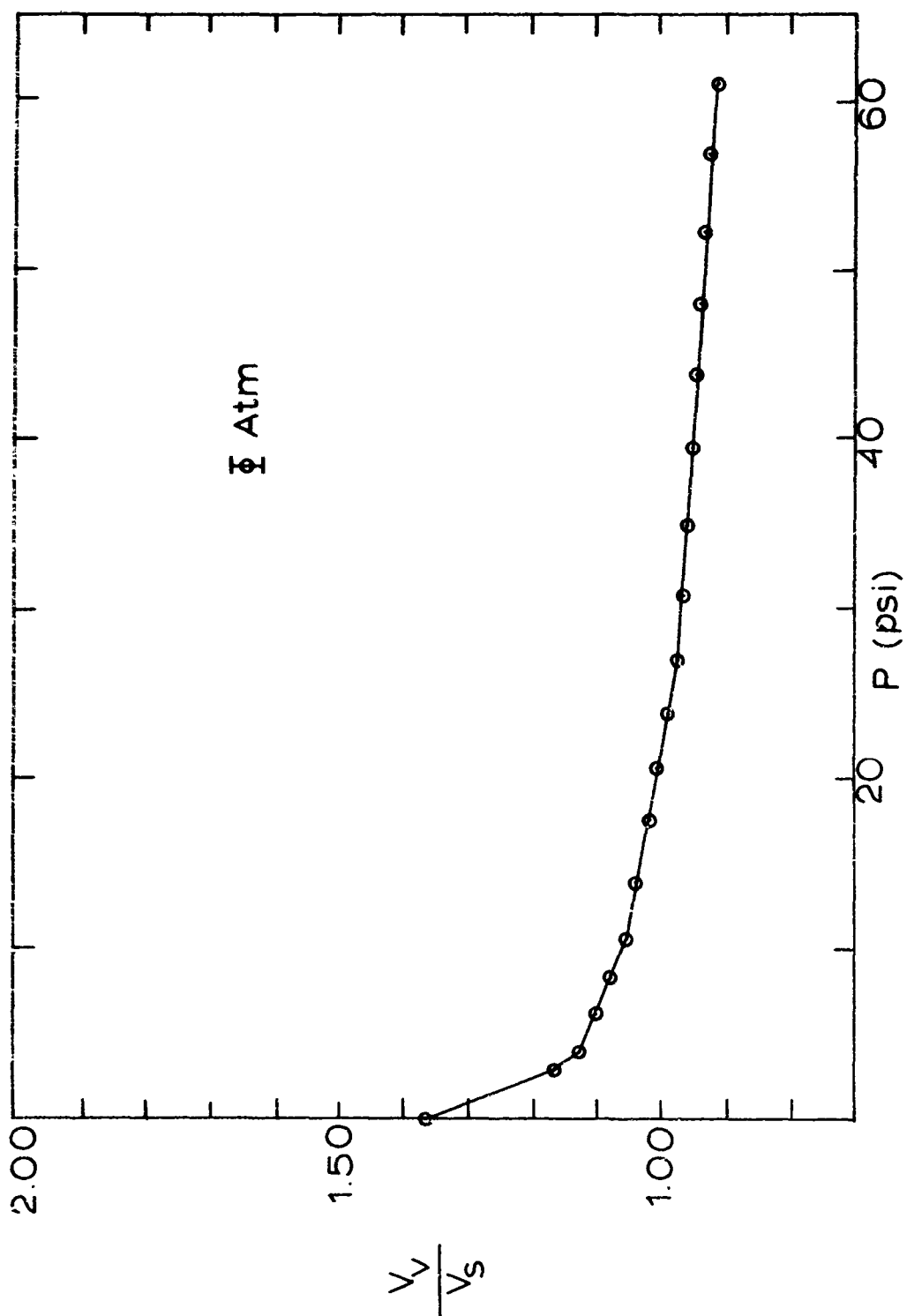


Fig.27 Data Run No. 21

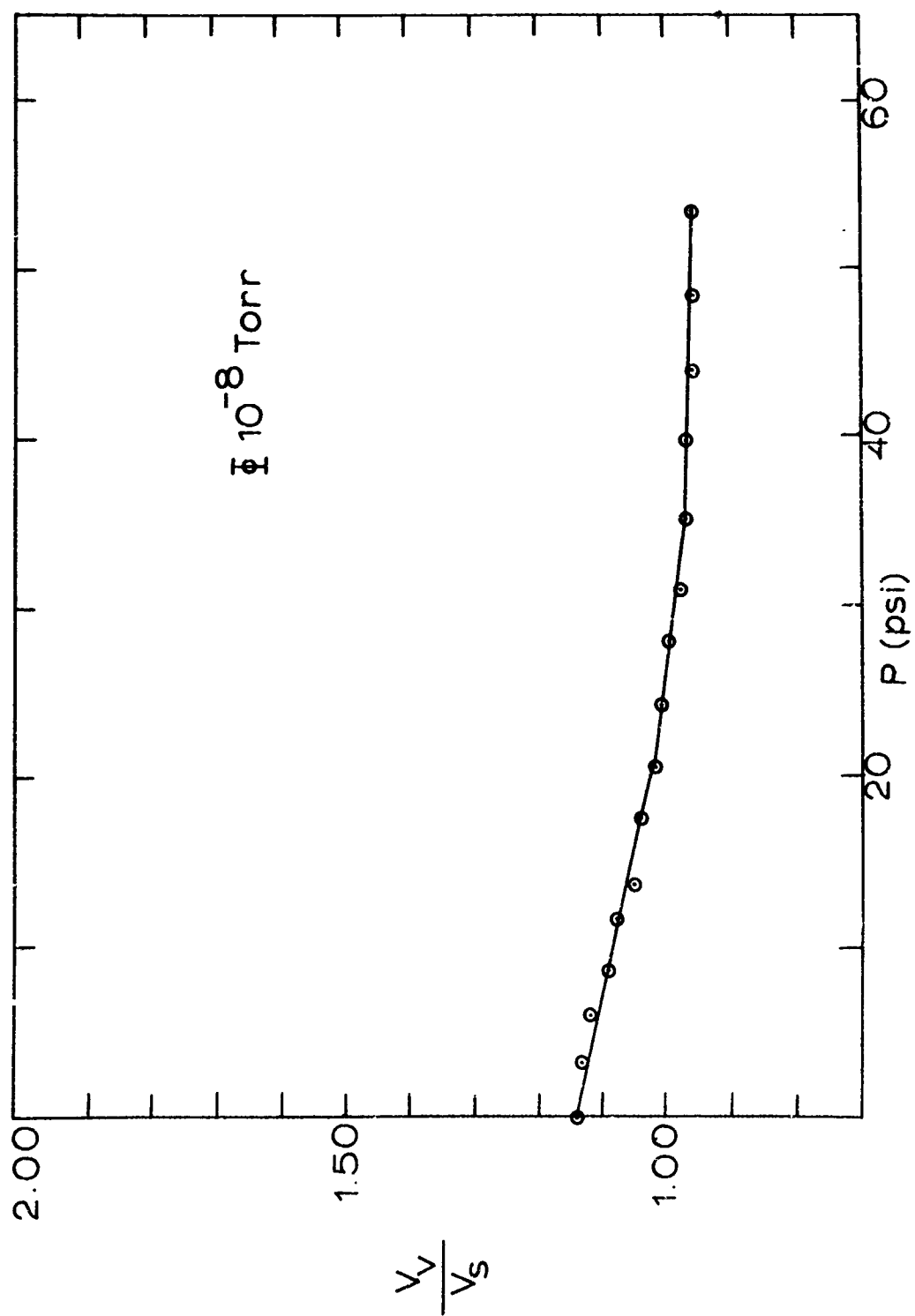


Fig.28 Data Run No.2

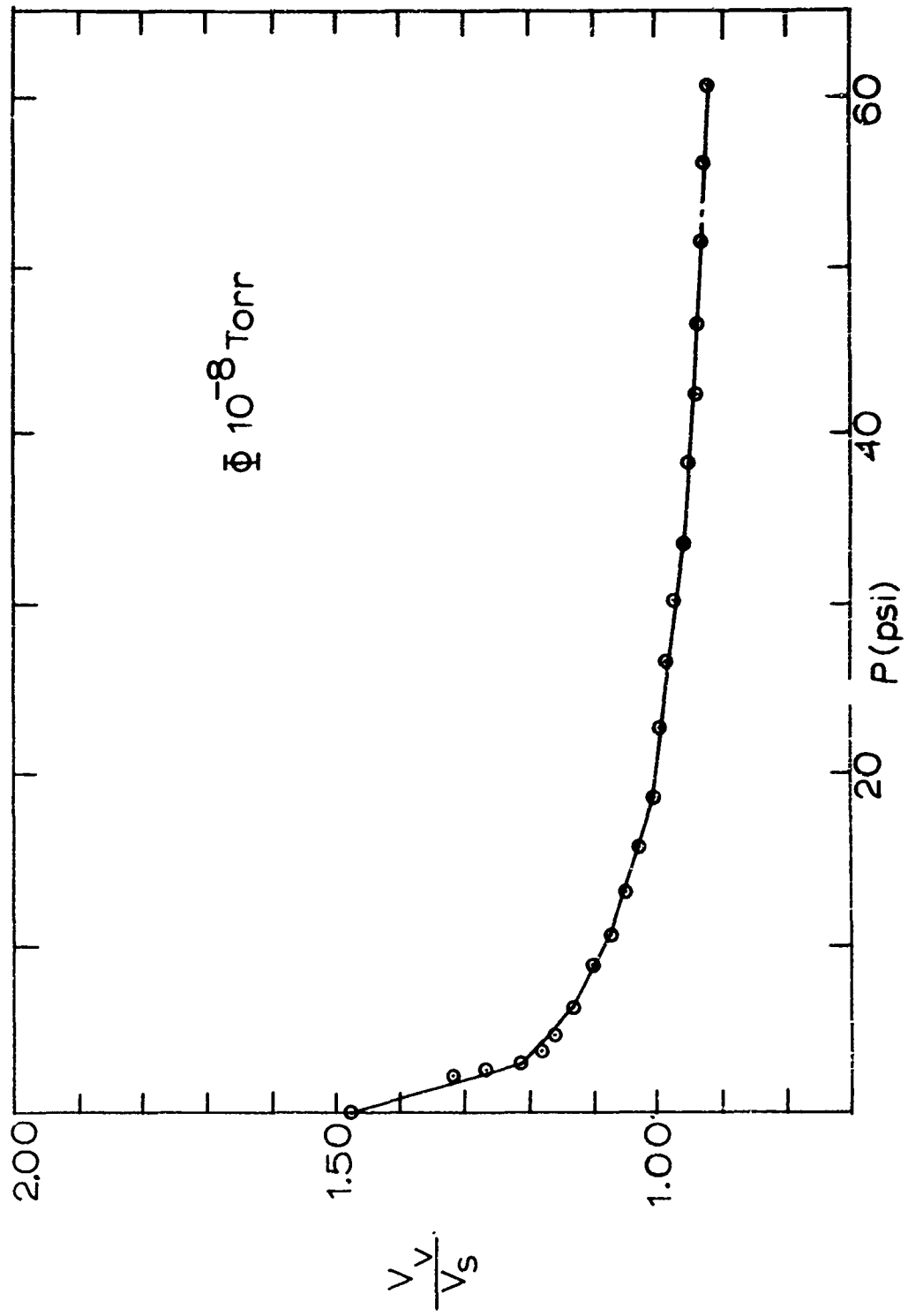


Fig.29 Data Run No.10

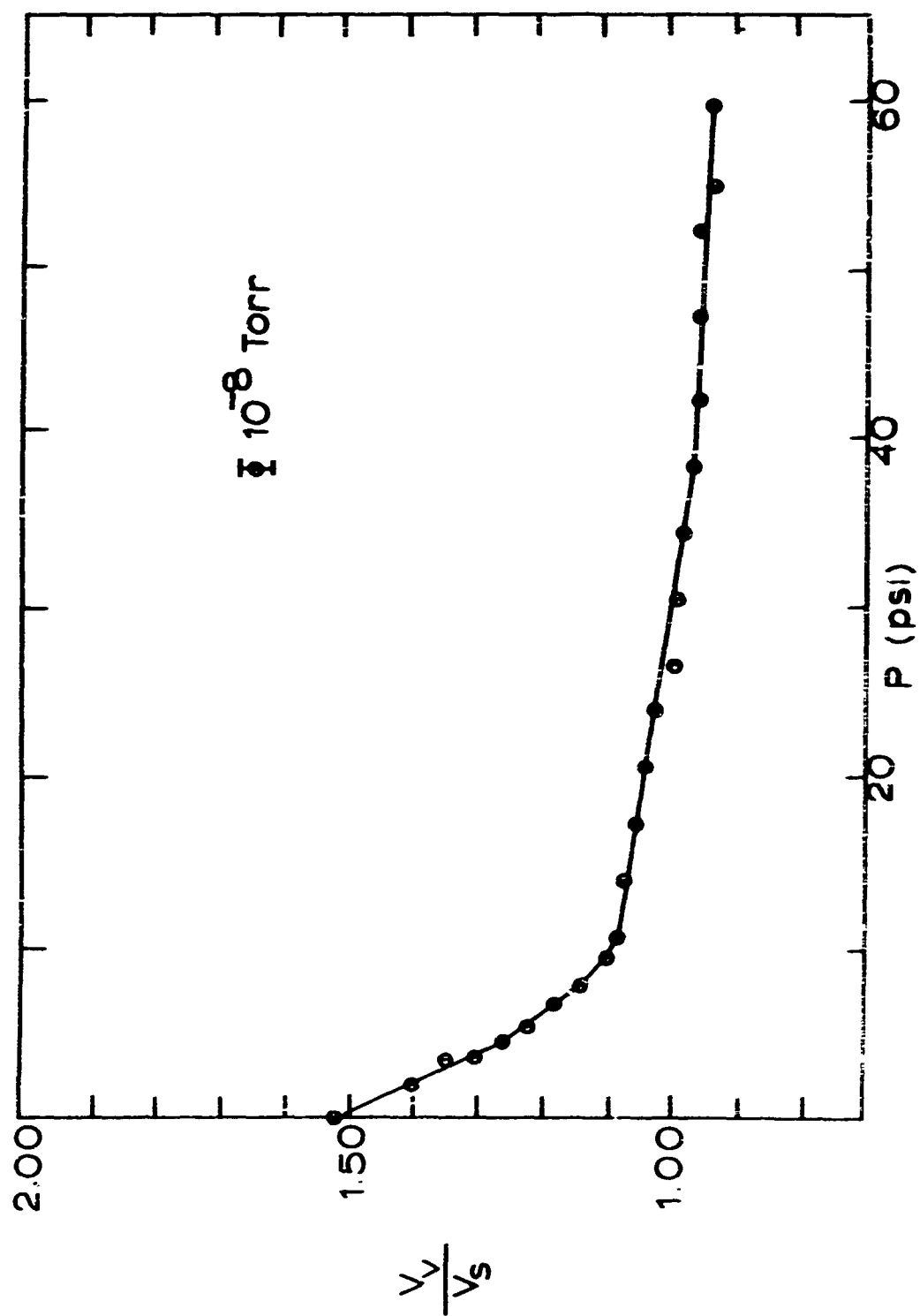


Fig 30 Data Runs Nos 6

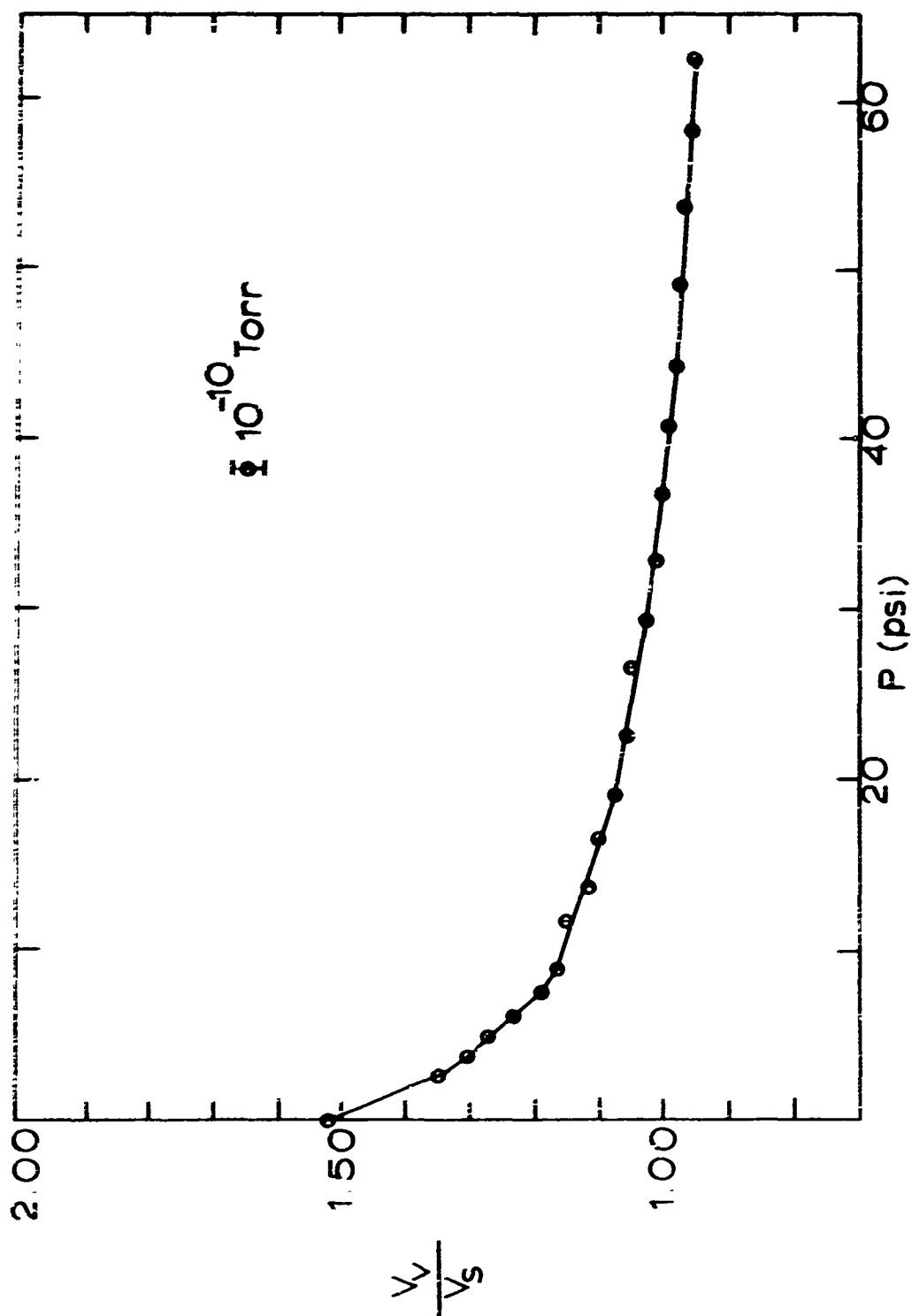


Fig.31 Data Run No.13

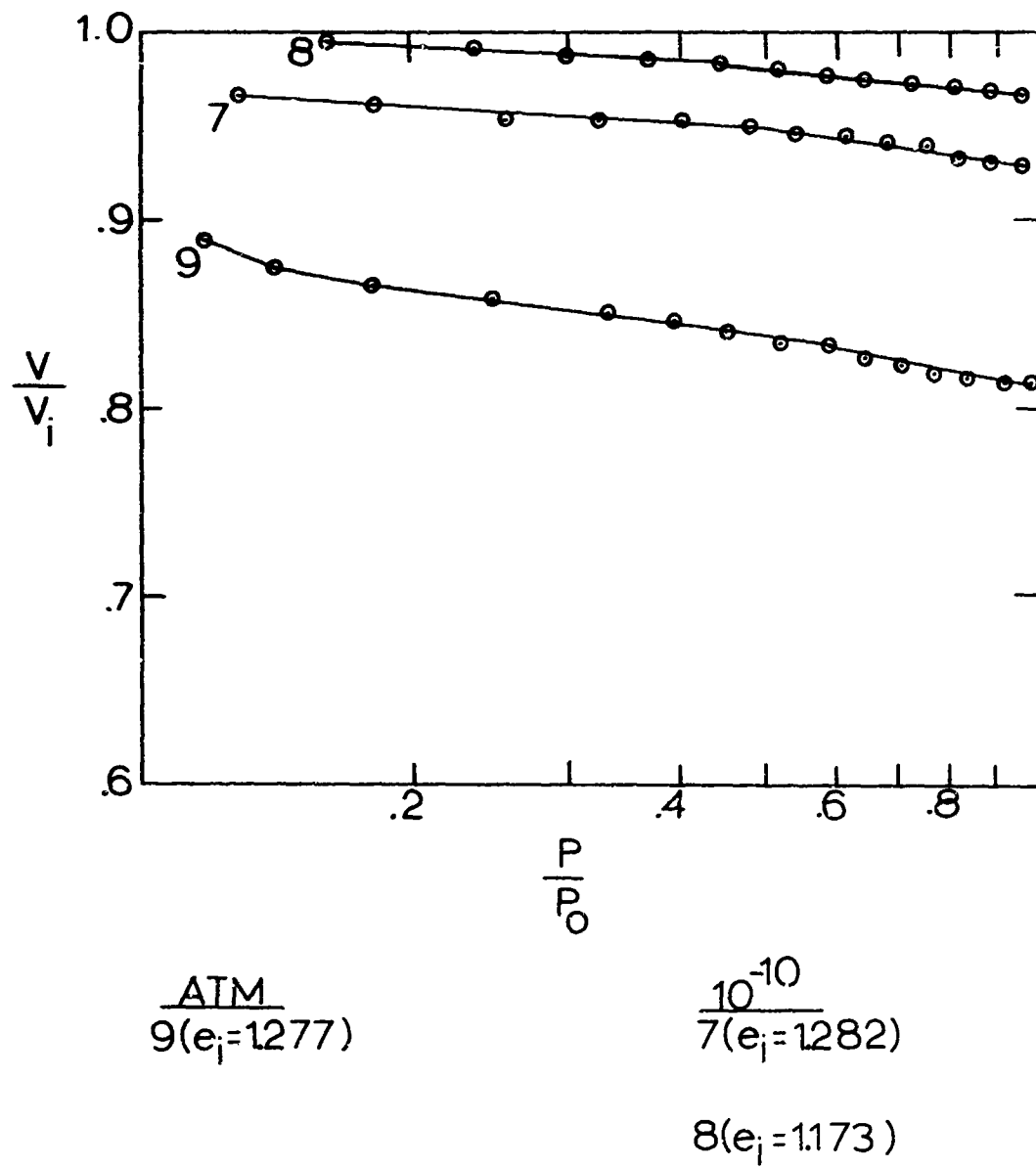


Fig.32 Range on e_i from 1.10 to 1.40

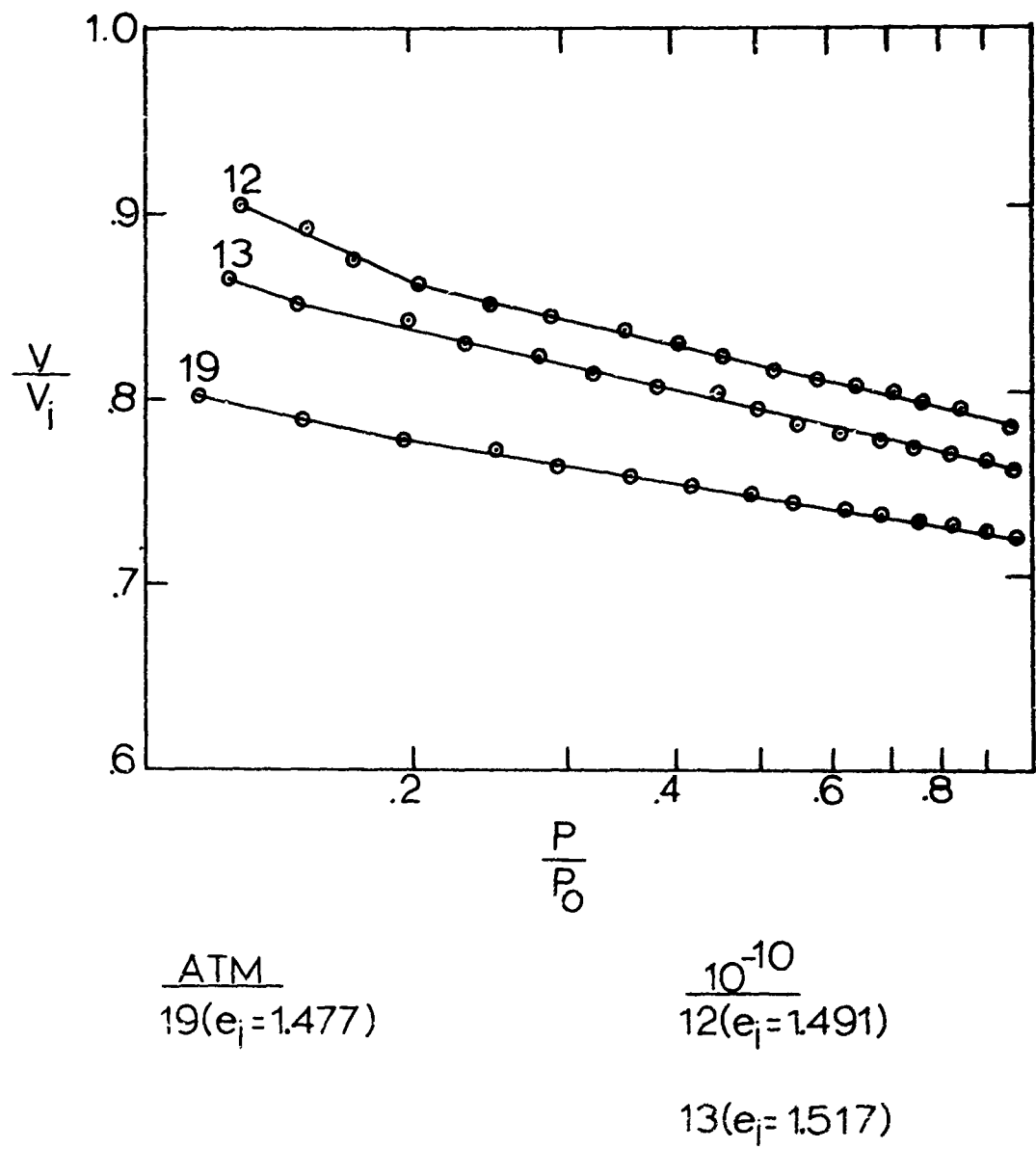


Fig.33 Range on e_i from 1.40 to 1.70

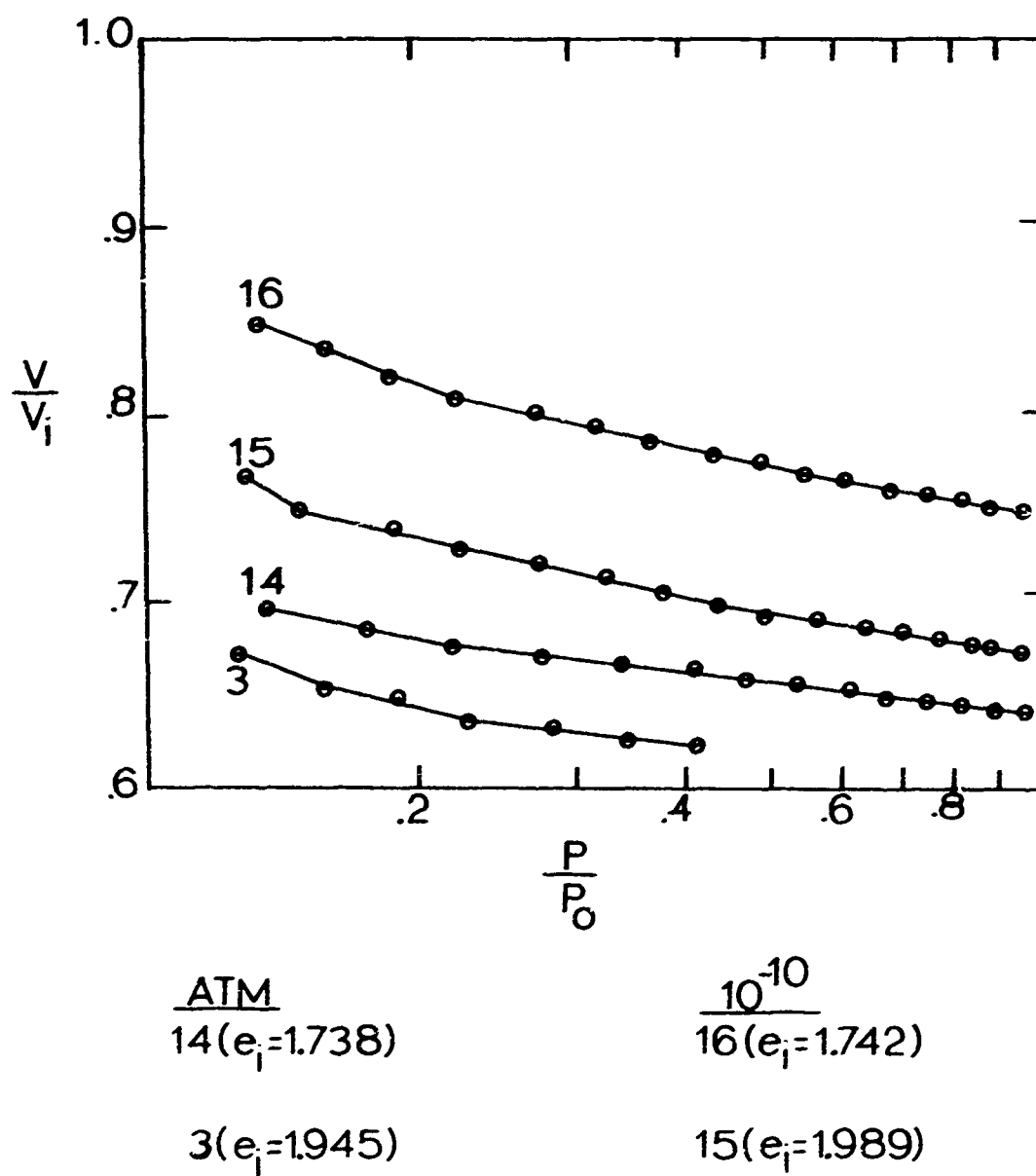


Fig.34 Range on e_i from 1.70 to 2.00

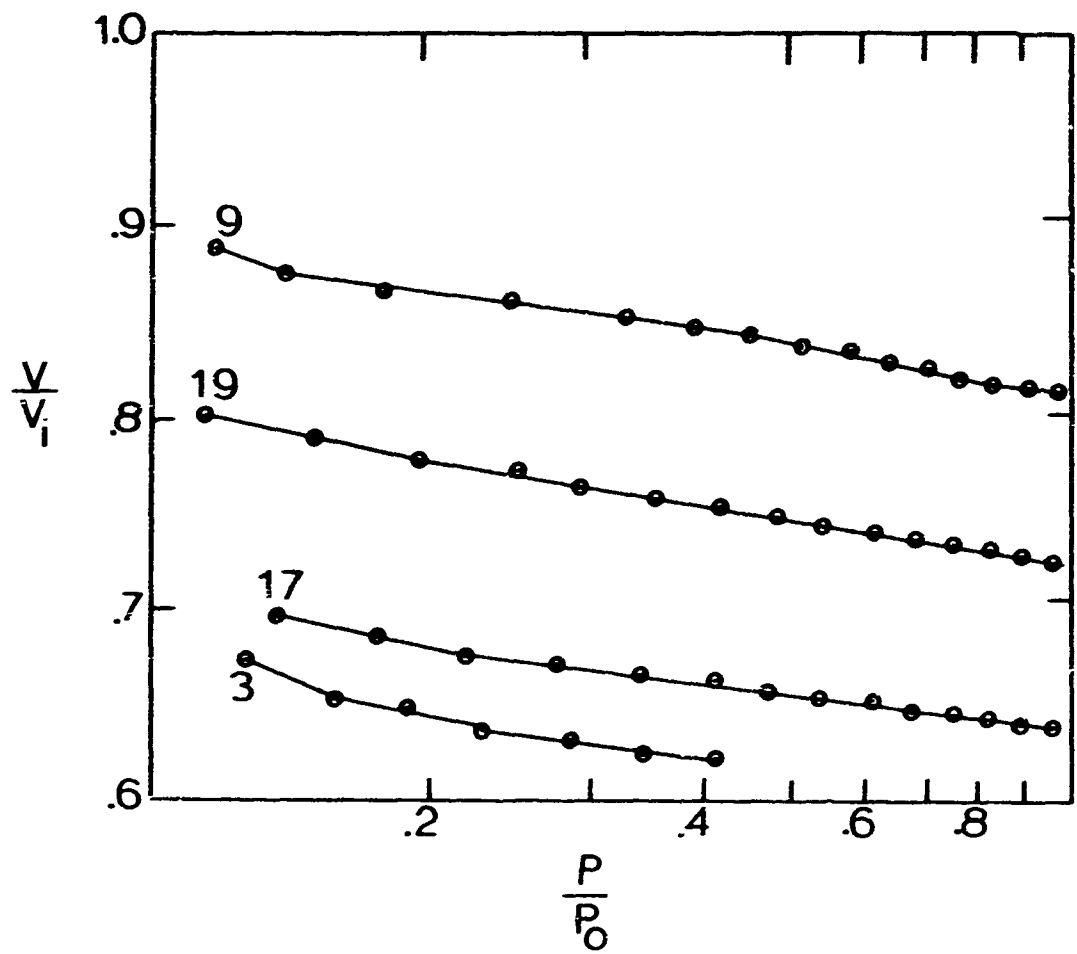


Fig.35 Atmospheric Tests

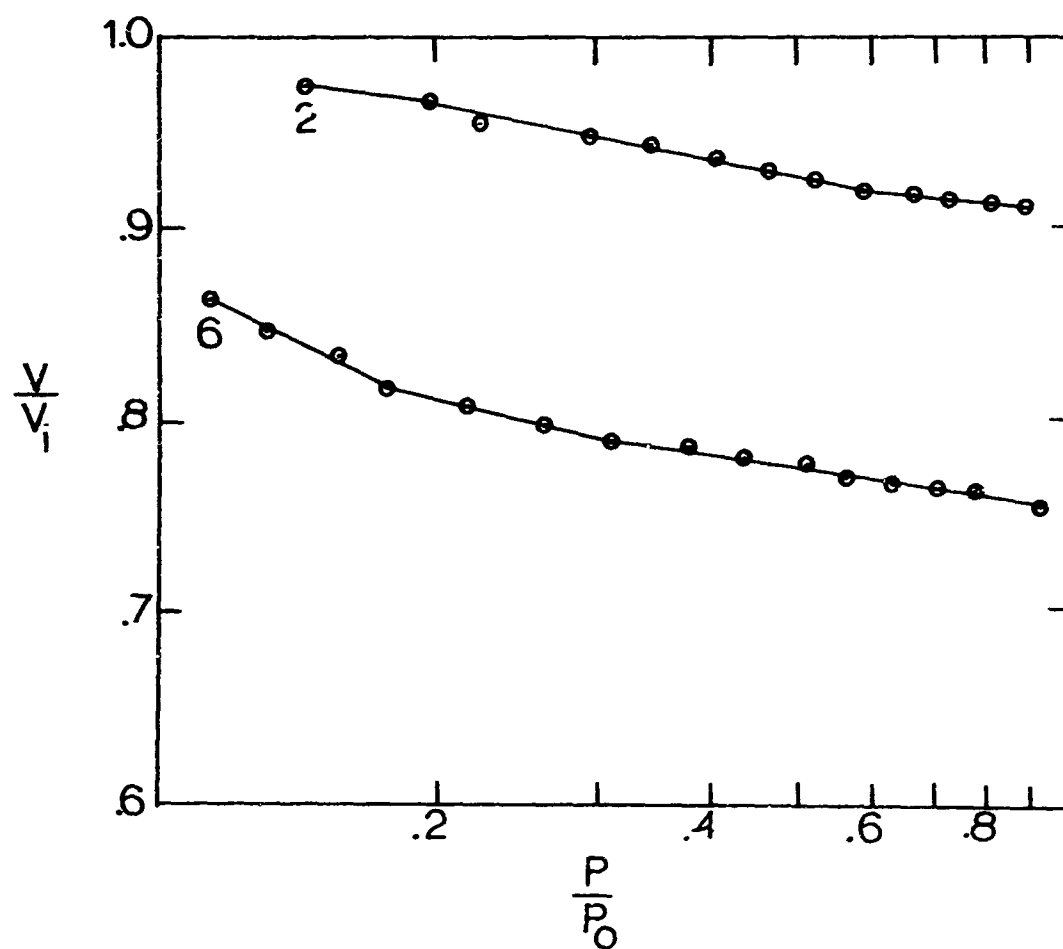


Fig.36 10^{-8} Torr Tests

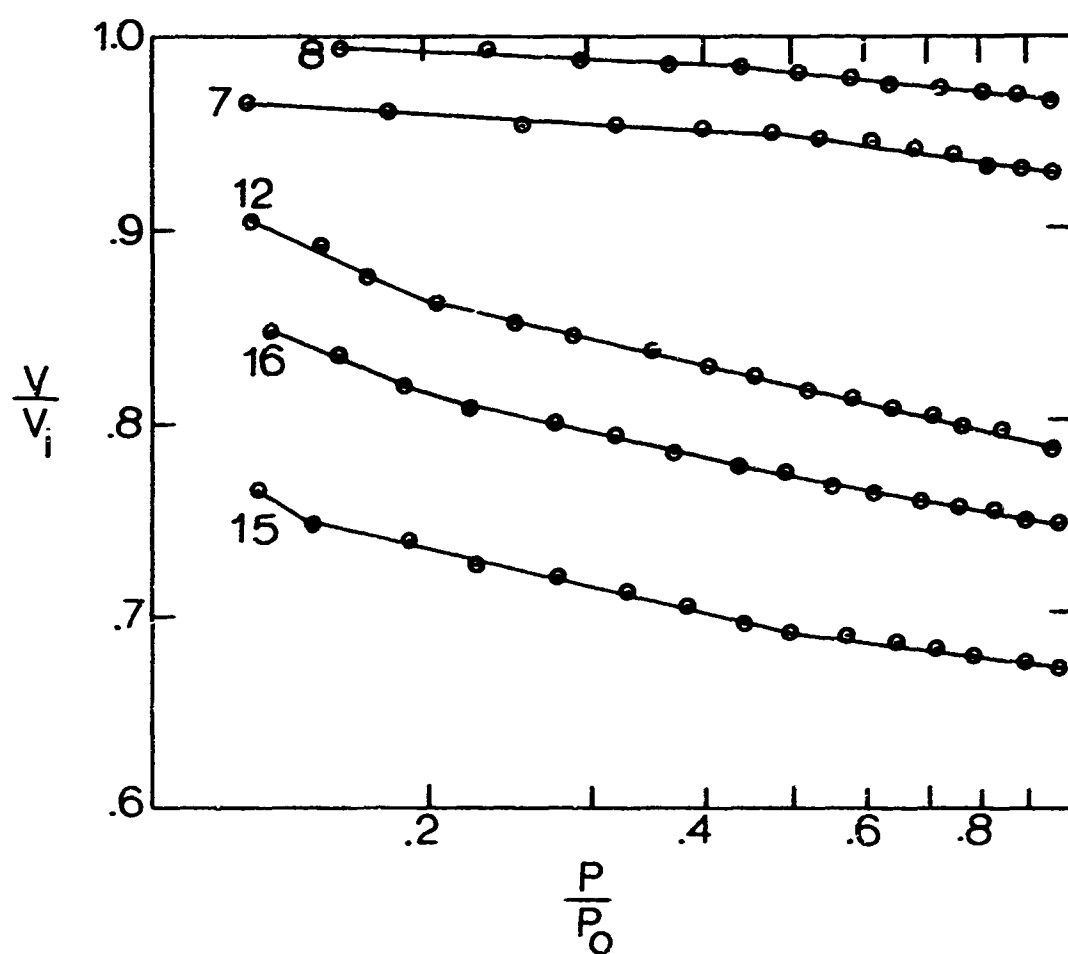
Fig.37 10^{-10} Torr Tests

Table IXI
Data Run # 2

<u>Feedthrough</u>	<u>Microscope</u>	<u>Void Ratio</u>	<u>Load (psi)</u>
200	11.18	1.143	0
225	11.30	1.127	3.23
250	11.45	1.108	6.91
275	11.61	1.087	8.65
300	11.73	1.072	11.88
325	11.94	1.045	13.78
350	12.02	1.034	17.61
375	12.14	1.019	20.84
400	12.25	1.005	24.22
425	12.33	0.994	28.04
450	12.46	0.978	31.13
475	12.51	0.970	35.24
500	12.52	0.968	40.10
525	12.60	0.958	43.92
550	12.64	0.953	48.53
575	12.65	0.952	53.38

Table IV

Data Run # 3

<u>Feedthrough</u>	<u>Microscope</u>	<u>Void Ratio</u>	<u>Load (psi)</u>
215	12.50	1.954	0
240	12.81	1.902	0.44
265	13.14	1.848	0.58
290	13.49	1.790	0.58
315	13.83	1.733	0.58
340	14.18	1.675	0.58
365	14.53	1.671	0.58
390	14.83	1.567	1.16
415	15.20	1.506	1.16
440	15.49	1.458	1.88
465	15.88	1.393	1.88
490	16.23	1.335	1.88
515	16.57	1.279	1.88
540	16.83	1.236	3.07
565	17.12	1.188	3.79
590	17.36	1.144	4.96
515	17.66	1.098	5.84
640	17.88	1.062	7.60
665	18.09	1.027	9.50
690	18.30	0.992	11.40
715	18.48	0.962	13.76
740	18.59	0.944	17.14
765	18.68	0.929	20.81
790	18.75	0.917	24.78

Table V

Data Run # 5

<u>Feedthrough</u>	<u>Microscope</u>	<u>Void Ratio</u>	<u>Load (psi)</u>
200	12.90	1.263	0
225	13.02	1.263	0
250	13.35	1.218	0.14
275	13.57	1.188	1.90
300	13.76	1.162	4.20
325	13.98	1.132	5.96
350	14.20	1.102	7.72
375	14.35	1.081	10.50
400	14.48	1.064	13.59
425	14.62	1.045	16.53
450	14.70	1.034	20.35
475	14.80	1.020	23.88
500	14.87	1.011	27.85
525	14.96	0.998	31.52
550	15.00	0.993	36.13
575	15.07	0.983	40.10
600	15.10	0.979	44.66
625	15.15	0.972	48.92
650	15.16	0.971	53.77
675	15.23	0.961	57.74
700	15.26	0.957	62.30

Table VI

Data Run # 6

<u>Feedthrough</u>	<u>Microscope</u>	<u>Void Ratio</u>	<u>Lead (psi)</u>
200	12.34	1.517	0
225	12.61	1.481	1.02
250	12.93	1.436	1.32
275	13.22	1.395	2.04
300	13.47	1.360	3.36
325	13.83	1.309	4.83
350	14.07	1.275	5.41
375	14.37	1.232	6.88
400	14.61	1.198	7.90
425	14.88	1.160	9.37
450	15.12	1.126	10.69
475	15.37	1.091	14.07
500	15.49	1.075	14.07
525	15.61	1.058	17.30
550	15.70	1.046	20.97
575	15.83	1.027	24.06
600	15.98	1.006	26.84
625	16.06	0.995	30.66
650	16.13	0.985	34.63
675	16.23	0.971	38.16
700	16.28	0.964	42.42
725	16.29	0.962	47.28
750	16.29	0.962	52.28
775	16.44	0.941	55.06

Table VII

Data Run # 7

<u>Feedthrough</u>	<u>Microscope</u>	<u>Void Ratio</u>	<u>Load (psi)</u>
000	12.71	1.282	0
025	12.86	1.262	2.78
050	13.08	1.231	4.53
075	13.21	1.214	7.63
100	13.31	1.200	11.15
125	13.34	1.196	15.71
150	13.40	1.187	19.83
175	13.46	1.179	23.94
200	13.50	1.174	28.56
225	13.58	1.163	32.38
250	13.61	1.159	36.94
275	13.66	1.152	41.20
300	13.78	1.143	45.32
325	13.84	1.135	49.43
350	13.89	1.128	56.70
375	13.93	1.123	58.31
400	13.96	1.119	62.87
425	14.00	1.113	67.48
450	14.03	1.109	72.04
475	14.11	1.098	75.86
500	14.12	1.097	80.71

Table VIII

Data Run # 1

<u>Feedthrough</u>	<u>Microscope</u>	<u>Void Ratio</u>	<u>Load (psi)</u>
000	12.42	1.173	0
025	12.42	1.173	5.00
050	12.46	1.167	9.61
075	12.51	1.161	13.82
100	12.59	1.150	17.70
125	12.65	1.142	21.82
150	12.67	1.140	26.52
175	12.74	1.131	30.49
200	12.79	1.124	34.75
225	12.82	1.120	38.31
250	12.87	1.114	43.52
275	12.89	1.111	48.23
300	12.92	1.107	52.84
325	12.96	1.102	57.45
350	12.97	1.101	62.30
375	13.01	1.095	66.92

Table IX

Data Run $\frac{2}{7} 9$

<u>Feedthrough</u>	<u>Microscope</u>	<u>Void Ratio</u>	<u>Load (psi)</u>
075	12.51	1.277	0
100	12.86	1.232	0
125	13.25	1.182	0
150	13.49	1.152	1.47
175	13.76	1.117	2.49
200	14.00	1.086	3.96
225	14.26	1.053	5.13
250	14.47	1.026	7.03
275	14.72	0.994	8.35
300	14.89	0.971	10.71
325	14.99	0.959	14.84
350	15.13	0.941	19.80
375	15.21	0.930	23.62
400	15.30	0.919	27.30
425	15.39	0.907	30.97
450	15.45	0.900	35.09
475	15.54	0.888	38.76
500	15.62	0.878	42.58
525	15.71	0.866	46.26
550	15.76	0.860	50.52
575	15.79	0.856	55.08
600	15.84	0.850	59.34
625	15.89	0.843	63.61

Table X

Data Run # 10

<u>Feedthrough</u>	<u>Microscope</u>	<u>Void Ratio</u>	<u>Load (psi)</u>
050	12.84	1.497	0
075	13.20	1.447	0
100	13.50	1.405	0.58
125	13.77	1.367	1.61
150	14.06	1.326	2.32
175	14.39	1.280	2.46
200	14.69	1.238	3.04
225	14.98	1.197	3.76
250	15.26	1.158	4.64
275	15.47	1.128	6.54
300	15.65	1.103	8.90
325	15.88	1.071	10.52
350	16.05	1.047	13.02
375	16.20	1.026	15.80
400	16.34	1.006	18.74
425	16.40	0.998	22.86
450	16.48	0.987	26.68
475	16.57	0.974	30.25
500	16.67	0.960	33.88
525	16.71	0.954	38.49
550	16.79	0.943	42.32
575	16.83	0.939	46.88
600	16.87	0.933	51.49
625	16.91	0.928	56.10

Table XI

Data Run # 12

<u>Feedthrough</u>	<u>Microscope</u>	<u>Void Ratio</u>	<u>Load (psi)</u>
050	12.43	1.491	0
075	12.78	1.442	0
100	13.03	1.407	1.32
125	13.25	1.376	3.08
150	13.50	1.341	4.49
175	13.76	1.305	5.57
200	13.96	1.277	7.63
225	14.20	1.243	9.10
250	14.46	1.207	10.27
275	14.66	1.179	12.33
300	14.83	1.155	14.93
325	15.00	1.131	17.33
350	15.08	1.120	21.15
375	15.21	1.102	24.24
400	15.32	1.086	27.63
425	15.42	1.073	31.15
450	15.50	1.061	34.97
475	15.59	1.049	38.64
500	15.65	1.040	42.76
525	15.73	1.029	46.58
550	15.77	1.024	51.20
575	15.80	1.019	55.75
600	15.97	0.996	58.25
625	15.99	0.993	63.16

Table XII

Data Run # 13

<u>Feedthrough</u>	<u>Microscope</u>	<u>Void Ratio</u>	<u>Load (psi)</u>
050	12.47	1.517	0
075	12.77	1.474	0.58
100	13.20	1.425	0.58
125	13.40	1.385	1.46
150	13.66	1.349	2.63
175	13.92	1.312	3.80
200	14.18	1.275	4.97
225	14.44	1.238	6.14
250	14.69	1.203	7.46
275	14.93	1.169	8.93
300	15.07	1.149	11.87
325	15.28	1.120	13.77
350	15.42	1.100	16.71
375	15.59	1.076	19.21
400	15.69	1.062	22.74
425	15.75	1.053	26.85
450	15.90	1.032	29.63
475	16.01	1.017	33.01
500	16.08	1.007	36.98
525	16.15	0.997	40.95
550	16.24	0.984	44.62
575	16.28	0.978	49.23
600	16.32	0.973	53.85
625	16.37	0.966	58.11

Table XIII

Data Run #14

<u>Feedthrough</u>	<u>Microscope</u>	<u>Void Ratio</u>	<u>Load (psi)</u>
050	12.12	1.380	0
075	12.47	1.328	0
100	12.70	1.296	1.76
125	12.96	1.259	2.93
150	13.20	1.225	4.40
175	13.38	1.199	6.76
200	13.57	1.171	8.97
225	13.74	1.147	11.47
250	13.88	1.127	14.41
275	14.01	1.108	17.50
300	14.15	1.088	20.44
325	14.18	1.084	24.99
350	14.25	1.074	28.96
375	14.32	1.064	32.93
400	14.41	1.051	36.60
425	14.45	1.045	41.22
450	14.51	1.037	45.33
475	14.54	1.032	49.89
500	14.58	1.027	54.50
525	14.63	1.019	58.77
550	14.69	1.011	62.88

Table XIV

Data Run # 15

<u>Feedthrough</u>	<u>Microscope</u>	<u>Void Ratio</u>	<u>Load (psi)</u>
050	12.48	1.989	0
075	12.82	1.932	0
100	13.11	1.883	0.72
125	13.43	1.830	1.02
150	13.75	1.776	1.32
175	14.09	1.719	1.32
200	14.39	1.669	1.90
225	14.71	1.615	2.20
250	15.02	1.562	2.64
275	15.29	1.518	3.66
300	15.56	1.472	4.68
325	15.87	1.420	5.12
350	16.14	1.375	6.14
375	16.37	1.336	7.76
400	16.63	1.293	8.93
425	16.80	1.264	11.43
450	17.00	1.231	13.49
475	17.12	1.210	16.72
500	17.25	1.189	19.81
525	17.37	1.168	23.04
550	17.48	1.150	26.42
575	17.58	1.133	29.95
600	17.62	1.127	34.56
625	17.66	1.120	39.17

Table XIV
(continued)

<u>Feedthrough</u>	<u>Microscope</u>	<u>Void Ratio</u>	<u>Load (psi)</u>
650	17.72	1.110	43.29
675	17.73	1.100	47.40
700	17.83	1.091	51.67
725	17.86	1.086	54.22
750	17.91	1.078	56.84

Table XV

Data Run # 16

<u>Feedthrough</u>	<u>Microscope</u>	<u>Void Ratio</u>	<u>Load (psi)</u>
050	12.85	1.742	0
075	13.13	1.699	0.88
100	13.42	1.654	1.50
125	13.73	1.606	2.04
150	14.03	1.560	2.62
175	14.33	1.514	3.20
200	14.67	1.462	3.20
225	14.92	1.423	4.52
250	15.16	1.386	5.90
275	15.35	1.355	8.05
300	15.60	1.319	9.52
325	15.83	1.283	11.14
350	16.02	1.254	13.35
375	16.15	1.234	16.44
400	16.30	1.211	19.22
425	16.43	1.191	22.30
450	16.52	1.177	25.93
475	16.61	1.163	29.65
500	16.72	1.146	33.63
525	16.81	1.132	36.70
550	16.84	1.123	41.26
575	16.90	1.117	45.38
600	16.96	1.109	49.40
625	17.03	1.098	53.46

Table XV
(continued)

<u>Feedthrough</u>	<u>Microscope</u>	<u>Void Ratio</u>	<u>Load (psi)</u>
650	17.06	1.094	58.02
675	17.08	1.091	62.72

Table XVI

Data Run # 17

<u>Feedthrough</u>	<u>Microscope</u>	<u>Void Ratio</u>	<u>Load (psi)</u>
050	13.04	1.738	0
075	13.38	1.685	0
100	13.71	1.635	0.14
125	14.12	1.572	0.14
150	14.45	1.521	0.28
175	14.81	1.456	0.28
200	15.13	1.416	0.58
225	15.48	1.363	0.58
250	15.81	1.312	0.72
275	16.16	1.258	0.72
300	16.47	1.210	1.16
325	16.82	1.157	1.16
350	17.08	1.117	2.33
375	17.38	1.071	2.91
400	17.64	1.031	4.08
425	17.88	0.994	5.55
450	18.04	0.960	8.19
475	18.22	0.941	10.55
500	18.38	0.917	13.19
525	18.48	0.901	16.72
550	18.56	0.889	20.54
575	18.61	0.881	24.81
600	18.70	0.868	28.46
625	18.77	0.857	32.45

Table XVI
(continued)

<u>Feedthrough</u>	<u>Microscope</u>	<u>Void Ratio</u>	<u>Load (psi)</u>
650	18.50	0.852	37.01
675	18.88	0.840	40.83
700	18.91	0.835	45.30
725	18.96	0.828	49.65
750	19.00	0.822	54.26
775	19.02	0.818	58.97
800	19.04	0.815	63.68

Table XVII

Data Run # 19

<u>Feedthrough</u>	<u>Microscope</u>	<u>Void Ratio</u>	<u>Load (psi)</u>
050	13.47	1.477	0
075	13.83	1.427	0
100	14.16	1.361	0.14
125	14.50	1.334	0.14
150	14.83	1.268	0.28
175	15.16	1.239	0.28
200	15.50	1.195	0.58
225	15.76	1.159	1.75
250	16.05	1.118	2.47
275	16.30	1.084	3.78
300	16.56	1.048	4.96
325	16.75	1.016	6.86
350	16.94	0.992	9.07
375	17.12	0.967	11.43
400	17.22	0.953	14.96
425	17.38	0.931	17.60
450	17.47	0.916	21.27
475	17.55	0.907	25.10
500	17.62	0.897	29.06
525	17.72	0.883	32.59
550	17.75	0.880	37.15
575	17.82	0.869	41.12
600	17.87	0.863	45.31
625	17.90	0.858	49.94

Table XVII
(continued)

<u>Feedthrough</u>	<u>Microscope</u>	<u>Void Ratio</u>	<u>Load (psi)</u>
550	17.96	0.850	54.06
675	18.01	0.843	58.32
700	18.04	0.839	62.88

Table XVIII

Data Run # 21

<u>Feedthrough</u>	<u>Microscope</u>	<u>Void Ratio</u>	<u>Load (psi)</u>
650	13.41	1.359	0
075	13.65	1.327	1.47
100	13.97	1.285	1.76
125	14.30	1.241	1.91
150	14.63	1.197	2.05
175	14.90	1.162	3.07
200	15.18	1.124	3.95
225	15.37	1.099	6.16
250	15.56	1.074	8.37
275	15.74	1.050	10.73
300	15.86	1.034	13.96
325	16.01	1.015	16.74
350	16.07	1.007	20.86
375	16.20	0.989	23.94
400	16.32	0.973	27.18
425	16.40	0.963	31.00
450	16.46	0.955	35.12
475	16.49	0.952	39.67
500	16.54	0.944	43.94
525	16.59	0.938	48.20
550	16.65	0.930	52.32
575	16.69	0.924	56.93
600	16.75	0.917	61.05

Table XIX

Data Run # 22

<u>Feedthrough</u>	<u>Microscope</u>	<u>Void Ratio</u>	<u>Load (psi)</u>
075	13.24	1.238	0
100	13.51	1.204	1.02
125	13.77	1.171	2.10
150	14.12	1.127	2.10
175	14.34	1.100	3.05
200	14.61	1.066	4.07
225	14.74	1.050	8.06
250	14.95	1.023	11.06
275	15.07	1.008	15.10
300	15.22	0.989	17.97
325	15.33	0.975	21.35
350	15.40	0.967	25.31
375	15.50	0.954	28.84
400	15.63	0.938	31.93
425	15.71	0.928	35.75
450	15.74	0.924	40.31
475	15.75	0.923	45.16
500	15.83	0.913	48.99
525	15.90	0.904	52.95
550	15.93	0.900	57.51
575	15.96	0.896	62.07

Table XX

Data Run # 23, 24, and 31

<u>Force</u>	<u>Total Deflection</u>	<u>Void Ratio</u>	<u>Load (psi)</u>
0	0	1.496	0
1.24	0.0936	1.163	2.48
1.90	0.0999	1.140	3.80
2.48	0.1158	1.084	4.96
3.43	0.1258	1.048	6.86
4.54	0.1337	1.020	9.08
5.72	0.1401	0.997	11.44
7.48	0.1467	0.974	14.96
8.80	0.1509	0.959	17.60
10.63	0.1557	0.942	21.26
12.55	0.1596	0.928	25.10
14.53	0.1630	0.916	29.06
16.30	0.1657	0.906	32.60
18.58	0.1688	0.895	37.16
20.56	0.1714	0.886	41.12
22.69	0.1737	0.877	45.38
24.97	0.1759	0.870	49.94
27.03	0.1778	0.863	54.06
29.16	0.1795	0.857	58.32
31.44	0.1814	0.850	62.88

Table XXI

Data Run # 25

<u>Force</u>	<u>Total Deflection</u>	<u>Void Ratio</u>	<u>Load (psi)</u>
0	0	1.744	0
0.50	0.1200	1.275	1.00
1.00	0.1470	1.169	2.00
1.50	0.1699	1.079	3.00
2.00	0.1840	1.024	4.00
2.75	0.1943	0.984	5.50
4.00	0.2043	0.945	8.00
5.25	0.2111	0.918	10.50
6.50	0.2160	0.899	13.00
8.50	0.2222	0.875	17.00
10.25	0.2265	0.858	20.50
12.50	0.2309	0.841	25.00
14.25	0.2337	0.830	28.50
16.00	0.2361	0.820	32.00
18.50	0.2394	0.808	37.00
21.00	0.2420	0.797	42.00
23.00	0.2440	0.789	46.00
25.00	0.2458	0.782	50.00
27.00	0.2474	0.776	54.00
29.50	0.2492	0.767	59.00
31.80	0.2503	0.765	63.60

Table XXII

Data Run # 26

<u>Force</u>	<u>Total Deflection</u>	<u>Void Ratio</u>	<u>Load (psi)</u>
0	0	1.140	0
0.50	0.0080	1.137	1.00
1.50	0.0139	1.094	3.00
3.00	0.0220	1.068	6.00
4.25	0.0286	1.046	8.50
6.00	0.0361	1.022	12.00
7.00	0.0397	1.010	14.00
8.75	0.0450	0.992	17.50
10.50	0.0496	0.977	21.00
12.00	0.0530	0.966	24.00
14.00	0.0570	0.953	28.00
15.50	0.0595	0.945	31.00
17.50	0.0627	0.934	35.00
20.00	0.0663	0.923	40.00
22.00	0.0687	0.915	44.00
24.25	0.0714	0.906	48.50
27.00	0.0743	0.896	54.00
29.50	0.0767	0.889	59.00
32.50	0.0793	0.880	65.00

Table XXIII

Data Run # 27

<u>Force</u>	<u>Total Reflection</u>	<u>Void Ratio</u>	<u>Load (psi)</u>
0	0	2.030	0
0.25	0.1400	1.333	0.50
1.00	0.1820	1.244	2.50
1.50	0.1950	1.188	3.00
2.50	0.2076	1.133	5.00
4.00	0.2182	1.085	8.00
5.00	0.2240	1.062	10.00
6.00	0.2277	1.046	12.00
8.00	0.2336	1.021	15.00
10.00	0.2384	1.000	20.00
12.50	0.2427	0.931	25.00
15.00	0.2462	0.956	30.00
17.50	0.2492	0.953	35.00
20.00	0.2515	0.942	40.00
22.50	0.2540	0.933	45.00
25.00	0.2560	0.924	50.00
27.50	0.2578	0.916	55.00
30.00	0.2594	0.909	60.00

Table XXIV

Data Run # 29

<u>Force</u>	<u>Total Deflection</u>	<u>Void Ratio</u>	<u>Load (psi)</u>
0	0	1.912	0
0.50	0.1567	1.253	1.00
1.00	0.1800	1.165	2.00
2.00	0.2093	1.079	3.00
3.00	0.2103	1.037	4.00
5.00	0.2223	0.989	10.00
7.50	0.2316	0.953	15.00
10.00	0.2371	0.927	20.00
12.50	0.2416	0.909	25.00
15.00	0.2452	0.894	30.00
17.50	0.2483	0.881	35.00
20.00	0.2508	0.871	40.00
22.50	0.2533	0.860	45.00
25.00	0.2552	0.852	50.00
27.50	0.2571	0.844	55.00
30.00	0.2588	0.837	60.00
32.50	0.2603	0.831	65.00

Table XIV

Data Run # 32

<u>Force</u>	<u>Total Deflection</u>	<u>Fold Ratio</u>	<u>Load (nsi)</u>
0	0	1.316	c
0.50	0.0396	1.280	1.00
1.00	0.0655	1.190	2.00
1.50	0.0809	1.103	3.00
2.50	0.0978	1.070	5.00
4.00	0.1122	1.035	7.00
6.00	0.1234	0.991	12.00
8.00	0.1312	0.963	15.00
10.00	0.1368	0.945	20.00
12.50	0.1424	0.925	25.00
15.00	0.1468	0.910	30.00
17.50	0.1506	0.897	35.00
20.00	0.1539	0.886	40.00
22.50	0.1567	0.876	45.00
25.00	0.1593	0.867	50.00
27.50	0.1615	0.860	55.00
30.00	0.1636	0.852	60.00
32.50	0.1657	0.845	65.00

USF/30/60-3

Table XVI

Data Run # 33

<u>Force</u>	<u>Total Deflection</u>	<u>Void Ratio</u>	<u>Load (psi)</u>
0	0	1.120	0
0.50	0.0064	1.100	1.00
1.00	0.0086	1.092	2.00
1.50	0.0104	1.087	3.00
2.50	0.0144	1.074	5.00
5.00	0.0247	1.040	10.00
7.50	0.0335	1.012	15.00
10.00	0.0404	0.989	20.00
12.50	0.0459	0.971	25.00
15.00	0.0505	0.956	30.00
20.00	0.0578	0.933	40.00
22.50	0.0608	0.923	45.00
25.00	0.0636	0.914	50.00
27.50	0.0661	0.906	55.00
30.00	0.0684	0.898	60.00
32.50	0.0706	0.891	65.00

Table XIVII

Data Run # 34

<u>Force</u>	<u>Total Deflection</u>	<u>Void Ratio</u>	<u>Load (psi)</u>
0	0	1.805	0
1.00	0.1602	1.164	2.00
2.00	0.1816	1.079	4.00
3.00	0.1937	1.030	6.00
4.00	0.2019	0.997	8.00
5.00	0.2071	0.977	10.00
7.50	0.2173	0.936	15.00
10.00	0.2239	0.909	20.00
12.50	0.2286	0.891	25.00
15.00	0.2327	0.874	30.00
17.50	0.2357	0.862	35.00
20.00	0.2386	0.851	40.00
22.50	0.2410	0.841	45.00
25.00	0.2433	0.832	50.00
27.50	0.2453	0.824	55.00
30.00	0.2471	0.817	60.00
32.50	0.2487	0.810	65.00

Table XXVIII

Data Run # 35

<u>Force</u>	<u>Total Deflection</u>	<u>Void Ratio</u>	<u>Load (psi)</u>
0	0	1.715	0
1.00	0.1431	1.162	2.00
2.00	0.1636	1.083	4.00
3.00	0.1743	1.041	6.00
4.00	0.1812	1.014	8.00
5.00	0.1866	0.993	10.00
7.50	0.1959	0.957	15.00
10.00	0.2023	0.933	20.00
12.50	0.2070	0.914	25.00
15.00	0.2109	0.899	30.00
17.50	0.2141	0.887	35.00
20.00	0.2169	0.876	40.00
22.50	0.2194	0.866	45.00
25.00	0.2215	0.858	50.00
27.50	0.2236	0.850	55.00
30.00	0.2255	0.843	60.00
32.50	0.2271	0.837	65.00

SSS/ C/69-3

Table XXIX

Data Run # 36

<u>Force</u>	<u>Total Deflection</u>	<u>Void Ratio</u>	<u>Load (psi)</u>
0	0	1.361	0
1.00	0.0449	1.193	2.00
2.00	0.0750	1.109	4.00
3.00	0.0860	1.065	6.00
4.00	0.0962	1.037	8.00
5.00	0.1025	1.016	10.00
7.50	0.1137	0.978	15.00
10.00	0.1214	0.952	20.00
12.50	0.1271	0.933	25.00
15.00	0.1317	0.932	30.00
17.50	0.1356	0.918	35.00
20.00	0.1390	0.905	40.00
22.50	0.1420	0.893	45.00
25.00	0.1446	0.883	50.00
27.50	0.1469	0.874	55.00
30.00	0.1491	0.859	60.00
32.50	0.1511	0.852	65.00

532/35/69-4

Table XXX

Data Run # 37

<u>Force</u>	<u>Total Deflection</u>	<u>Void Ratio</u>	<u>Load (psi)</u>
0	0	1.236	0
1.00	0.0267	1.170	2.00
2.00	0.0453	1.111	4.00
3.00	0.0567	1.074	6.00
4.00	0.0644	1.049	8.00
5.00	0.0705	1.030	10.00
7.50	0.0814	0.994	15.00
10.00	0.0889	0.970	20.00
12.50	0.0946	0.952	25.00
15.00	0.0992	0.937	30.00
17.50	0.1031	0.925	35.00
20.00	0.1065	0.914	40.00
22.50	0.1095	0.904	45.00
25.00	0.5917	0.895	50.00
27.50	0.1146	0.888	55.00
30.00	0.1169	0.880	60.00
32.50	0.1189	0.874	65.00

Table XXXI

Data Run # 38

<u>Force</u>	<u>Total Deflection</u>	<u>Void Ratio</u>	<u>Load (psi)</u>
0	0	1.681	0
1.00	0.1406	1.116	2.00
2.00	0.1500	1.038	4.00
3.00	0.1707	0.995	6.00
4.00	0.1772	0.968	8.00
5.00	0.1824	0.947	10.00
7.50	0.1913	0.912	15.00
10.00	0.1973	0.888	20.00
12.50	0.2019	0.869	25.00
15.00	0.2055	0.856	30.00
17.50	0.2086	0.842	35.00
20.00	0.2112	0.832	40.00
22.50	0.2135	0.822	45.00
25.00	0.2155	0.814	50.00
27.50	0.2174	0.807	55.00
30.00	0.2191	0.800	60.00
32.50	0.2206	0.794	65.00

Table XXXII

Data Run # 39

<u>Force</u>	<u>Total Deflection</u>	<u>Void Ratio</u>	<u>Load (psi)</u>
0	0	1.544	0
1.00	0.1124	1.115	2.00
2.00	0.1307	1.045	4.00
3.00	0.1406	1.007	6.00
4.00	0.1474	0.981	8.00
5.00	0.1525	0.962	10.00
7.50	0.1617	0.927	15.00
10.00	0.1678	0.904	20.00
12.50	0.1725	0.886	25.00
15.00	0.1763	0.871	30.00
17.50	0.1795	0.859	35.00
20.00	0.1822	0.849	40.00
22.50	0.1846	0.840	45.00
25.00	0.1864	0.833	50.00
27.50	0.1884	0.825	55.00
30.00	0.1903	0.818	60.00
32.50	0.1918	0.812	65.00

GSF/X/67-4

Table XXXIII

Data Run # 40

<u>Force</u>	<u>Total Deflection</u>	<u>Void Ratio</u>	<u>Load (psi)</u>
0	0	1.242	0
1.00	0.0455	1.475	2.00
2.00	0.0646	1.825	4.00
3.00	0.0734	2.995	6.00
4.00	0.0796	0.974	8.00
5.00	0.0847	2.957	10.00
7.50	0.0934	0.923	15.00
10.00	0.0997	0.907	20.00
12.50	0.1044	0.391	25.00
15.00	0.1082	0.375	30.00
17.50	0.1115	0.367	35.00
20.00	0.1144	0.657	40.00
22.50	0.1168	0.649	45.00
25.00	0.1191	0.841	50.00
27.50	0.1212	0.634	55.00
30.00	0.1230	0.828	60.00
32.50	0.1243	2.822	65.00

CS / 5/59-1

Table XXXIV

Data from Fig. 41

<u>Force</u>	<u>Total Deflection</u>	<u>Void Ratio</u>	<u>Load (psi)</u>
0	0	1.666	0
1.00	0.0296	0.974	2.00
2.00	0.0332	0.926	4.00
3.00	0.0351	0.925	6.00
4.00	0.0394	0.913	8.00
5.00	0.0529	0.962	10.00
7.50	0.0999	0.920	15.00
10.00	0.0646	0.845	20.00
12.50	0.0689	0.852	25.00
15.00	0.0723	0.842	30.00
17.50	0.0752	0.832	35.00
20.00	0.0778	0.825	40.00
22.50	0.0801	0.815	45.00
25.00	0.0822	0.811	50.00
27.50	0.0842	0.805	55.00
30.00	0.0859	0.800	60.00
32.50	0.0875	0.795	65.00

CSF/11/59-4

Table XXIV

Data Run # 32

<u>Force</u>	<u>Total Deflection</u>	<u>Total Ratio</u>	<u>Load (psi)</u>
0	0	1.910	0
1.00	0.1310	1.125	2.00
2.00	0.1395	1.039	4.00
3.00	0.2092	0.997	6.00
4.00	0.2154	0.970	8.00
5.00	0.2202	0.949	10.00
7.50	0.2284	0.913	15.00
10.00	0.2340	0.889	20.00
12.50	0.2381	0.871	25.00
15.00	0.2415	0.856	30.00
17.50	0.2442	0.844	35.00
20.00	0.2466	0.834	40.00
22.50	0.2485	0.825	45.00
25.00	0.2506	0.816	50.00
27.50	0.2522	0.809	55.00
30.00	0.2537	0.803	60.00
32.50	0.2552	0.796	65.00

CSF/10/60-4

Table XXXVI

Data Run # 43

<u>Force</u>	<u>Total Deflection</u>	<u>Void Ratio</u>	<u>Load (psi)</u>
0	0	1.332	0
1.00	0.0575	1.096	2.00
2.00	0.0882	1.024	4.00
3.00	0.0991	0.936	6.00
4.00	0.1064	0.960	8.00
5.00	0.1118	0.941	10.00
7.50	0.1215	0.907	15.00
10.00	0.1280	0.884	20.00
12.50	0.1330	0.867	25.00
15.00	0.1370	0.853	30.00
17.50	0.1404	0.841	35.00
20.00	0.1435	0.830	40.00
22.50	0.1460	0.822	45.00
25.00	0.1483	0.813	50.00
27.50	0.1504	0.806	55.00
30.00	0.1522	0.800	60.00
32.50	0.1540	0.794	65.00

Table XXXVII

Data Run # 44

<u>Force</u>	<u>Total Deflection</u>	<u>Void Ratio</u>	<u>Load (psi)</u>
0	0	1.143	0
1.00	0.0360	1.027	2.00
2.00	0.0510	0.979	4.00
3.00	0.0596	0.951	6.00
4.00	0.0657	0.932	8.00
5.00	0.0704	0.917	10.00
7.50	0.0793	0.888	15.00
10.00	0.0855	0.868	20.00
12.50	0.0902	0.853	25.00
15.00	0.0941	0.841	30.00
17.50	0.0976	0.829	35.00
20.00	0.1006	0.820	40.00
22.50	0.1032	0.811	45.00
25.00	0.1055	0.804	50.00
27.50	0.1077	0.797	55.00
30.00	0.1096	0.791	60.00
32.50	0.1115	0.785	65.00

GSF/MC/69-4

Table XXXVIII

Data Run # 45

<u>Force</u>	<u>Total Deflection</u>	<u>Void Ratio</u>	<u>Load (psi)</u>
0	0	1.341	0
1.00	0.0580	1.137	2.00
2.00	0.0785	1.065	4.00
3.00	0.0890	1.029	6.00
4.00	0.0961	1.004	8.00
5.00	0.1017	0.984	10.00
7.50	0.1114	0.950	15.00
10.00	0.1180	0.927	20.00
12.50	0.1231	0.909	25.00
15.00	0.1273	0.894	30.00
17.50	0.1307	0.882	35.00
20.00	0.1338	0.871	40.00
22.50	0.1364	0.862	45.00
25.00	0.1388	0.854	50.00
27.50	0.1419	0.843	55.00
30.00	0.1430	0.839	60.00
32.50	0.1448	0.833	65.00

Table XXXIX

Data Run # 46

<u>Force</u>	<u>Total Deflection</u>	<u>Void Ratio</u>	<u>Load (psi)</u>
0	0	1.245	0
1.00	0.0415	1.105	2.00
2.00	0.0564	1.055	4.00
3.00	0.0655	1.025	6.00
4.00	0.0720	1.003	8.00
5.00	0.0770	0.986	10.00
7.50	0.0860	0.956	15.00
10.00	0.0921	0.935	20.00
12.50	0.0970	0.918	25.00
15.00	0.1010	0.905	30.00
17.50	0.1043	0.894	35.00
20.00	0.1072	0.884	40.00
22.50	0.1098	0.875	45.00
25.00	0.1120	0.868	50.00
27.50	0.1142	0.861	55.00
30.00	0.1161	0.854	60.00
32.50	0.1179	0.848	65.00

GSF/10/69-4

Table XL

Data Run # 47

<u>Force</u>	<u>Total Deflection</u>	<u>Void Ratio</u>	<u>Load (psi)</u>
0	0	1.138	0
1.00	0.0330	1.032	2.00
2.00	0.0449	0.924	4.00
3.00	0.0516	0.972	6.00
4.00	0.0563	0.957	8.00
5.00	0.0606	0.947	10.00
7.50	0.0679	0.920	15.00
10.00	0.0733	0.903	20.00
12.50	0.0774	0.890	25.00
15.00	0.0809	0.878	30.00
17.50	0.0840	0.869	35.00
20.00	0.0867	0.860	40.00
22.50	0.0890	0.853	45.00
25.00	0.0912	0.845	50.00
27.50	0.0932	0.839	55.00
30.00	0.0950	0.833	60.00
32.50	0.0966	0.828	65.00

Appendix E

Assumptions

Introduction

The assumptions involved are not numerous but they are important to the development of the concepts presented. In order that the full significance of these assumptions be considered, they are discussed in detail in this appendix.

Simulated Lunar Soil

The rock powders that were used were assumed to simulate the fine fraction of the lunar surface layer. As mentioned previously, these rocks are one of Green's standards for lunar research and a comparison of the chemical analysis of these rocks and the results of Surveyor V, VI, and VII are included in Table XLI. The data in this table indicates that the chemical analysis of the rocks is a good approximation of the lunar surface material. The results of Surveyor V indicate that the finest fraction of the lunar surface layer is probably in the 2-60 micron range (Ref 4:87). The grain size analysis of the powders used is shown in Fig. 17 and is comparable to the results of Surveyor V. Therefore within the bounds of existing information, these rocks powders seem to be the closest terrestrial approximation to the fine fraction of the lunar surface material.

Table XLI

Comparison of Green's Standards and Surveyor Results

Element	Chemical Composition, Atomic %			
	Sur. V *	Sur. VI *	Sur. VII *	Green's Std. **
C	3	2	2	0.01
O	58+ <u>5</u>	57+ <u>5</u>	58+ <u>5</u>	44.67
Na	2	2	3	2.50
Mg	3+ <u>3</u>	3+ <u>3</u>	4+ <u>3</u>	2.70
Al	6.5+ <u>2</u>	6.5+ <u>2</u>	8+ <u>3</u>	7.40
Si	18+ <u>3</u>	22+ <u>4</u>	18+ <u>4</u>	23.80
"Ca" ^a	13+ <u>3</u>	6+ <u>2</u>	6+ <u>2</u>	18.60
"Fe" ^b		5+ <u>2</u>	2+ <u>1</u>	9.20

* Reference 6:257

** Reference 8

a. "Ca" here denoted elements with mass numbers between approximately 30 and 47 and includes for example, P, S, K, and Ca.

b. "Fe" here denotes elements with mass numbers between 47 and 65 and includes for example, Cr, Fe, Co, and Ni.

Grain Density

The density of the soil grains in the sample was assumed to be the same as the rock prior to comminution. This is the same as saying the rock contained no voids. This assumption is not precisely accurate but the error associated with it is small enough that the error introduced from the instrumentation is orders of magnitude greater. The basalt is not vesicular and does not contain voids that are visible to the eye. Upon bakeout of the rocks prior to comminution, the weight loss was about 1% which verifies that the rocks were not highly vesicular.

Initial Void Ratio

The initial void ratio of the soil mass when placed in the container prior to the test was assumed to be distributed uniformly throughout the container. There was no way to check this assumption and it is probably not correct. The reproducibility of the results from the Instron tests indicated that whatever the initial void ratio distribution was, it was uniform from test to test. The compatibility of results from tests where the sample had been prepared by application of a uniform pressure on its surface and the sample that had been initially packed by a rodding technique indicates that the same distribution of void ratio was obtained by the two methods. An alternate possibility is that the results were not sensitive to the initial void ratio distribution; however, this possibility seems remote and is

rejected. The material in the bottom of the container probably was at a lower void ratio than the material near the surface because it would see a larger total force during the preparation process. In either case, the experiments indicate that whatever the distribution of the initial void ratio, it was consistent from one test to another.

Lateral Strain

The assumption was made in the process of calculating the change in void ratio under the tamper as the load increased that there was no loss of mass from the volume of soil under the tamper. This is the same as assuming that the soil under the tamper was compressed under the condition of no lateral strain. This assumption is known not to be precisely correct for reasons that are discussed fully in Appendix F. The soil did move out from under the tamper but the extent of this movement was not known; however it is felt to be insignificant for several reasons. First the soil failed principally in compression and only for the samples with a low initial void ratio was an extrusion of material above the level of the container noted. This extrusion was in all cases extremely small and just visible to the naked eye. For the samples with an initial void ratio greater than 1.50, this extrusion did not occur at all. Because of the visual evidence of this lack of plastic behavior at the surface, it appears that the movement of mass internally was also small. If a large degree of plastic behavior had been observed, then this assumption would be quite invalid.

Secondly, any expansion of the container during the loading would indicate that the soil was moving outward and thus invalidate the assumption. Such deflections in the walls of the container were calculated using the classical methods of elasticity and the change in the original volume was found to be less than 0.05% which supports the assumption as made.

The effect of this assumption was to compute a value of the void ratio that was too low. The total mass of the soil under the tamper was assumed to remain constant when in fact it decreased. The true value of the void ratio then was less than the value actually computed. The difference between these values is not known but the assumption was made for all computations thus the relative error associated with comparing data would be less than the absolute error involved. This assumption then is probably the least valid of all of the assumptions made in the analysis but its effect on the relative importance of the results is considered negligible.

Time Dependence

In the testing phase the assumption was made that the response of the soil to the load was almost instantaneous and not time dependent. This assumption was made for several reasons. The material was a granular material with essentially a zero water content. Yong and Warkentin state that the compression deformation of a granular soil occurs in a short time whereas the time dependence of clay is

quite complex due to the presence of moisture in the soil (Ref 28:179). Scott states that there is a time dependence for sand but that it is quite short. This short time allows for particle readjustment caused by particle imbalances and movements (Ref 22:263). Gilboy tested the compressibility of sand-mica mixtures and found that there was no time lag observed in compression (Ref 7:559). It was possible to check this assumption during the experimentation. On Data Runs #13 and 15, the final load of approximately 60 psi was held on the sample at the end of the normal test and the tamper was checked for additional movement every 15 minutes for a total time of two hours. At each reading the scope was moved off of the focusing point and then realigned to detect movement. There was no additional deflection within the sensitivity of the instrument within a two hour period. The assumption then seems valid.

Appendix F

Analysis of the Boundary Effects

Introduction

In order to determine the magnitude of the effect of the boundaries of the container in the compression tests that were performed, several tests were performed and certain calculations were made. This appendix deals with those attempts. Some idea as to the importance of this effect was necessary to insure that all of the observed differences between the atmospheric and vacuum data was not caused by changes in the frictional properties of the boundaries alone.

Frictional Shear at the Wall

As the normal load was applied to the surface of the soil, frictional shear forces developed along the interface of the wall and the soil. This shear force reduced the effective load on the soil so that the actual load seen by the soil was

$$P_{act} = P_{app} - \text{Frictional Shear Pressure}$$

In order to determine the order of magnitude of this frictional shear pressure, several assumptions were made and a very conservative estimate was made. To be consistent with the assumption of no lateral strain, the coefficient of earth pressure at rest was assumed to be 0.30 (Ref 24:140) and the coefficient of friction between the soil

and the wall was assumed to be 1.0. The pressure distribution on the sides of the sample for a normal surface load of 60 psi was assumed to be triangular with a zero value at the surface and a maximum value at the bottom. The normal force on the wall was computed as the resultant of this triangular distribution, the frictional force was then computed for the resulting normal force, and the result was integrated around the perimeter of the container. Making these assumptions the frictional shear pressure was approximately 2% of the applied surface pressure. This result is consistent with the results of Leonards and Girault who determined that the effect of side friction in a one dimensional consolidometer was less than 6% of the applied pressure for a total pressure in excess of approximately 14 psi (Ref 15:216). Their result however was for a container with a diameter to height ratio of 6 while the container used in these experiments had a similar ratio of 1.33. Hendron also measured the ring friction in his experiment and found it to be less than 5% (Ref 10:279). The conclusion may be drawn from this calculation, the work of Leonards and Girault, and Hendron that the frictional shear force developed at the wall of the container was less than 10% of the force applied to the surface of the sample.

Tests

Tests were performed on the Instron with several types of containers to determine the nature of the soil behavior as it was loaded

and the relative importance of the boundary effects along the walls and on the bottom. These tests were run in a steel container, a teflon container, and a teflon container with an aluminium foil bottom. The steel container was the same as the one used for the vacuum tests and consequently represented the same boundary conditions as were present in all of the atmospheric tests on the chamber apparatus. The teflon container had the same internal dimensions as the steel container so that the geometry of the soil sample was not varied. With the teflon container, the frictional resistance of the boundaries of the container was reduced to its lowest possible value. By addition of the aluminium foil to the bottom of the teflon container, the walls of the container retained their low frictional resistance but the bottom of the container had approximately the same frictional resistance as the steel bottom. By comparison of the results of these three tests, a qualitative determination of the behavior of the soil in the steel container as it was loaded could be made. The results of the tests for the steel and teflon containers are shown in Figs. 6 through 10. The conclusions from these results are that the larger the initial void ratio the less the effects of the boundary while for samples with an initial void ratio of less than 1.20 the effect of the boundary was significant. The difference between these two curves represents a change in the frictional properties of the walls and bottom of the container. Such a difference would only be noted if the soil were moving rela-

tive to either the walls or the bottom or both. Upon placing the aluminium foil in the bottom of the container the resulting e-P curve fell intermediate to the results of the steel and the teflon. Under this condition, the frictional resistance of the walls of the teflon container was unchanged while the resistance of the bottom approximated the steel container. Because the results fell intermediate to the two previous tests, the conclusion may be drawn that in the tests with the teflon container, the soil was moving relative to the walls and the bottom. The predominance of one over the other could not be determined. With the steel container it was not apparent whether the soil was in motion at the boundaries or not. The only conclusive statement that can be made is that the steel container caused a higher frictional response at the boundaries than the teflon caused. Whether this increase in friction was significant enough to prevent grain movement is not known, although it is felt that some movement did occur in the steel container. From the results of these tests the flow pattern of the soil in the steel container tested at atmospheric pressure is assumed to be as shown in Fig. 38. A semiquantitative idea of the degree of change of the frictional resistance between the steel and the teflon container was obtained from the work of two other reports. Mohr and Karafiath measured the coefficient of friction of basalt powders on the 38-62 micron size range with 1020 steel and obtained a value of 0.25 (Ref 17:14). Bowers, Clinton and Zisman researched

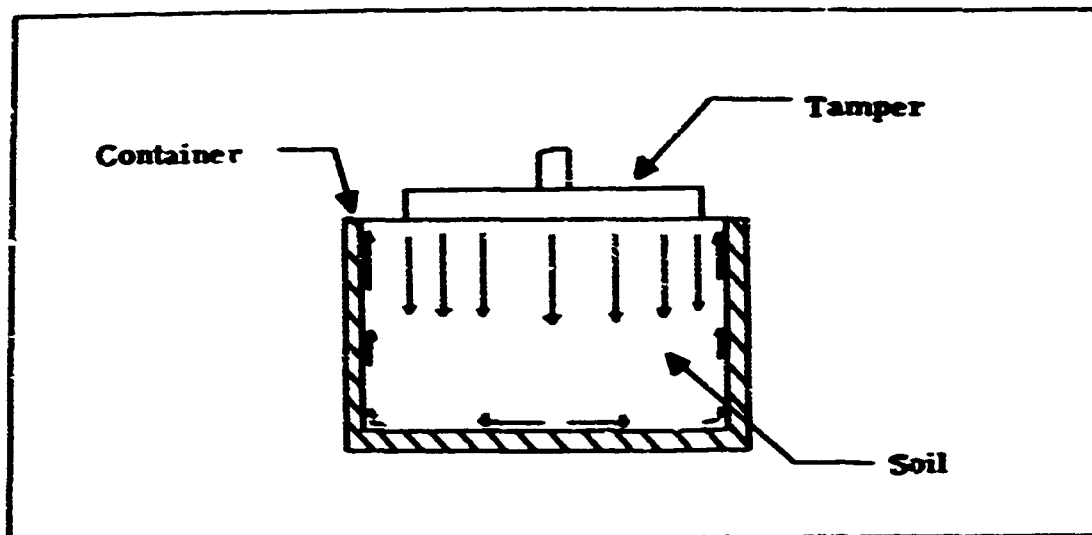


Fig. 38 Flow Pattern of the Soil

the frictional properties of teflon and found the coefficient of friction for steel sliding at low speeds on teflon to be 0.15 (Ref 2:136). The ratio of these values is

$$\frac{u \text{ (basalt on steel)}}{u \text{ (steel on teflon)}} = 1.50$$

Thus the change in the frictional response of the teflon and the steel containers represents a change of the frictional characteristics of the boundaries by a factor of about 1.50.

Correction of Vacuum Data

The intended purpose of these above-discussed tests was to determine an upper limit of the effects of the boundaries of the container as the environment was changed from atmospheric pressure to 10^{-10} Torr. Accepting the flow pattern of the soil as shown in Fig. 38, it would be essentially the same for vacuum except that the frictional resistance of the boundaries would have increased even further. It

could be that movement did not occur along either boundary because of the increase or movement might have occurred but had been more restricted. The increased frictional resistance of the wall introduced a larger error in the calculation and should be corrected for. The increased resistance of the bottom is helpful because this restricts the soil movement in that region and there is less transfer of mass out from under the tamper which improves the assumption of no lateral strain. The effect of the vacuum then by changing the frictional characteristics of the wall has compensating effects; however, the individual magnitude of these effects is not known.

Mohr and Karafiath performed some experiments in air and in vacuum with basalt powders and steel to determine the effect of the vacuum on the coefficient of friction between the basalt and the steel (Ref 17). They used basalt powders in the 38-62 micron range on a 1020 steel and performed their vacuum tests in the 10^{-10} Torr range. Thus all of their work dealt with essentially the same materials in the same type of environment as the experiments of this report. The result of their work was the ratio

$$\frac{u \text{ (basalt on steel in vacuum)}}{u \text{ (basalt on steel in air)}} = 1.50 \text{ (Ref 17:19)}$$

Consequently the change in the frictional characteristics of the basalt on steel with the change in environment is about 1.50.

A direct way to interpret the results of the tests on the Instron and apply those results to the vacuum tests was not available. Since

the effect of the vacuum was to produce compensating effects at the boundary and since the corresponding ratios of the steel-teflon in air tests and the work of Mohr and Karafiath are the same, the vacuum data was corrected by the same amount as the difference that resulted between the steel-teflon in air tests. This correction is felt to be quite conservative and more than compensates for the effects of the boundaries in the vacuum tests. The remaining difference that exists between the curves in Figs. 6 through 10 can be attributed to an increase in the internal friction of the soil mass and the soil cohesion and hence to a decrease in the compressibility of the soil.

Personally Identifiable
Information Redacted

Vita

Dwayne Goldsmith Lee [REDACTED]

[REDACTED] and was awarded a Bachelor of Science degree from the United States Military Academy in June 1964. At that time he was commissioned as a 2nd Lieutenant in the U.S. Army Corps of Engineers and was assigned to the 10th Engineer Battalion in Kitzigen, West Germany. In June 1966 he was assigned to the 168th Combat Engineer Battalion in the Republic of Vietnam where he served as an engineer company commander until reassignment at the Air Force Institute of Technology in the Graduate Space Facilities program in June 1967.

Permanent address: [REDACTED]

UNCLASSIFIED

Security Classification

DOCUMENT CONTROL DATA - R & D		
<small>(Security Classification of title, body of abstract and indexing information must be entered when the overall report is classified)</small>		
1. ORIGINATING ACTIVITY (Corporate author)		2. REPORT SECURITY CLASSIFICATION
Air Force Institute of Technology (AFIT-SE) Wright-Patterson AFB, Ohio 45433		Unclassified
3. REPORT TITLE		4. GROUP
Compressibility of Simulated Lunar Soils in Air and in Ultrahigh Vacuum		
5. DESCRIPTIVE NOTES (Type of report and inclusive dates)		
AFIT Thesis		
6. AUTHOR(S) (First name, middle initial, last name)		
Dwayne G. Lee		
Captain CE		
7. REPORT DATE	8. TOTAL NO. OF PAGES	9. NO. OF REFS
June 1969		
10. CONTRACT OR GRANT NO.	11. ORIGINATOR'S REPORT NUMBER(S)	
A. PROJECT NO.	GSF/MC/69-4	
C.	12. OTHER REPORT NO(S) (Any other numbers that may be assigned this report)	
N/A		
13. DISTRIBUTION STATEMENT		
This document is subject to special export controls transmittal to foreign governments or foreign nationals may be made only with prior approval of the Dean of Engineering, Air Force Institute of Technology (AFIT-SE), Wright-Patterson AFB, Ohio 45433		
14. SUPPLEMENTARY NOTES		15. SPONSORING MILITARY ACTIVITY
16. ABSTRACT		
<p>A simulated lunar soil of comminuted tholeiitic basalt powder with particles less than 60 microns in size was tested in one dimensional compression to determine the effect of the initial void ratio and the ambient pressure on the compressibility of the soil. The initial void ratio ranged from 1.12 to 2.00 and the ambient pressure was restricted to three levels; atmospheric pressure, 10^{-8} Torr, and 10^{-10} Torr. The results of the tests indicate that the compressibility of the powders increased as the initial void ratio increased. Also the powders tended to become less compressible as the ambient pressure decreased.</p>		

DD FORM 1 NOV 65 1473

Unclassified

Security Classification

Security Classification

14	KEY WORDS	TEST A		TEST B		TEST C	
		HOLE	WT	HOLE	WT	HOLE	WT
	Compressibility Simulated lunar soil One dimensional compression						

Security Classification